LV-2016-129

Landsvirkjun

Vatnajökull

Mass balance, meltwater drainage and surface velocity of the glacial year 2015-16

Lykilsíða

Landsvirkjun

Skýrsla nr:	**Dags:**	**Dreifing:**	
LV-2016-129	28. des. 2016		☒ Opin ☐ Birt á vef LV ☐ Takmörkuð til

Titill: Vatnajökull: Mass balance, meltwater drainage and surface velocity of the glacial year 2015-16	**Upplag:**
	Fjöldi síðna: 53

Höfundar / fyrirtæki	Finnur Pálsson, Jarðvísindastofnun Háskólans
Verkefnisstjóri:	Andri Gunnarsson
Samvinnuaðilar:	

Útdráttur:

The autumn of 2015 was wet and windy, followed by a winter colder than average this century. The spring weather was calm, and unusually dry. In spite of an extremely calm and dry summer in Iceland, on Vatnajökull most of the summer was cloudy, less than 1/3 of the summer-days were close to cloud free. Latter half of September and first weeks of October were unusually favorable for ablation, both warm and windy. The total winter balance was 5% higher than average. The total summer balance was more negative than on average since 1995 by ~2%. The net balance was negative as it has been since 1994-95 (except 2014-15); the mass loss was close to average, 0,1 m_{we} less negative than average since 1994-95.

Flokkun:	
Landsvæði: Þjórsársvæði	Flákar:
Tegund: Rannsóknir	Flokkur: Vatn
Lykilorð: Vatnajökull, afkoma, mass balance, runoff, ablation, melt	**Samþykki verkefnisstjóra LV:** Andri Gunnarsson

LV-2016-129

Landsvirkjun

Vatnajökull

Mass balance, meltwater drainage and surface velocity of the glacial year 2015_16

UNIVERSITY OF ICELAND

December 2016

Contents:

Figures:

Tables:

Appendixes:

1. INTRODUCTION

In 1992 (glacial year 1991_92) a program of mass balance measurements was started for Vatnajökull by the Science Institute University of Iceland (now Institute of Earth Sciences, IES) in collaboration with the National Power Company (NPC). For the first year the program was limited to the western part of the glacier, but then expanded to include the northern outlets as well. In 1996 this study was further expanded to include southern outlets, with support from The European Union (Framework IV - Environment and Climate, TEMBA project 1996-1997). This program was extended 1998–2000 with further support from EU (Framework IV - Environment and Climate, ICEMASS project, 1998-2000). In 2000-2002 NPC and IES continued the program. In 2003-2005 IES participated in a multinational research project, which was financially supported by The European Union (EVK2-CT-2002-00152 SPICE). IES was responsible for obtaining data sets for calibration of models of the mass balance and dynamics of Vatnajökull. This work was also supported by The National Power Company of Iceland and The National Road Authority, and is a continuation of the TEMBA-project of 1996-97 and ICEMASS project 1998-2001.
In 2015_2016 IES and NPC continued a similar program. Mass balance measurements on the southeast outlets Breiðamerkurjökull and Hoffellsjökull is financially supported by the National Road Authority.
The aim of the collaborative work of NPC and IES is to improve our understanding of the mass balance and melt water runoff from glaciers. This work in combination with energy balance measurements by NPC and IES on Vatnajökull will be used for calibration of models of the energy and mass balance of Vatnajökull.
This report describes the field measurements, GPS survey, mass balance and melt water runoff for the glacial year 2015_16.

2. DIARY

January 18 - 19: installation of melt wires, maintenance of AWSs on Breiðamerkurjökull
May 4 - 10: measurements of the winter balance
June 3-10: measurements of the winter balance.
October 9 – 11 and 13 – 17: summer balance measurements, maintenance of AWSs on Breiðamerkurjökull

In all expeditions and short visits to the glacier the locations of mass balance stakes were measured with Kinematic GPS (or fast static GPS and a few with DGPS) for surface velocity calculation.
In the June expedition Tinna Jónsdóttir led a program to drill towards and sample the Grímsvötn tephra layer deposited in 2011. The cores from the boreholes were measured in a traditional way, and are named TJ01 to TJ09 in the winter mass balance data set.

The following members of staff of the Institute of Earth Sciences, University of Iceland, carried out the fieldwork on Vatnajökull: Finnur Pálsson, Þorsteinn Jónsson, Sveinbjörn Steinþórsson also Andri Gunnarsson and Gestur Jónsson (National Power Company) and Hlynur Skagfjörð Pálsson (Reykjavík Rescue Team).
Members of the Iceland Glaciological Society assisted in the June fieldwork.

3. MASS BALANCE MEASUREMENTS

The purpose of the mass balance measurements is to describe the temporal and spatial distribution of the components of the mass balance. The mean annual values of the components and their variation from year to year are analyzed and related to meteorological conditions and climatic variability. The results will be used in studies of changes in the glacier volume, estimates of meltwater contribution to glacial rivers, mass balance modeling, evaluation of altitudinal and regional variations of mass balance in response to climatic variations, and to assess the hydrometeorological and dynamic response of the ice cap to climate change.

The mass balance was determined by a stratigraphic method, measuring changes in thickness and density relative to the summer surface. The winter balance was estimated by drilling ice cores through the winter layer in the spring. Ablation was monitored from markers; snow stakes were put up on the glacier and wires were drilled down in the ablation area. The summer balance was measured in the autumn.

3.1 Methods

Measurements of the surface mass balance on a large ice cap like Vatnajökull are impractical in terms of cost with conventional techniques and sampling density that are typically used on small glaciers. The spatial variability of the mass balance may, however, be predictable on the flat large outlets of such an ice cap given data on several profiles extending over the elevation range of the glacier. The precipitation generally increases with elevation and decreases with the distance from the coast, but both the distribution of snowfall and redistribution of snow by drift depend on the prevailing wind direction during the winter. The summer melting depends mainly on the altitude and the albedo of the glacier surface. Therefore, we have used observations along a limited number of flowlines, which span the elevation range of the outlets to assess aerial estimates of surface mass balance. Each profile describes the variation with elevation, but together they also describe the lateral variation of the mass balance. Recently, modern over-snow vehicles and helicopters have allowed fast traverses to ensure successful fieldwork in spite of frequently poor weather conditions. The error for individual point measurement is estimate ~30 cm_{we} for both summer and winter balance. The error for the area integral of mass balance is however considered smaller, since the error for individual survey sites is independent.

The winter mass balance (b_w) is defined as the mass of snow accumulated during the winter months, the summer balance (b_s) is the mass balance during the summer, and the net balance (b_n) is defined as their sum. The specific mass balance is expressed in terms of the equivalent thickness of water. All mass balance components apply to a time interval between given measurement dates, which are not fixed from one year to another. The dates in the autumn are separated by approximately one calendar year, which roughly coincides with the glaciological year defined as October 1st to September 30th. Snow cores are drilled in April-May through the winter layer and profiles of the density are measured. The summer balance is derived in the autumn from measurements of the changes in the snow core density during the summer in the accumulation area and from readings at stakes and wires drilled into the ice in the ablation areas.

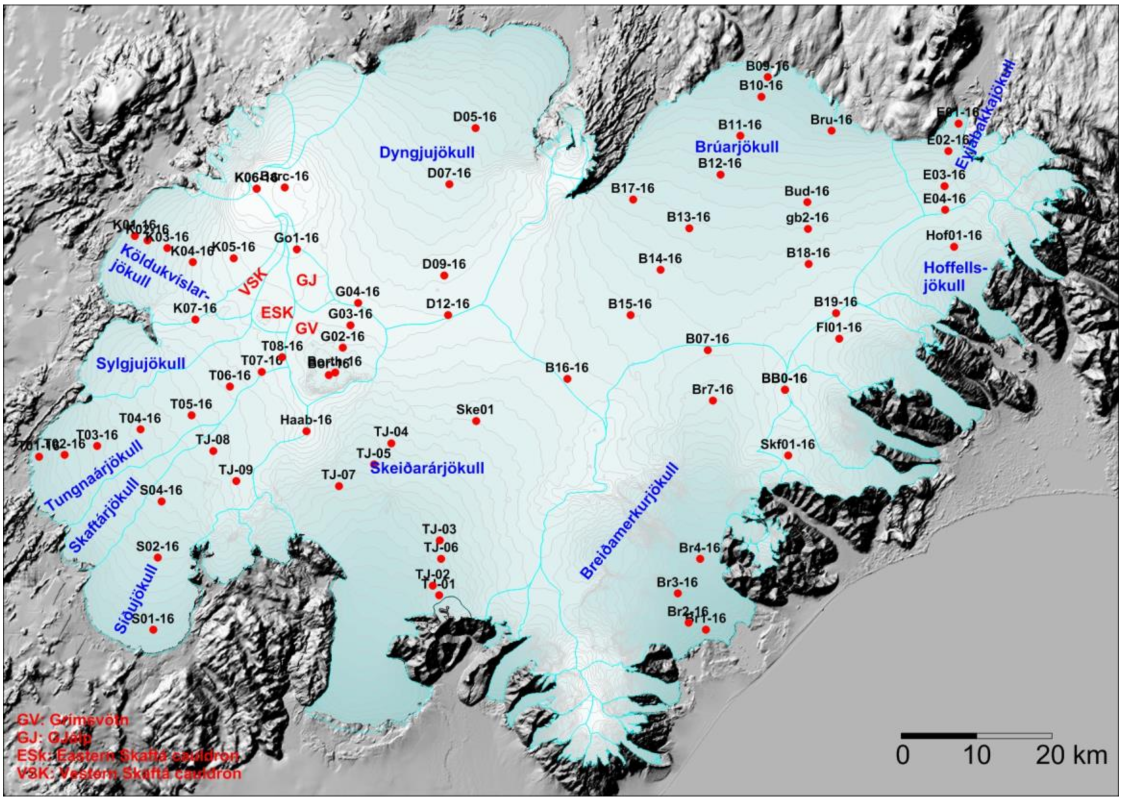

Figure 1. Outlets of Vatnajökull and location of mass balance survey sites 2015_16.

Digital maps are created for winter, summer and net balance for the whole ice cap based on site measurements. The mass balance is calculated over both the ice and water drainage basins. The summer balance over the water basin is an estimate of meltwater contribution to rivers and groundwater storage. This estimate, however, does not include precipitation that falls as rain on the glacier or snow, which falls and melts during the summer. The meltwater contribution is compared with river runoff at stream flow gauges closest to the glacier. For this comparison, we define the glaciological year from the start of October to the end of September and the period draining meltwater from the glacier during the summer from June through September. It would be misleading to include May in the summer period because runoff from the glacier melt in May is delayed due to refreezing during elimination of the cold wave.

3. 2 Results of mass balance measurements.

Mass balance measurements were done at 67 sites in spring 2016 (Fig. 1). The specific mass balance at individual sites is shown in Fig. 2. Most sites are on central flow lines at individual outlets. The specific mass balance along approximate flow lines is given in Fig 3. for the glacier outlets: Síðujökull, Tungnaárjökull, Köldu-kvíslarjökull, Dyngjujökull, Brúar-jökull (west and east), Eyjabakka-jökull, Hoffellsjökull and Breiða-merkurjökull.
Digital maps for winter, summer and net balance are shown in Figure 4. Although no balance measurements are available for Skeiðarárjökull, the balance has been estimated by interpolating the balance values from the neighboring outlets, based on our experience from previous years. The mass balance of individual outlet is discussed in the following subsections.

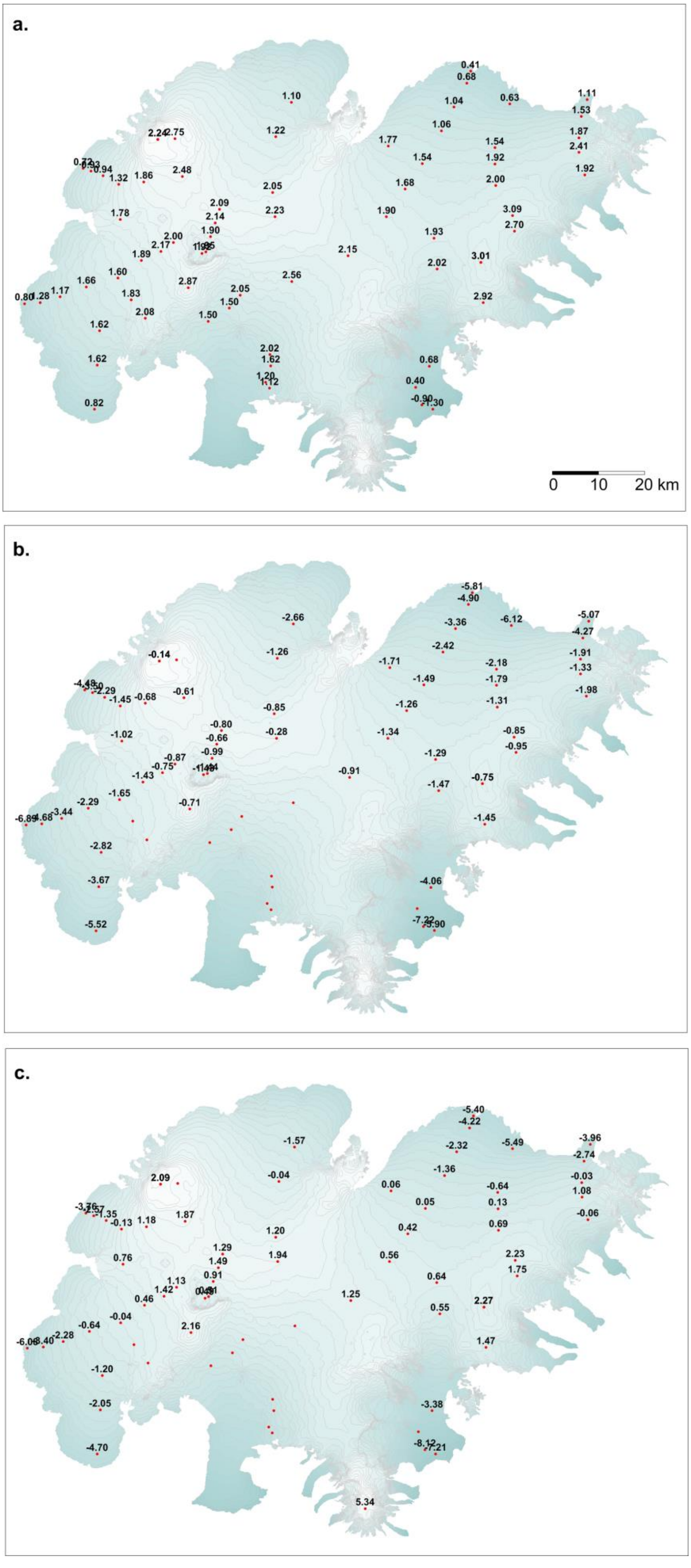

Figure 2. Maps showing point values of specific mass balance in m water equivalent (m_{we}), 2015_16. a. winter, b. summer, c. net balance.

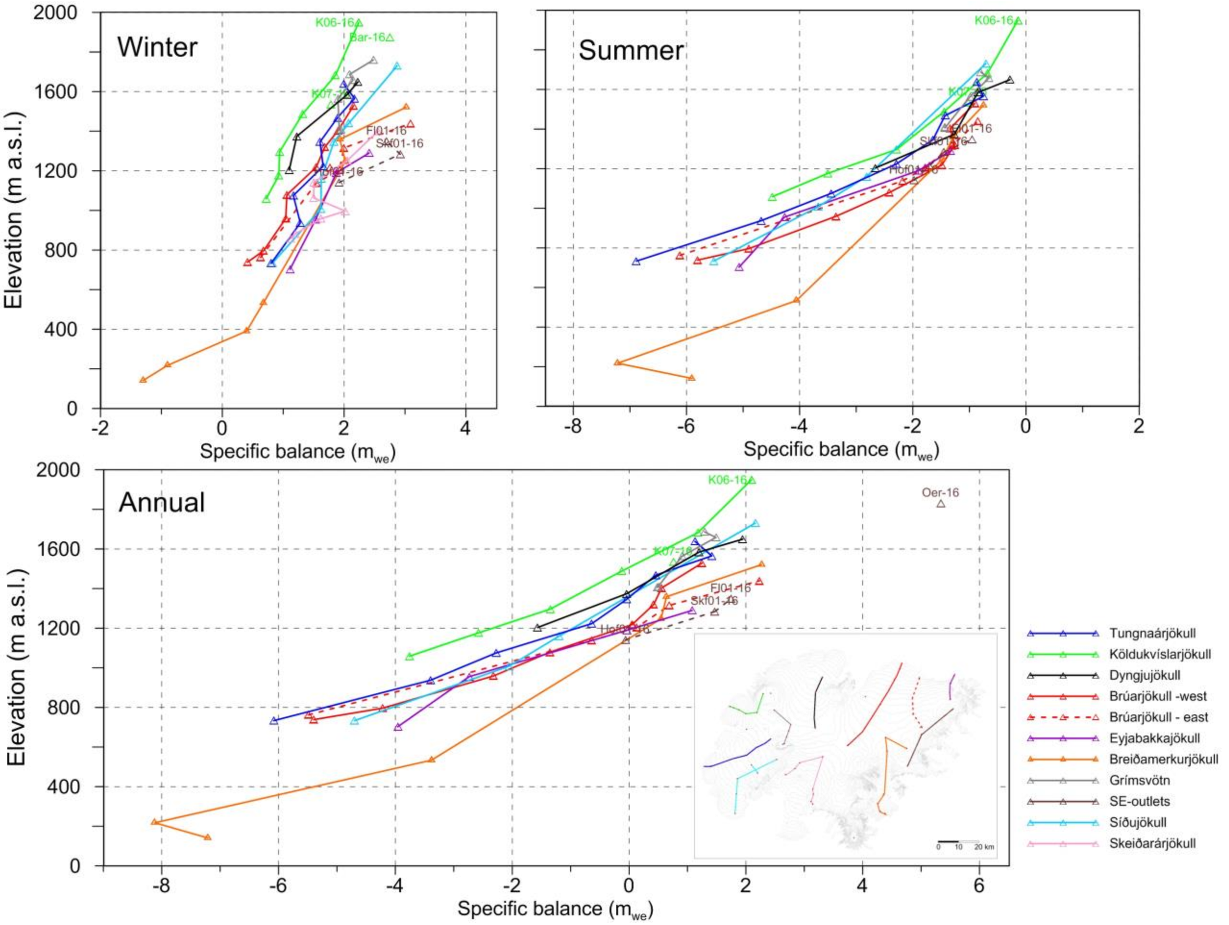

Figure 3. a. Specific mass balance (m_{we}), along all mass balance profiles 2015_16.

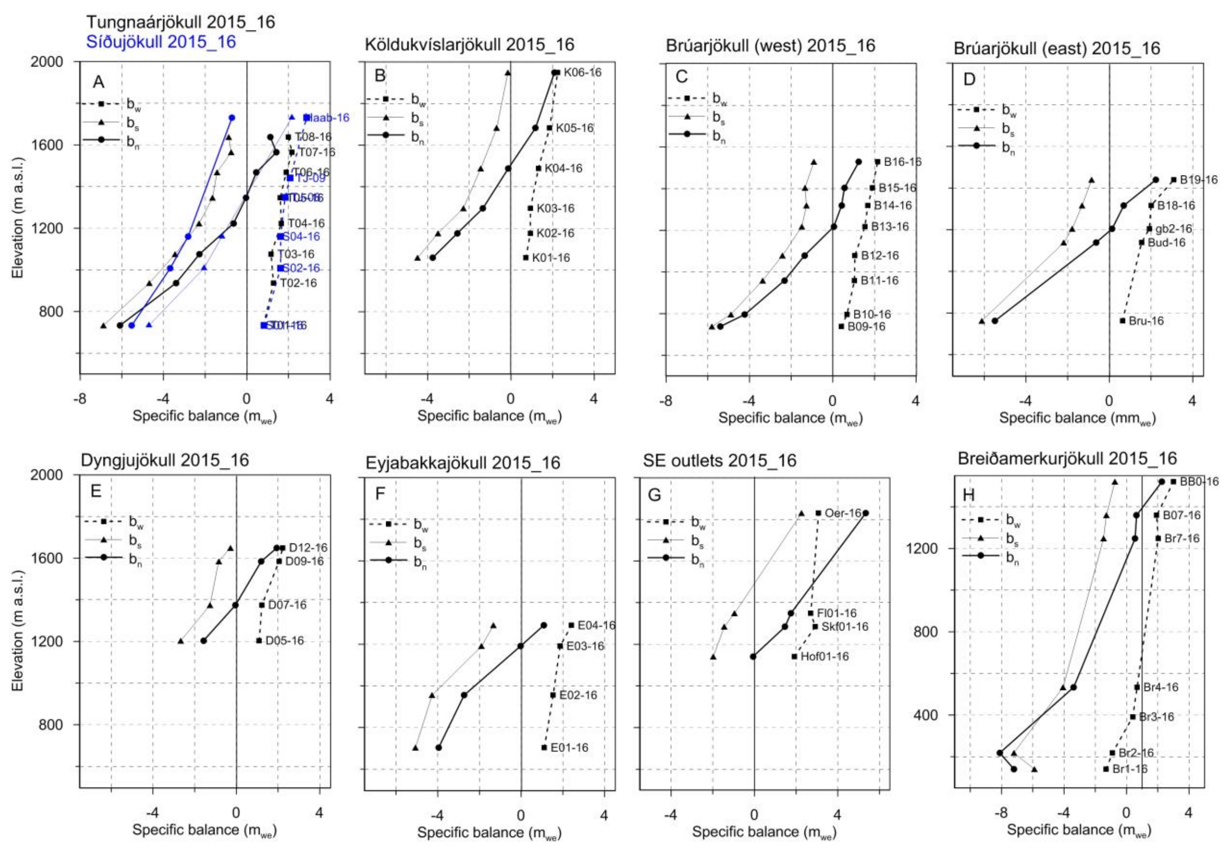

Figure 3b. Specific mass balance (m_{we}) 2015_16 as a function of elevation on central flow lines on Vatnajökull outlets.

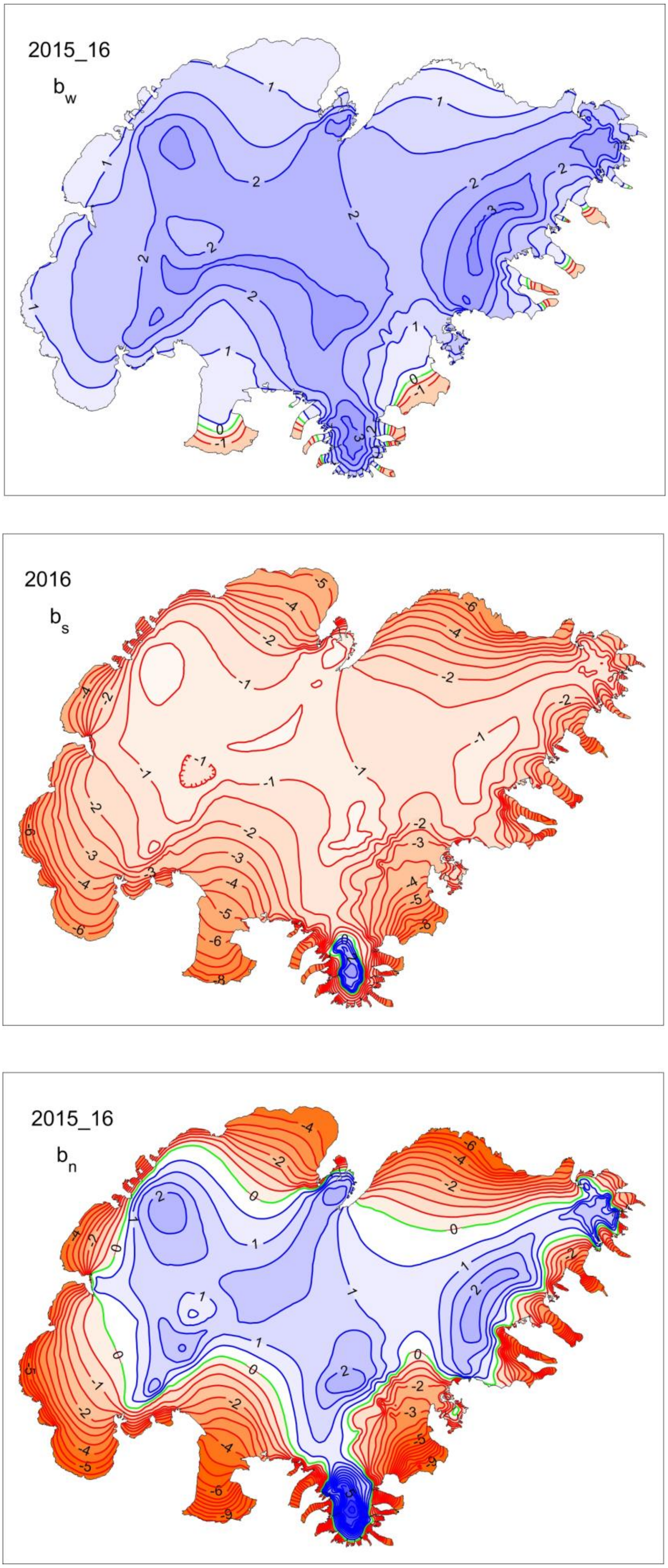

Figure 4. Specific mass balance (m_{we}) maps of Vatnajökull 2015_16. Top: winter, Centre: summer, Bottom: net balance.

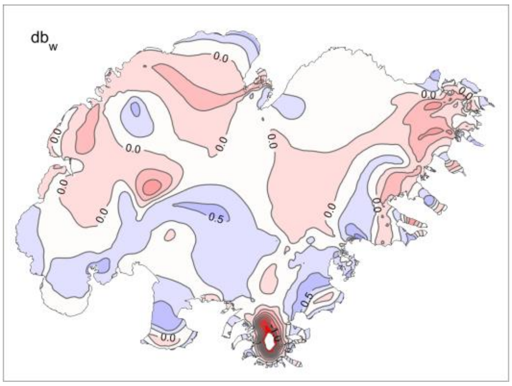

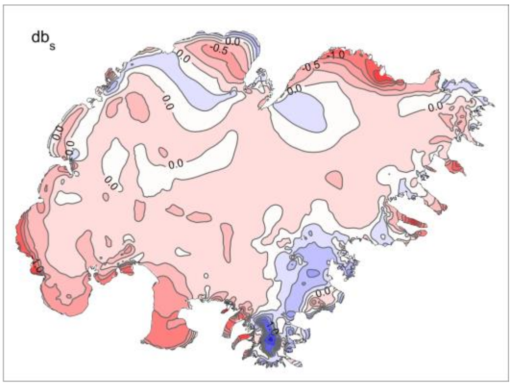

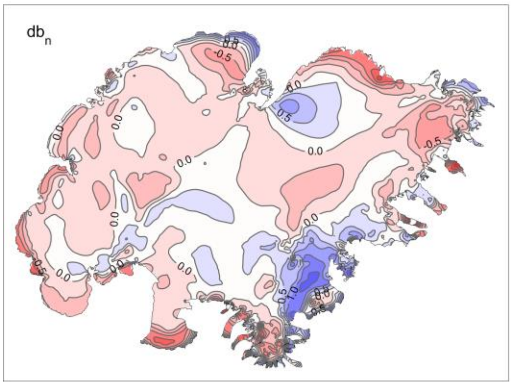

Figure 5. Top left: The difference between winter balance in 2015_16 and the average winter balance 1995_96 to 2014_15. Top right: The difference between summer balance in 2016 and the average summer balance 1996 to 2015. (Red is higher than average ablation). Lower left: The difference between net balance in 2015_16 and the average net balance 1995_96 to 2014_15. (Blue is higher than average balance and red lower).

A surface DEM is needed for surface area distribution and delineation of ice divides for individual outlets and catchments. A new surface DEM was created of Vatnajökull for this work. The DEM is mostly based on SPOT5 satellite images in 2010, and partly from LiDAR survey 2010, -11 and -12, but the large GPS profile set measured in spring 2015 was used to locally shift the older DEMs. This new representing the surface of 2015 was used in all area distributions, but ice and water divides were not reworked.

The autumn weather, 2015, was wet but not cold, the winter into March rather cold with average precipitation. The spring was relatively cold but dry.

Figure 5 (top left) shows that the winter accumulation is not far from average all over Vatnajökull. There is less than average winter snow in the higher accumulation zone, but higher than average in the mid elevation range of the south facing outlets.

Summer weather was extremely calm and mostly dry, but cloudy in the SE over Vatnajökull. The autumn was extremely warm, commonly accompanied with high wind. Melting at lower ablation zone extended well into October. This resulted in total melt more than average except in vicinity of Breiðamerkurjökull, where thicker than average winter snow and cloudy summer reduced the melt.

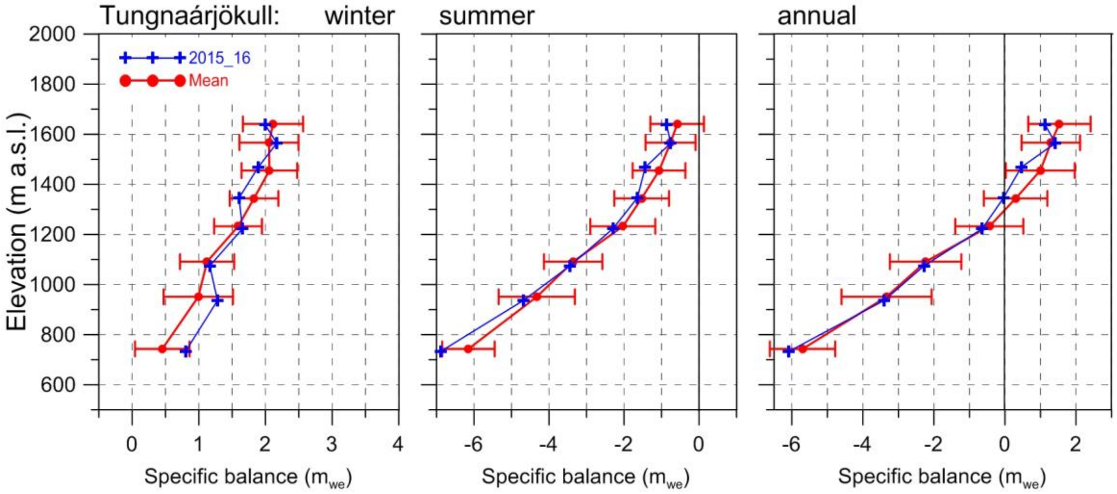

Figure 6. Mass balance at a central flow line of Tungnaárjökull 2015_16, and average mass balance 1991_92 to 2014_15.

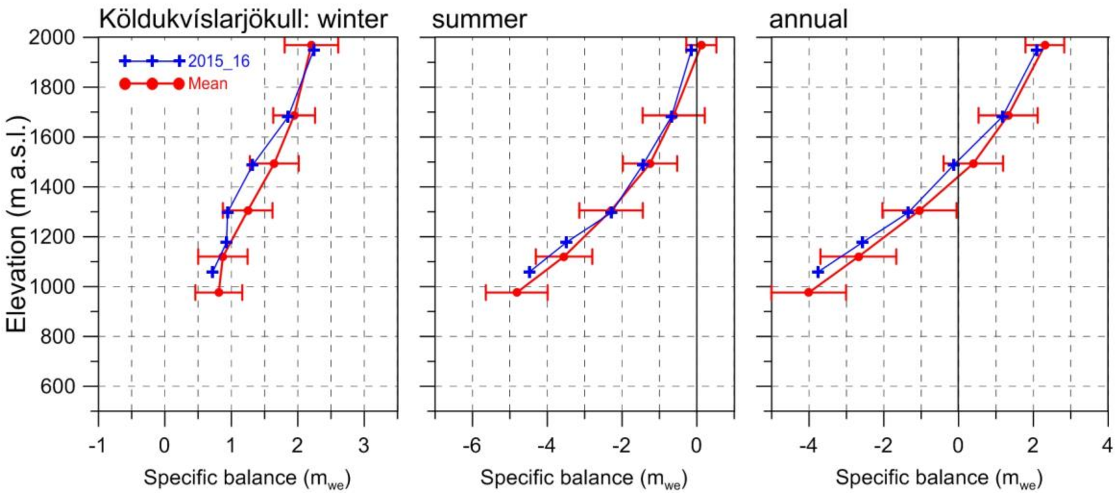

Figure 7. Mass balance at a central flow line of Köldukvíslarjökull 2015_16, and average mass balance 1991_92 to 2014_15.

3.2.1 Tungnaárjökull.

Area = 340 km^2
B_w= 0,52 $km^3{}_{we}$; b_w= 1,52 m_{we}
B_s = -1,00 $km^3{}_{we}$; b_s = -2,94 m_{we}
B_n = -0,48 $km^3{}_{we}$; b_n = -1,42 m_{we}
ELA = 1355 m a.s.l. (at profile)
AAR = 33 %
(The terms are defined at the foot of this page)

Variation of mass balance along a central flow line on Tungnaárjökull is shown in Fig. 6. The winter accumulation was close to average at all survey sites, except the lowest where it was ~1 std. over. The total winter balance was 3% over average. Summer melting was also close to average at all survey sites. At T08, T06 melting was enhanced due to dirt on the surface, but the almost one std. more melt at the lowest site is explained with extremely warm and windy condition in autumn. The summer balance was 13% more negative the average during the survey period. The net balance was more negative than on average by -0,3 m_{we}. This is the 22 year out 25 surveyed with negative net balance.

3.2.2 Köldukvíslarjökull

Area = 298 km^2
B_w = 0,41 $km^3{}_{we}$; b_w = 1,38 m_{we}
B_s = -0,60 $km^3{}_{we}$; b_s = -2,02 m_{we}
B_n = -0,19 $km^3{}_{we}$; b_n = -0,64 m_{we}
ELA = 1510 m a.s.l. (at profile)
AAR = 46 %

For each ice catchment basin, B_w, B_s and B_n are water equivalent volumes of winter, summer and net balance, ELA the equilibrium line altitude, and AAR is the accumulation area ratio.

Variation of mass balance along a central flow line on Köldukvíslarjökull is shown in Fig. 7. Accumulation was close to average except at the mid elevation sites (K03 and K04) where it was ~1 std. less than average. The total winter balance was about 94% of the average since 1991_92. Summer balance was almost average at all survey sites. In all, the summer balance was 4% more negative than in an average summer of the survey period. The net balance was slightly (-0,07m_{we}) more negative than in an average year.

3.2.3 Dyngjujökull

Area = 1059 km^2
B_w = 1,67 $km^3{}_{we}$; b_w= 1,57 m_{we}
B_s = -1,92 $km^3{}_{we}$; b_s = -1,81 m_{we}
B_n = -0,25 $km^3{}_{we}$; b_n = -0,24 m_{we}
ELA = 1385 m a.s.l. (at profile)
AAR = 60 %

Variation of mass balance along a flow line on Dyngjujökull is shown on Fig. 8. Mass balance is not measured at the lowest elevations, but assumed to be correlated (as a function of elevation) to that of Brúarjökull and Köldukvíslarjökull. The winter balance in 2015_16 was close to average at all sites except D07 at 1400 m a.s.l. where it was 1 std. less than average. This is similar as on both Tungnaárjökull and Köldukvíslarjökull. Inspection of the winter Modis images shown in appendix F suggest that at the glacier snout snow cover was very thin, In total the winter balance was at average. Summer balance was very close to average at all survey sites, and summer snow accumulation more than the melt at the highest site. The summer balance was 12% more negative than in an average summer. The net balance was slightly negative, now 0,2 m_{we} more negative than average during the survey. The AAR of 60% reflects this.
Dyngjujökull has often has had mass balance close to zero, and the net balance has been slightly positive in some years of the two decade period of continuous mass loss for Vatnajökull as a whole.

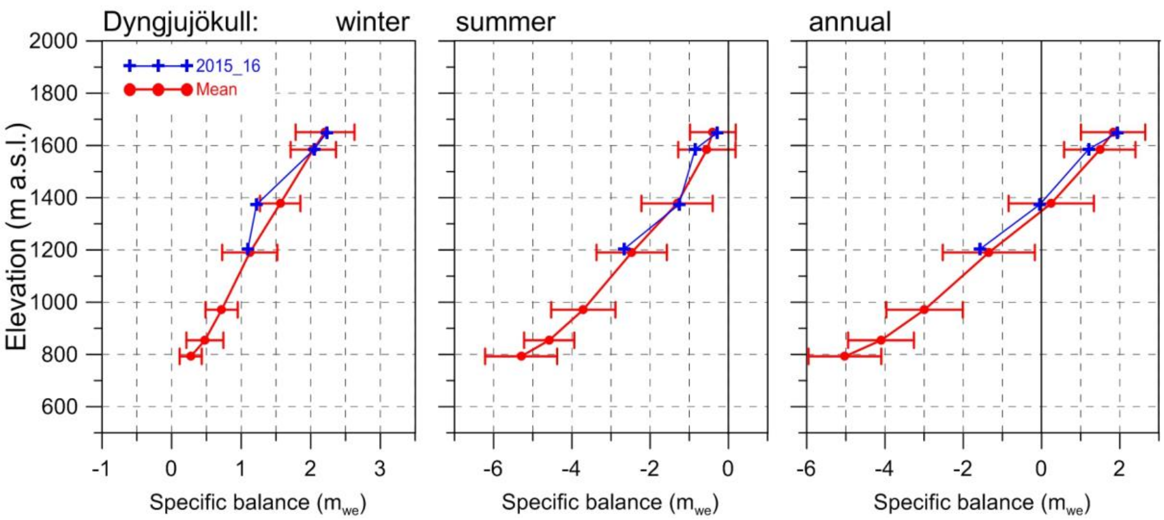

Figure 8. Mass balance at a central flow line on Dyngjujökull 2015_16, and average mass balance 1991_92 to 2014_15 (except 1998_99 – 2003_04 at all but the top elevation).

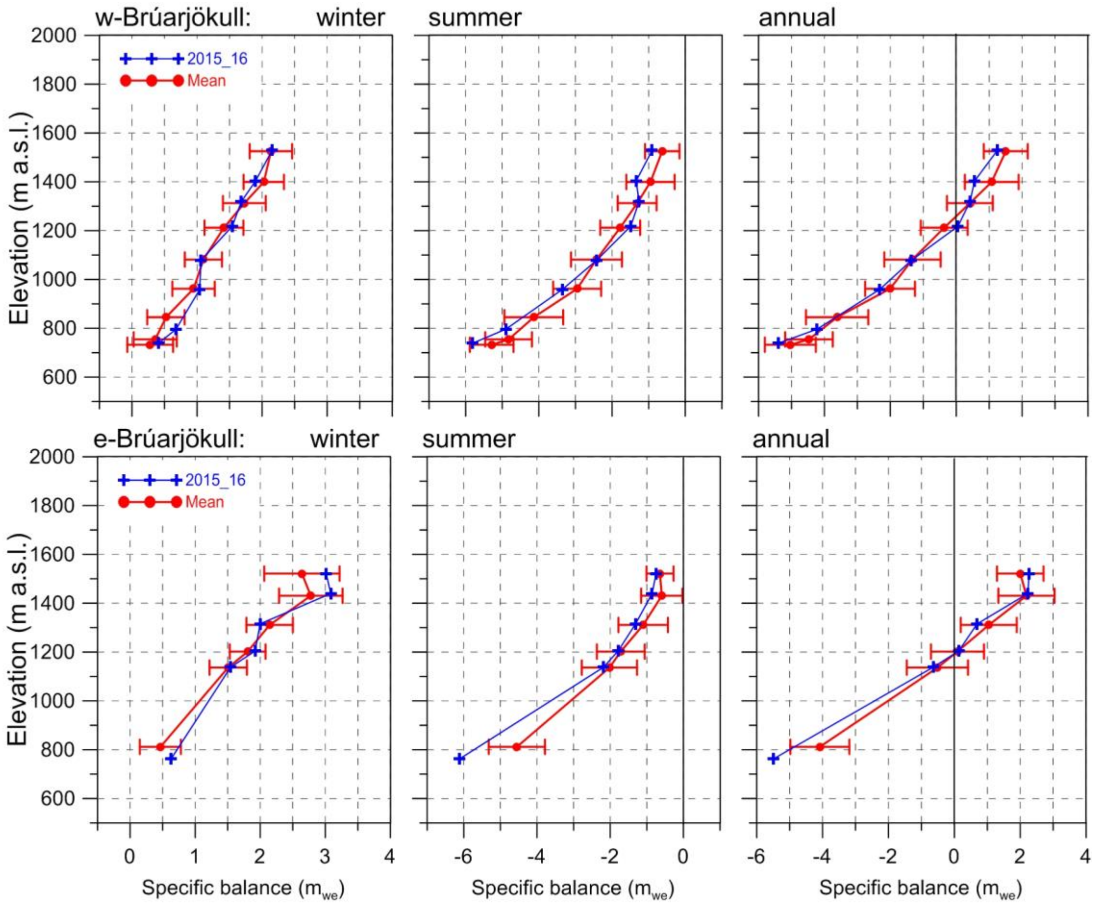

Figure 9. Mass balance at two flow lines on Brúarjökull 2015_16, and average mass balance 1992_93 to 2014_15.

3.2.4 Brúarjökull

Area = 1524 km^2
B_w = 2,55 $km^3{}_{we}$;b_w = 1,67 m_{we}
B_s = -3,07 $km^3{}_{we}$; b_s = -2,01 m_{we}
B_n = -0,52 $km^3{}_{we}$; b_n = -0,34 m_{we}
ELA = 1200 m a.s.l. (western flow line)
ELA = 1195 m a.s.l. (eastern flow line)
AAR = 61 %

Variation of mass balance along two flow lines on Brúarjökull is shown on Fig. 9. Accumulation was close to average at mid elevations survey sties, ~1/2 std. over average at the highest sites (on Breiðabunga) and the lowest sites. The winter balance was about 6% higher than average since 1991_92. Summer balance was close to average at all survey sites, except the highest and lowest where it exceeded the average by ½ to 1 std.. The summer balance was 6% more negative than in an average summer of the survey period. Surface dust enhanced melting at the topmost sites and the warm autumn at prolonged the melting season at the lowest sites. The net balance was negative very close to the average of the survey period.
During the survey period, there have been 6 years of positive balance but 18 years with negative balance.

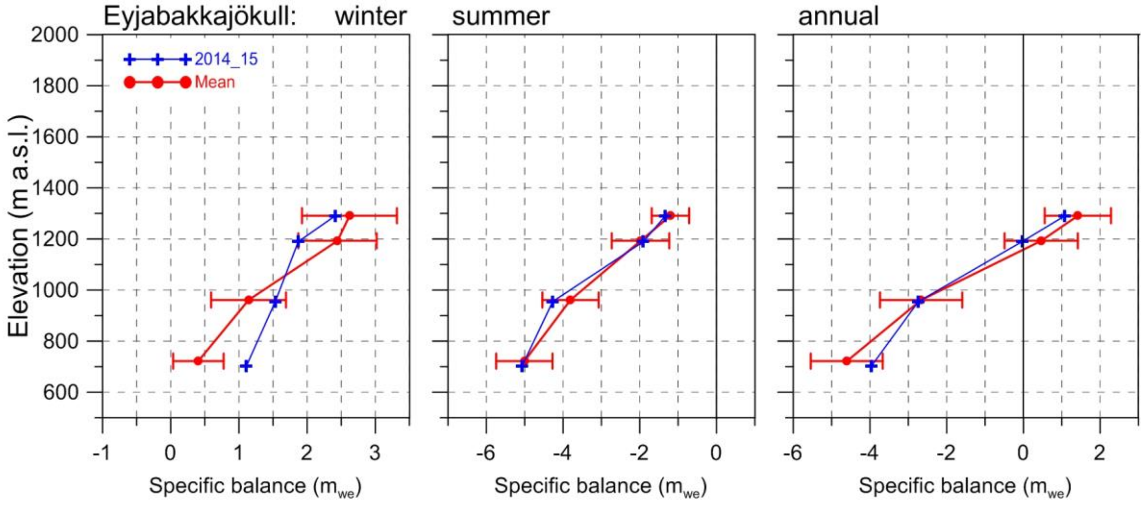

Figure 10. Mass balance at a central flow line of Eyjabakkajökull 2015_16 and average mass balance 1995_96 to 2014_15.

3.2.5 Eyjabakkajökull

Area = 112 km^2
B_w= 0,20 km^3 $_{we}$; b_w = 1,78 m_{we}
B_s = -0,30 km^3 $_{we}$; b_s = -2,71 m_{we}
B_n = 0,10 km^3 $_{we}$; b_n = -0,93 m_{we}
ELA = 1192 m a.s.l. (at profile)
AAR = 37 %

Variation of mass balance along a central flow line on Eyjabakkajökull is shown on Fig. 10. Accumulation was close to 1 std. more than average at the 2 lower sites, reflecting cold latter half of winter (no melting, and snow rather than rain in precipitation events), but much less than average at the two higher sites. The total winter balance 2015_16 was almost same as the average 1995_96 to 2014_15. Summer melting was not far from average at all survey sites. There was slight mass loss at the upper sites but as expect the unusually thick snow on the snout resulted in net balance less negative than average. In total the net balance was at average.

3.2.6 Breiðamerkurjökull

Area = 936 km^2
B_w = 1,50 km^3$_{we}$; b_w = 1,60 m_{we}
B_s = -2,18 km^3$_{we}$; b_s = -2,33 m_{we}
B_n = -0,68 km^3$_{we}$; b_n= -0,73 m_{we}
ELA = 1150 m a.s.l. (at profile)
AAR = 55 %

Variation of mass balance along a central flow line on Breiðamerkurjökull is shown on Fig. 11.

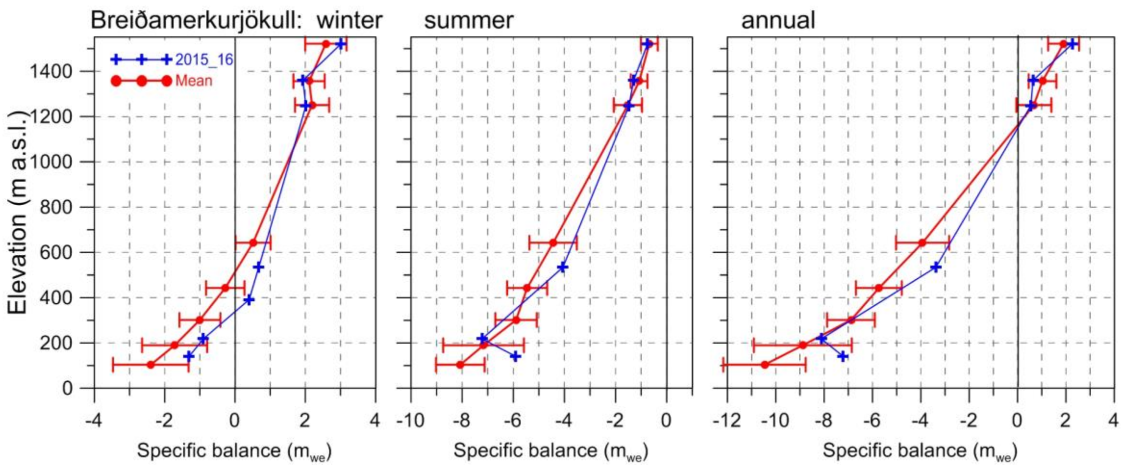

Figure 11. Mass balance at a central flow line of Breiðamerkurjökull 2015_16, and average mass balance 1995_96 to 2014_15.

Winter accumulation was well over average at the highest station (Breiðabunga), but close average at the other two accumulation survey sites. At the lowest sites the relatively cold winter is reflected in about 1 std. less mass loss in winter. The total winter balance was ~12% over average. Summer balance was average at the tope sites, but ~1 std less mass loss ata the lower sites. At Bre2 much more melt was measured than at the lowest; we think this is not typical for this elevation on Breiðamerkurjökull; the site is now biased (more melt) by dirt from the nearby Mávabyggða moraine. The total negative summer balance was only 90% of the average during the survey period. The net balance was ~0,4 m_{we} less negative than in an average year.

3.2.7 Síðujökull

Area = 423 km^2
B_w= 0,69 $km^3{}_{we}$; b_w = 1,64 m_{we}
B_s = -1,34 $km^3{}_{we}$; b_s = -3,16 m_{we}
B_n = -0,64 $km^3{}_{we}$; b_n= -1,52 m_{we}
ELA = 1361 m a.s.l. (at profile)
AAR = 35 %

Variation of mass balance along a central flow line on Síðujökull is

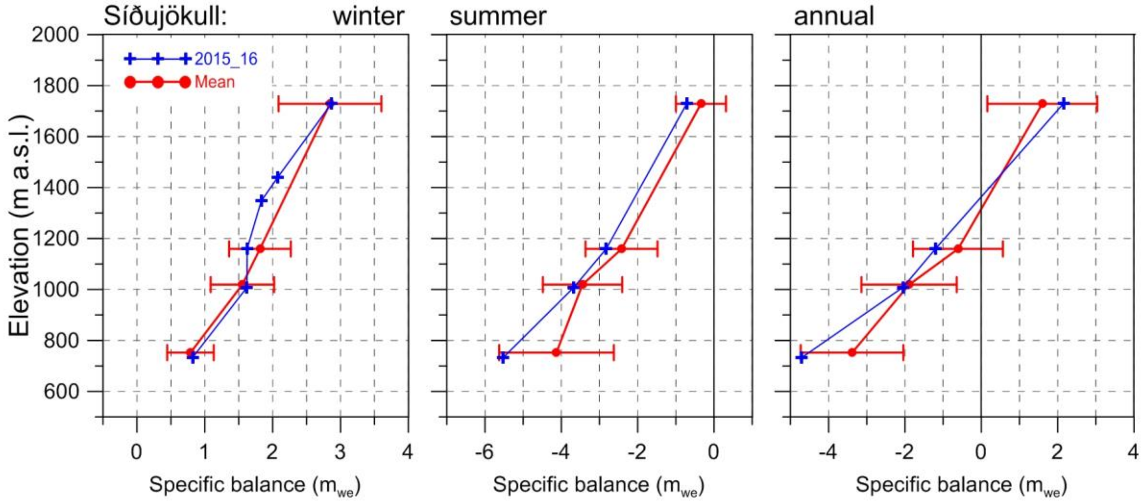

Figure 12. Mass balance at a central flow line of Síðujökull 2015_16, and average mass balance 2004_05 to 2014_15.

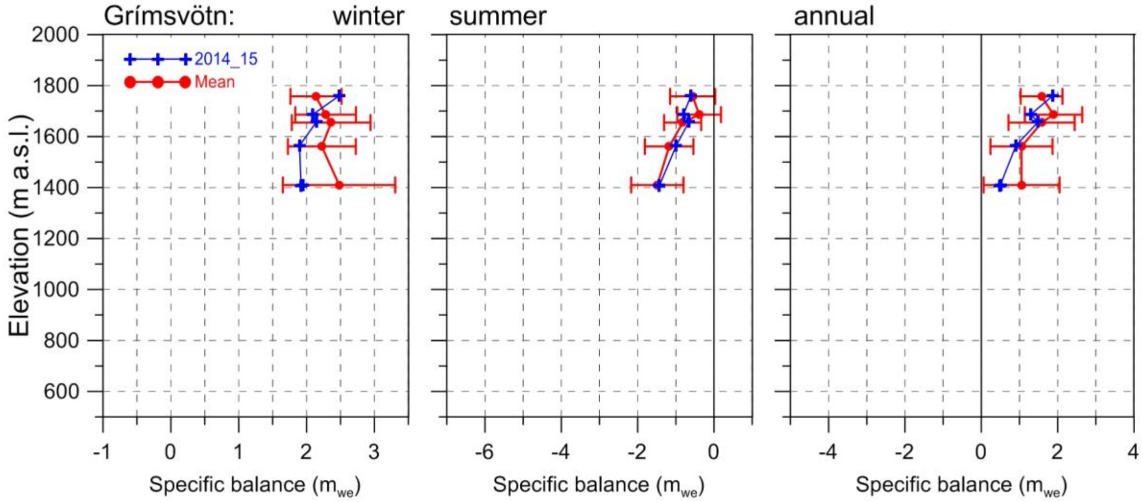

Figure 13. Mass balance at a central flow line towards Grímsvötn 2015_16, and average mass balance 1991_92 to 2014_15.

shown on Fig. 12. Snow accumulation close to average at all sites. Two extra sites were surveyed in the JÖRFI spring trip. The total winter balance was 8% over the average (past decade). Summer balance was slightly over average, except at the lowest site where ablation was 1 std. over. The total summer balance was 8% more negative than the average during the survey period. The net balance slightly was more negative than average (by -0,1 m_{we}).

3.2.6 Grímsvötn-Gjálp

Area = 174 km^2
B_w = 0,36 km^3_{we}; b_w = 2,07 m_{we}
B_s = -0,15 km^3_{we}; b_s = -0,87 m_{we}
B_n = 0,21 km^3_{we}; b_n= 1,20 m_{we}

Variation of mass balance close to a central flow line from Bárðarbunga towards Grímsvötn center is shown in Fig. 13. Snow accumulation varied from about 0,75 std. less than average at the lowest site up to +1 std. at the highest. The total winter balance was 91% of average. Summer balance was close to average at most survey sites except one, and in total mass loss was 15% over average. The net balance was positive but only 80% of the average of the survey period.

3.3 The mass balance record for Vatnajökull.

From the digital maps the total volumes of winter, summer and net balance for Vatnajökull (and selected outlets) have been calculated by integration (appendix D, gives balance values as a function of elevation) and are as follows:

B_w = 13,23 km^3_{we} ; b_w = 1,66 m_{we}
B_s = -17,89 km^3_{we} ; b_s = -2,25 m_{we}
B_n = -4,65 km^3_{we} ; b_n = -0,59 m_{we}
AAR = 55%

The autumn of 2015 was wet and windy, followed by a winter colder than average this century. In winter the precipitation in NE and E Iceland was over average reflecting snowfall in E, and NE wind directions. The spring weather was calm, and unusually dry. The total winter balance was 5% higher than average (over the observation period from 1991_92, Fig. 14). The zero mass balance turnover for Vatnajökull (current topography) is close to 13,5 km^3_{we} (1,7 m_{we}) and the winter balance 2015_16 is ~3% lower. In spite of an extremely calm and dry summer in Iceland, on Vatnajökull most of the summer was cloudy, less than 1/3 of the summer-days were

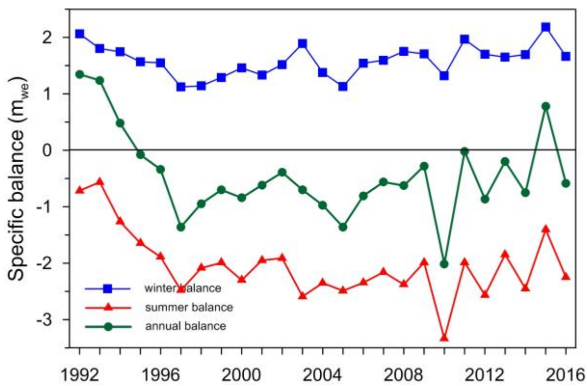

Figure 14. Specific mass balance record for Vatnajökull 1991_92 – 2015_16.

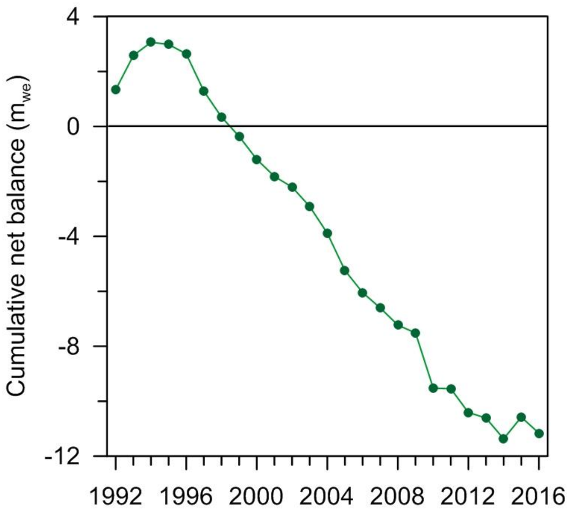

Figure 15. Cumulative specific mass balance of Vatnajökull 1991_92 – 2015_16.

close to cloud free (see Modis images in Appendix F). Latter half of September and first weeks of October were unusually favorable for ablation both warm and windy. The total summer balance was more negative by ~2% than on average since 1995. As mentioned above, zero mass balance turnover for Vatnajökull (current topography) is close to 13,5 km^3_{we} (1,7 m_{we}), the summer balance 2016 was 17,89 km^3_{we} or ~33 % more than the zero balance turnover. The net balance was negative as it has been since 1994_95 (except 2014_15), mass loss was close to average, 0.1 m_{we} less negative than average since 1994_ 95.

The temporal variability of mass balance for different outlets is shown in Fig. 16. The greatest variability of the winter balance is for Eyjabakkajökull the eastern most of the studied outlets. This part of the glacier is receives precipitation from

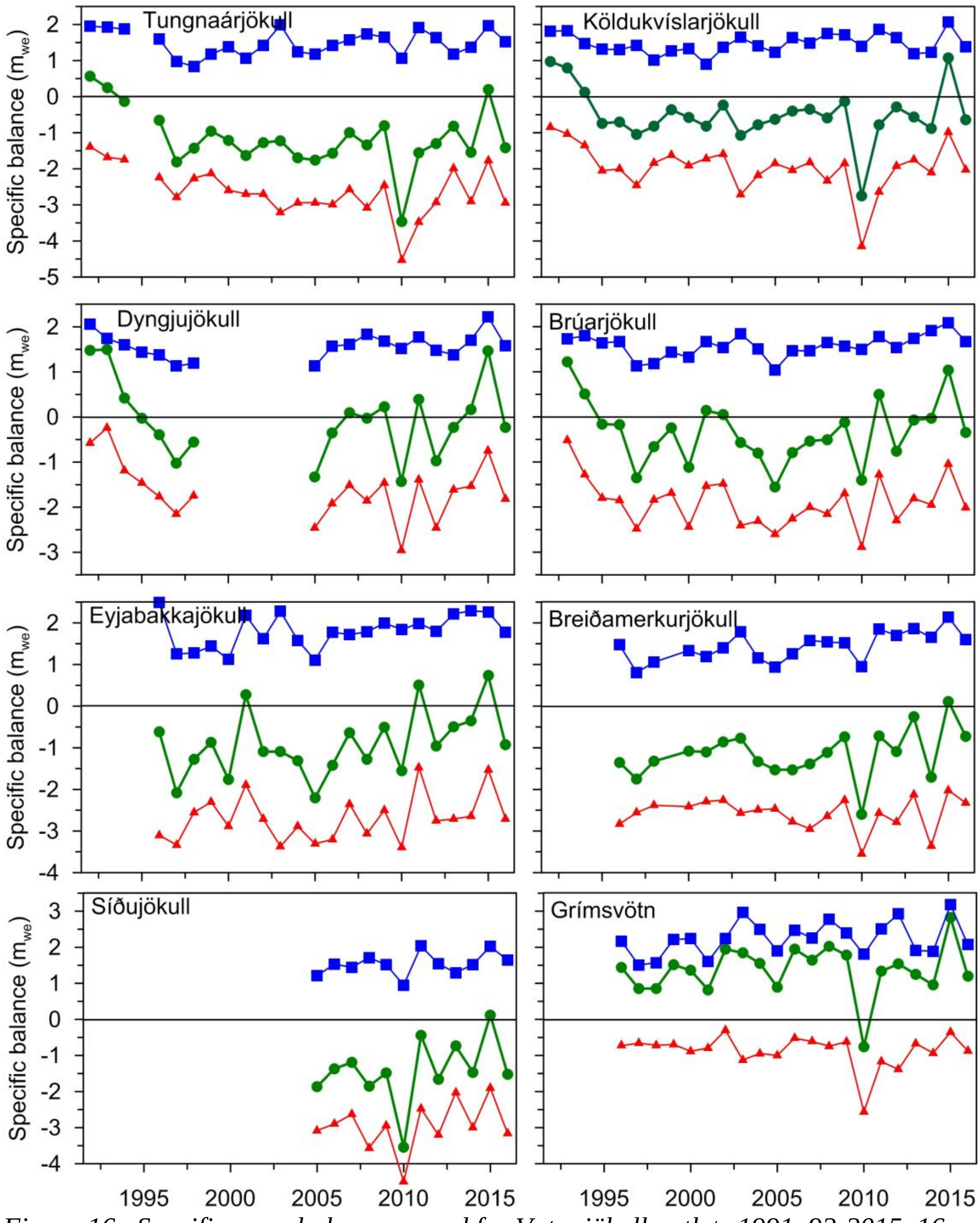

Figure 16. Specific mass balance record for Vatnajökull outlets 1991_92-2015_16.

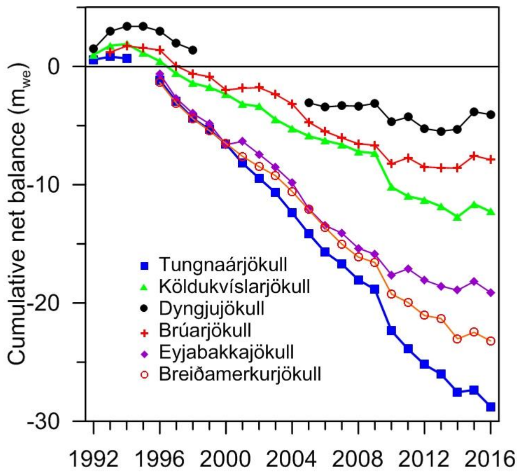

Figure 17. Cumulative specific mass balance for several of Vatnajökull outlets 1991_92 – 2015_16.

all south- and east- and north-easterly wind directions, and thus has high snow accumulation in winters when the paths of the North Atlantic lows are just east of Iceland. This is also the case for the eastern part of Brúarjökull. During the period of net mass loss since 1994_95, the northern outlets have had several years of close to zero and positive mass balance.

The cumulative net balance curves for the outlets of Vatnajökull in Fig. 17 show that all outlets have been losing mass since 1994_95. The slope for mass loss is about 0,7 $m_{we}a^{-1}$ for the northern outlets but 1,5 $m_{we}a^{-1}$ for the south and western outlets.

In Fig. 18 the relation of the annual net balance to the accumulation area ratio (AAR) and equilibrium line altitude (ELA) is shown for different outlets over the survey period. The b_n-AAR gradient is similar for all outlets, about 0,5 m_{we} for 10% change in AAR. The zero-balance AAR varies for different outlets from about 60-65%, similar for all outlets except for the southern outlet Breiðamerkurjökull.

Breiðamerkurjökull is far from equilibrium, the ablation area is too large. A large part of the glacier has carved 200-300 m through the former sediment bed, and the surface elevation has lowered accordingly. Breiðamerkurjökull is now retreating at a high rate.

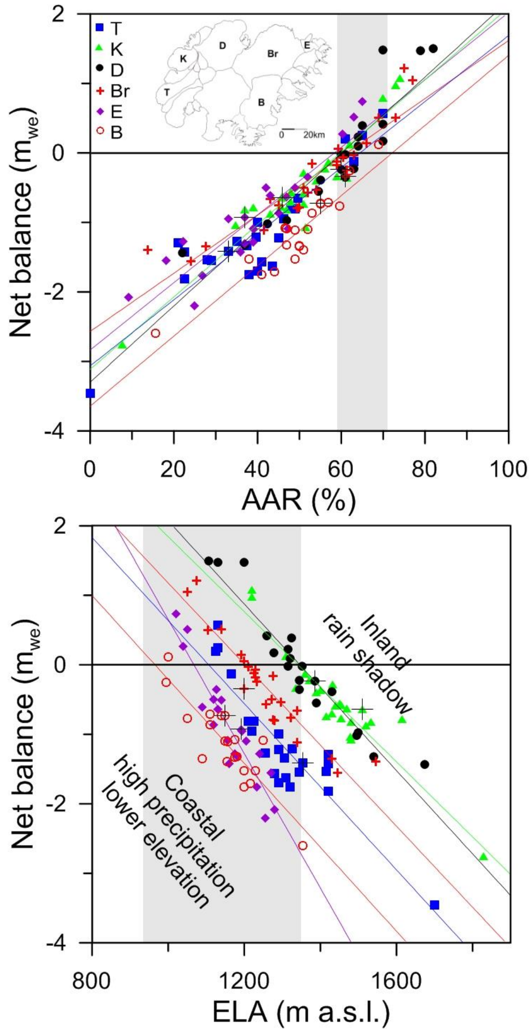

Figure 18. The relation between net annual balance (b_n) and accumulation area ratio (AAR)(upper) and b_n and equilibrium line altitude (ELA), for Vatnajökull outlets during the survey period. (This years points are marked with a black +).

Similarly the zero-balance ELA varies from about 1000-1100 m a.s.l. for the southern outlets to 1400 m a.s.l. for the NW outlets. The b_n-ELA slope is similar for all outlets -0,7 m_{we} per 100 m, except Eyjabakkajökull with a slope of -1 m_{we} per 100.

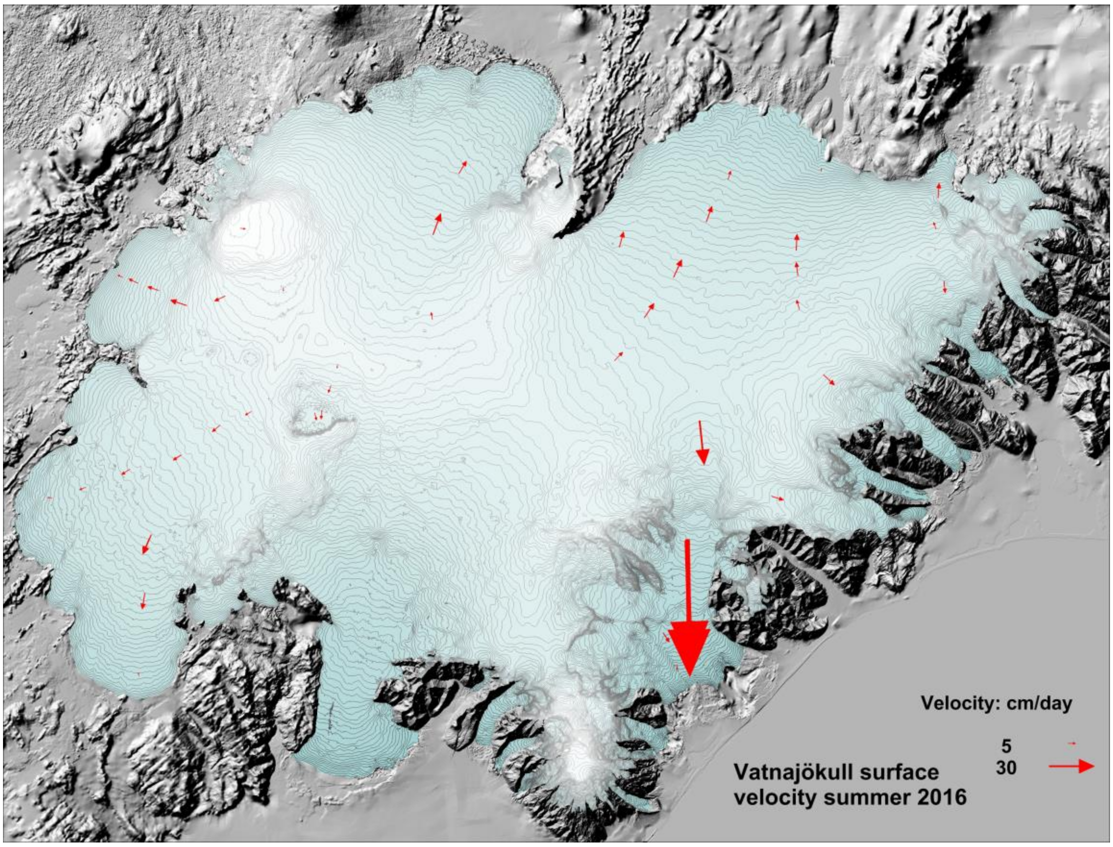

Figure 19. Average surface velocity at survey sites in 2015_16.

4. SURFACE VELOCITY MEASUREMENTS

The surface velocity of the glacier was calculated from DGPS (accuracy within 1 m), fast static (accuracy about 1 cm) and kinematic GPS (accuracy about 3 cm) positioning of the ablation stakes. All sites were surveyed in spring and autumn (most kinematic, some DGPS), and many also in June (kinematic), August (fast static) and October (kinematic). At a few sites stakes from previous years were found and resurveyed, making it possible to calculate surface velocity over a year or longer time span. The average summer surface velocity is shown on Figure 19.

At sites close to the glacier edge very small horizontal movement is measured. This indicates that the glacier snouts are almost stagnant. In the centre areas of some of the outlets especially close to the equilibrium line, there is an increase in velocity during summer compared to winter. The summer velocity is of the order of two-fold the winter velocity. This suggests that basal sliding is increased in the melting season, and is of the same magnitude as the deformation velocity.

To better understand this continuous GPS has been run during summer at several sites.

From previous velocity measurements, surging of outlets has been predicted. No signs of a starting surge are seen from this year’s survey.

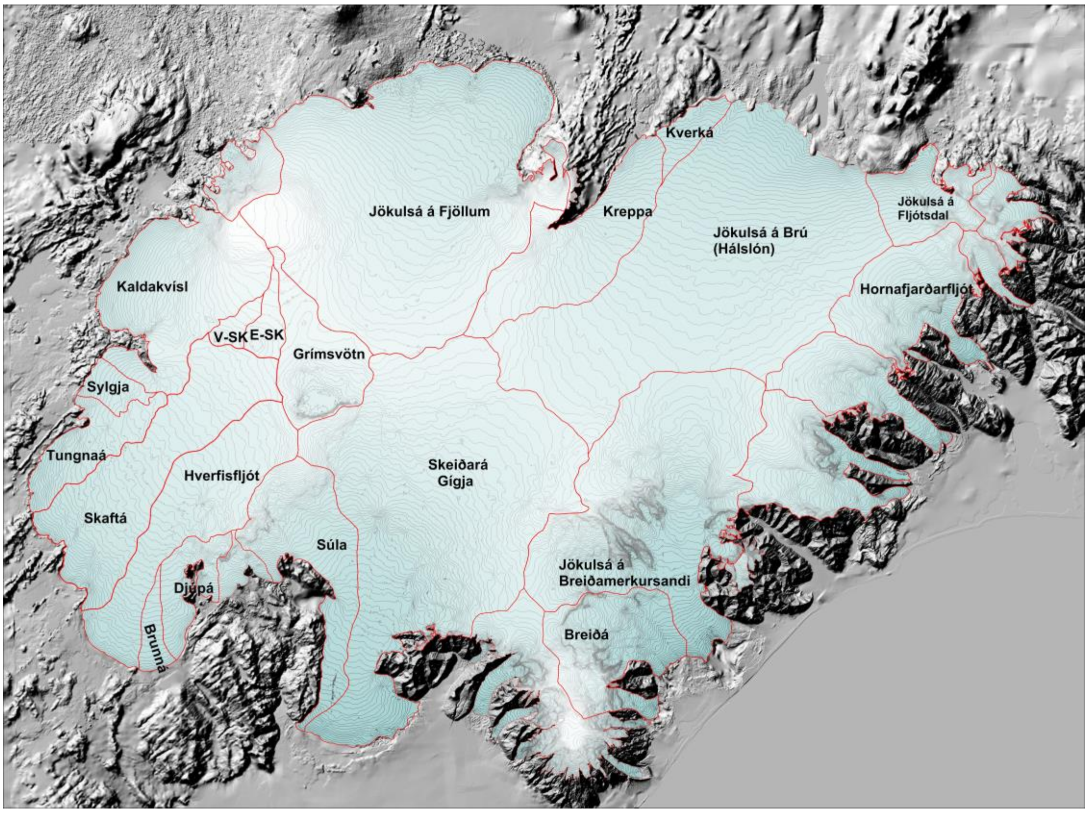

Figure 20. Water divides and drainage basins of selected rivers draining water from Vatnajökull.

5. Melt water runoff.

Water divides and drainage basins for rivers draining water from Vatnajökull have been defined from water pressure potential maps. The potential maps were produced from existing surface (year 2010) and bedrock digital elevation models.

Figure 20 shows the water divides and drainage areas for selected rivers draining melt water from Vatnajökull. The summer balance over the water basin is an estimate of meltwater contribution to rivers and groundwater storage. This estimate, however, does not include precipitation that falls as rain on the glacier, nor snow which falls and melts during the summer. The meltwater contribution can be compared with river runoff at stream flow gauges closest to the glacier. For this comparison, we define the glaciological year from the start of October to the end of September and the period draining meltwater from the glacier during the summer from June through September. It would be misleading to include May in the summer period because runoff from

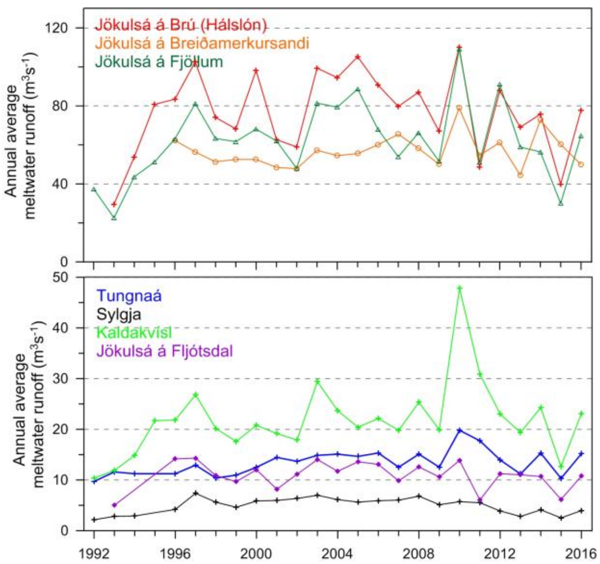

Figure 21. The temporal variation of average annual meltwater runoff to selected river catchments.

Table I. Melt water drainage to selected rivers.

Water Catchment:	Area (km^2)	ΣQ_s ($10^6 m^3$)	Q_s (m^3s^{-1})	Q_a (m^3s^{-1})	q_s ($ls^{-1}km^{-2}$)
Vatnajökull	7968,0	17971,7	1705,0	569,9	72,2
Tungnaá	121,8	478,3	45,4	15,2	127,5
Sylgja	39,7	124,8	11,8	4,0	100,4
Kaldakvísl	367,9	729,2	69,2	23,1	63,4
Jokulsa a Fjöllum	1188,3	2041,1	193,6	64,7	56,0
Kreppa	291,2	430,2	40,8	13,6	46,9
Kverka	47,0	213,2	20,2	6,8	144,8
Jokulsa a Brú	1214,8	2450,1	232,4	77,7	64,0
Jökulsá á Fljótsdal	130,6	339,8	32,2	10,8	82,4
Jökulsá í Lóni	101,3	243,4	23,1	7,7	76,2
Hornafjarðarfljót	239,1	585,5	55,5	18,6	77,7
Jökulsá á Breiðamerkursandi	739,5	1574,1	149,3	49,9	67,7
Breiðá-Fjallsá	234,6	740,8	70,3	23,5	109,6
Skeiðará-Gígja	1165,2	2565,9	243,4	81,4	70,5
Súla	255,8	826,7	78,4	26,2	103,7
Brunná	35,8	182,5	17,3	5,8	165,8
Djúpá	83,7	315,5	29,9	10,0	126,6
Hverfisfljót	317,7	804,8	76,4	25,5	80,9
Skaftá	394,9	1105,2	104,8	35,0	89,9
Grímsvötn	173,3	149,8	14,2	4,8	27,4
Eystri Skaftárketill	39,4	24,5	2,3	0,8	19,8
Vestari Skaftárketill	25,1	16,8	1,6	0,5	21,2
Hólmsá	164,9	403,5	38,3	12,8	77,6
Heinabergsvötn	229,6	604,6	57,4	19,2	83,5
Skjálfandafljót	71,9	135,2	12,8	4,3	44,1

ΣQ_s: total summer melt water; Q_s: average runoff (averaged over summer, 4 months, June – September)
Q_a: average runoff (averaged over a whole year); q_s : average runoff per km^2 (averaged over a whole year)

the glacier melt in May is delayed due to refreezing during elimination of the cold wave and because of the contribution of the spring melt from the highlands to the runoff. Some melting also occurs during winter, especially in the low snouts of the southern outlets.

Average melt water runoff to different rivers is given in Table I, and temporal variation of the average meltwater runoff in Fig. 21. The average specific runoff (q_s) differs from basin to basin from 21 to 165 $ls^{-1}km^{-2}$. This is mainly due to different elevation distributions, for example, the water drainage basins for Tungnaá and Kverká are within the ablation area, while that of Grímsvötn and Skaftárkatlar are high in the accumulation zone.

6. Conclusions

The autumn of 2015 was wet and windy, followed by a winter colder than average this century. In winter the precipitation in NE and E Iceland was over average, reflecting snowfall in E, and NE wind directions. The spring weather was calm, and unusually dry. In spite of an extremely calm and dry summer in Iceland, on Vatnajökull most of the summer was cloudy, less than 1/3 of the summer-days were close to cloud free (see Modis images in Appendix F). Latter half of September and first weeks of October were unusually favorable for ablation both warm and windy. The total winter balance was 5% higher than average (over the observation

period from 1991_92.
The total summer balance was more negative than on average since 1995 by ~2%. The net balance was negative as it has been since 1994_95 (except 2014_15); the mass loss was close to average, 0,1 m_{we} less negative than average since 1994_ 95.
The total mass loss over the 25 year survey period is 11,2 m_{we} (ice volume of ~99 km^3) since 1991_92 (or since 1994_95, 14,2 m_{we} (ice volume of 126 km^3)). The volume loss since 1991_92 amounts to ~3% of total ice volume (~4% since 1994_95).
Glacier meltwater runoff in summer 2016 (estimated from summer balance only, summer rain and snow that falls and melts during summer is not included; averages refer to the survey period of each outlet): to Tungnaá 14% over average, 6 % over average to Kaldakvísl, 4% over average to Jökulsá á Fjöllum, 1% over average to Hálslón, 98% of average to Jökulsá í Fljótsdal and 88% of average to Jökulsá á Breiðamerkursandi.

Mass balance summary 2015_16:

B_w = 13,23 km^3_{we}
B_s = -17,89 km^3_{we}
B_n = -4,65 km^3_{we}

AAR = 55%

Specific Values:

b_w = 1,66 m_{we}
b_s = -2,25 m_{we}
b_n = -0,59 m_{we}

Appendix A: Mass balance at measurement sites 2015_16.

b_w: specific winter balance, **b_s**: specific summer balance, **b_n**: specific net balance,
l_a: new snow in autumn (all in water equivalent).

Site	Position				Elevation	Date	Date	b_w	b_s	b_n	la
	Latitude		Longitude		(m a.s.l.)	in spring	in autumn	(m)	(m)	(m)	(m)
B09-16	64	45,049	16	5,458	738,2	20160507	20161011	0,410	-5,810	-5,400	0,035
B10-16	64	43,687	16	6,698	796,1	20160507	20161011	0,678	-4,899	-4,221	0,035
B11-16	64	40,944	16	10,494	959,2	20160507	20161011	1,040	-3,362	-2,322	0,070
B12-16	64	38,266	16	14,124	1078,9	20160507	20161011	1,060	-2,419	-1,359	0,070
B13-16	64	34,526	16	19,705	1218,2	20160507	20161011	1,540	-1,490	0,050	0,063
B14-16	64	31,634	16	24,699	1319,3	20160507	20161010	1,681	-1,261	0,420	0,140
B15-16	64	28,488	16	30,016	1403,4	20160506	20161011	1,899	-1,341	0,558	0,140
B16-16	64	24,119	16	40,848	1528,7	20160507	20161014	2,153	-0,905	1,248	0,315
B17-16	64	36,735	16	28,796	1215,0	20160507	20161010	1,770	-1,710	0,060	0,053
Br1-16	64	5,840	16	19,721	140,8	20160508	20161009	-1,305	-5,904	-7,209	0,000
Br2-16	64	6,380	16	22,540	218,1	20160508	20161009	-0,900	-7,220	-8,120	
Br3-16	64	8,489	16	24,076	391,6	20160508		0,400			
Br4-16	64	10,883	16	20,185	533,6	20160508	20161010	0,675	-4,059	-3,384	0,000
Br7-16	64	22,144	16	16,941	1247,9	20160508	20161010	2,020	-1,474	0,546	0,116
B07-16	64	25,786	16	17,456	1359,1	20160508	20161010	1,930	-1,290	0,640	0,123
BB0-16	64	22,715	16	5,054	1520,9	20160508	20161010	3,014	-0,748	2,266	0,280
Bru-16	64	41,003	15	55,225	762,3	20160507	20161010	0,628	-6,118	-5,490	0,021
Bud-16	64	35,990	15	59,876	1138,1	20160507	20161010	1,543	-2,182	-0,639	0,333
gb2-16	64	34,106	16	0,010	1204,6	20160507	20161010	1,920	-1,788	0,132	0,070
B18-16	64	31,583	16	0,128	1315,5	20160507	20161010	1,998	-1,308	0,690	0,116
B19-16	64	27,994	15	55,978	1439,8	20160508	20161010	3,086	-0,854	2,232	0,137
BB0-16	64	22,715	16	5,054	1520,9	20160508	20161010	3,014	-0,748	2,266	0,280
D05-16	64	42,246	16	54,648	1204,0	20160506	20161014	1,096	-2,662	-1,566	0,060
D07-16	64	38,292	16	59,231	1374,5	20160506	20161014	1,221	-1,263	-0,042	0,067
D09-16	64	31,810	17	0,558	1585,1	20160506	20161014	2,049	-0,850	1,199	0,245
D12-16	64	28,967	17	0,143	1649,6	20160506	20161014	2,228	-0,284	1,944	0,231
E01-16	64	41,062	15	34,096	703,0	20160508	20161010	1,110	-5,070	-3,960	0,035
E02-16	64	39,135	15	35,978	955,2	20160508	20161010	1,533	-4,269	-2,736	0,035
E03-16	64	36,664	15	36,913	1190,1	20160508	20161010	1,870	-1,905	-0,035	0,070
E04-16	64	34,953	15	37,090	1290,4	20160508	20161010	2,412	-1,332	1,080	0,123
K01-16	64	35,163	17	51,799	1058,7	20160506	20161015	0,719	-4,481	-3,762	0,000
K02-16	64	34,812	17	49,678	1177,1	20160506	20161015	0,926	-3,500	-2,574	0,035
K03-16	64	34,248	17	46,402	1296,7	20160506	20161015	0,940	-2,290	-1,350	0,042
K04-16	64	33,205	17	42,266	1488,4	20160506	20161015	1,321	-1,447	-0,126	0,231
K05-16	64	33,447	17	35,435	1682,0	20160506	20161015	1,856	-0,680	1,176	0,284
K06-16	64	38,352	17	31,366	1949,4	20160605	20161016	2,238	-0,144	2,094	0,385
K07-16	64	29,118	17	42,034	1534,6	20160506	20161015	1,785	-1,023	0,762	0,305
S01-16	64	7,012	17	49,975	733,2	20160504	20161015	0,820	-5,521	-4,701	0,035
S02-16	64	12,166	17	48,961	1008,7	20160504	20161015	1,620	-3,672	-2,052	0,074
S04-16	64	16,174	17	48,206	1160,2	20160504	20161015	1,624	-2,821	-1,197	0,095
Haab-16	64	20,974	17	24,116	1730,9	20160608	20161016	2,870	-0,710	2,160	0,875

T01-16	64	19,487	18	8,228	733,4	20160503	20161016	0,802	-6,886	-6,084	0,000
T02-16	64	19,599	18	3,964	937,0	20160503	20161016	1,280	-4,682	-3,402	0,035
T03-16	64	20,207	17	58,592	1074,9	20160504	20161016	1,165	-3,442	-2,277	0,109
T04-16	64	21,329	17	51,482	1223,5	20160504	20161016	1,655	-2,294	-0,639	0,182
T05-16	64	22,273	17	42,984	1345,9	20160504	20161015	1,603	-1,645	-0,042	0,238
T06-16	64	24,268	17	36,521	1468,2	20160504	20161016	1,889	-1,433	0,456	0,354
T07-16	64	25,290	17	31,185	1564,8	20160505	20161016	2,170	-0,754	1,416	0,455
T08-16	64	26,284	17	27,755	1638,1	20160505	20161016	1,995	-0,867	1,128	0,490
Borth-16	64	25,072	17	19,161	1410,0	20160508	20161016	1,950	-1,440	0,510	0,385
Bor-16	64	24,944	17	20,143	1406,0	20160606	20161016	1,920	-1,434	0,486	0,315
G02-16	64	26,849	17	17,718	1563,7	20160608	20161015	1,897	-0,991	0,906	0,315
G03-16	64	28,451	17	16,345	1658,0	20160608	20161015	2,144	-0,656	1,488	0,315
G04-16	64	30,027	17	15,048	1687,0	20160608	20161015	2,089	-0,799	1,290	0,343
Go1-16	64	33,973	17	24,939	1760,0	20160605	20161015	2,479	-0,607	1,872	
Hof01-16	64	32,307	15	35,843	1141,5	20160508	20161010	1,916	-1,979	-0,063	0,175
Skf01-16	64	17,995	16	4,979	1284,1	20160509	20161010	2,920	-1,450	1,470	0,238
Fl01-16	64	26,164	15	55,628	1348,6	20160508	20161010	2,700	-0,954	1,746	0,140
Barc-16	64	38,410	17	26,676	1879	20160605	20160000	2,750			
TJ-01	64	8,972	17	3,118	857,6	20160605	20160000	1,120			0,462
TJ-02	64	9,690	17	4,038	882,2	20160605	20160000	1,200			0,315
TJ-06	64	11,593	17	2,533	958,6	20160606	20160000	1,620			
TJ-03	64	12,890	17	2,723	996,6	20160605	20160000	2,020			0,455
TJ-07	64	17,001	17	18,991	1063,6	20160606	20160000	1,500			0,385
TJ-05	64	18,445	17	13,163	1142,0	20160606	20160000	1,503			
TJ-04	64	19,950	17	10,157	1251,6	20160606	20160000	2,050			
Ske01	64	21,357	16	56,143	1401	20160609	20160000	2,555			
TJ-08	64	19,712	17	39,553	1348	20160607	20160000	1,832			
TJ-09	64	17,518	17	35,855	1441	20160608	20160000	2,076			
Oer-16	63	59,790	16	39,040	1830	20160501	20160930			5,340	

Appendix B: Balance distribution by elevation in 2015_16.

ΔS : area in elevation range, $\sum\Delta S$: cumulative area above given elevation, b_w: specific winter balance, b_s: specific summer balance. b_n: specific winter balance, ΔB_w : winter balance at a given elevation range, $\sum\Delta B_w$: cumulative winter balance above given elevation, ΔB_s summer balance at a given elevation range, $\sum\Delta B_s$: cumulative summer balance above given elevation, ΔB_n: net annual balance in a given elevation range, $\sum B_n$: cumulative net annual balance above given elevation.

Vatnajökull

Elevation (m a.s.l.)			ΔS (km^2)	$\sum\Delta S$ (km^2)	b_w (mm)	b_s (mm)	b_n (mm)	ΔB_w (10^6m^3)	$\sum\Delta B_w$ (10^6m^3)	ΔB_s (10^6m^3)	$\sum\Delta B_s$ (10^6m^3)	ΔB_n (10^6m^3)	$\sum B_n$ (10^6m^3)
2000	2050	2025	0,4	0,4	3113	2412	5525	1,4	1,4	1,1	1,1	2,5	2,5
1950	2000	1975	8,8	9,2	2351	285	2637	20,6	22,0	2,5	3,6	23,1	25,6
1900	1950	1925	36,6	45,8	2390	-57	2332	87,4	109,4	-2,1	1,5	85,3	110,9
1850	1900	1875	47,4	93,2	2567	3	2571	121,8	231,2	0,2	1,7	122,0	232,8
1800	1850	1825	47,0	140,2	2571	157	2728	120,8	351,9	7,4	9,0	128,2	361,0
1750	1800	1775	54,5	194,7	2426	-186	2240	132,4	484,3	-10,2	-1,1	122,2	483,2
1700	1750	1725	104,3	299,0	2293	-471	1821	239,3	723,6	-49,2	-50,3	190,1	673,3
1650	1700	1675	222,4	521,4	2208	-623	1585	491,3	1214,8	-138,7	-189,0	352,6	1025,8
1600	1650	1625	373,0	894,4	2206	-652	1553	822,8	2037,6	-243,2	-432,2	579,6	1605,4
1550	1600	1575	353,6	1248,0	2161	-786	1375	764,4	2802,0	-278,1	-710,3	486,3	2091,7
1500	1550	1525	420,6	1668,6	2112	-912	1200	888,6	3690,6	-383,9	-1094,2	504,7	2596,4
1450	1500	1475	453,2	2121,8	2121	-1050	1070	961,3	4651,8	-476,1	-1570,3	485,2	3081,6
1400	1450	1425	503,8	2625,6	2158	-1148	1009	1087,4	5739,2	-578,7	-2148,9	508,7	3590,3
1350	1400	1375	548,7	3174,3	2083	-1271	811	1143,2	6882,4	-697,9	-2846,8	445,3	4035,6
1300	1350	1325	540,9	3715,2	1993	-1430	563	1078,3	7960,7	-773,7	-3620,5	304,6	4340,2
1250	1300	1275	512,0	4227,2	1905	-1613	291	975,6	8936,4	-826,2	-4446,7	149,5	4489,7
1200	1250	1225	453,3	4680,5	1759	-1899	-139	797,6	9734,0	-861,1	-5307,8	-63,5	4426,2
1150	1200	1175	403,5	5084,0	1630	-2241	-610	658,0	10392,0	-904,5	-6212,2	-246,5	4179,8
1100	1150	1125	362,5	5446,5	1531	-2565	-1034	555,2	10947,2	-930,0	-7142,2	-374,8	3804,9
1050	1100	1075	323,6	5770,1	1427	-2904	-1477	461,8	11409,0	-940,0	-8082,2	-478,1	3326,8
1000	1050	1025	301,1	6071,2	1334	-3231	-1896	401,9	11810,9	-972,8	-9055,0	-570,9	2755,9
950	1000	975	270,8	6342,0	1252	-3506	-2254	339,1	12150,0	-949,6	-10004,6	-610,5	2145,4
900	950	925	238,3	6580,3	1184	-3767	-2583	282,3	12432,3	-898,0	-10902,5	-615,6	1529,8
850	900	875	210,2	6790,5	1103	-4032	-2928	232,0	12664,3	-847,6	-11750,2	-615,7	914,1
800	850	825	192,1	6982,6	1012	-4349	-3336	194,6	12858,9	-835,8	-12585,9	-641,1	273,0
750	800	775	174,8	7157,4	906	-4698	-3791	158,5	13017,4	-821,3	-13407,2	-662,8	-389,8
700	750	725	141,2	7298,6	848	-4923	-4075	119,8	13137,2	-695,2	-14102,5	-575,5	-965,3
650	700	675	121,3	7419,9	815	-4946	-4131	98,9	13236,1	-599,9	-14702,4	-501,1	-1466,3
600	650	625	74,6	7494,5	785	-4760	-3975	58,6	13294,7	-355,2	-15057,6	-296,6	-1762,9
550	600	575	65,8	7560,3	766	-4664	-3897	50,5	13345,1	-307,0	-15364,6	-256,6	-2019,5
500	550	525	48,0	7608,3	716	-4984	-4268	34,4	13379,5	-239,1	-15603,7	-204,7	-2224,2
450	500	475	40,4	7648,7	635	-5209	-4573	25,7	13405,2	-210,4	-15814,1	-184,8	-2409,0
400	450	425	44,5	7693,2	492	-5531	-5038	21,9	13427,1	-246,3	-16060,5	-224,4	-2633,4
350	400	375	40,0	7733,2	188	-6011	-5823	7,5	13434,7	-240,5	-16301,0	-233,0	-2866,3
300	350	325	38,1	7771,3	-224	-6448	-6673	-8,5	13426,1	-245,6	-16546,6	-254,1	-3120,4
250	300	275	36,6	7807,9	-582	-6772	-7355	-21,3	13404,8	-248,1	-16794,6	-269,4	-3389,9
200	250	225	37,5	7845,4	-899	-7094	-7994	-33,7	13371,1	-265,8	-17060,5	-299,5	-3689,4
150	200	175	32,5	7877,9	-1166	-7496	-8662	-37,8	13333,2	-243,3	-17303,7	-281,1	-3970,5
100	150	125	28,3	7906,2	-1325	-7831	-9156	-37,5	13295,7	-221,7	-17525,4	-259,2	-4229,8
50	100	75	25,9	7932,1	-1414	-8057	-9471	-36,6	13259,1	-208,6	-17734,1	-245,2	-4475,0
0	50	25	18,3	7950,4	-1481	-8337	-9819	-27,1	13232,0	-152,7	-17886,7	-179,8	-4654,8

Tungnaárjökull

Elevation (m a.s.l.)			ΔS (km^2)	ΣΔS (km^2)	b_w (mm)	b_s (mm)	b_n (mm)	ΔB_w (10^6m^3)	$\Sigma\Delta B_w$ (10^6m^3)	ΔB_s (10^6m^3)	$\Sigma\Delta B_s$ (10^6m^3)	ΔB_n (10^6m^3)	ΣB_n (10^6m^3)
1650	1700	1675	1,8	1,8	1990	-784	1206	3,7	3,7	-1,5	-1,5	2,2	2,2
1600	1650	1625	12,7	14,5	2019	-804	1215	25,7	29,4	-10,2	-11,7	15,5	17,7
1550	1600	1575	15,7	30,2	2034	-781	1252	31,9	61,3	-12,3	-24,0	19,7	37,4
1500	1550	1525	15,5	45,7	1982	-991	991	30,8	92,1	-15,4	-39,4	15,4	52,8
1450	1500	1475	18,4	64,1	1886	-1283	602	34,6	126,8	-23,6	-62,9	11,1	63,8
1400	1450	1425	23	87,1	1812	-1454	358	41,6	168,4	-33,4	-96,3	8,2	72,1
1350	1400	1375	21,4	108,5	1729	-1571	157	36,9	205,3	-33,6	-129,9	3,4	75,4
1300	1350	1325	27,5	136,0	1650	-1745	-95	45,4	250,7	-48,0	-177,9	-2,6	72,8
1250	1300	1275	21,1	157,1	1616	-1982	-365	34,1	284,9	-41,9	-219,8	-7,7	65,1
1200	1250	1225	23,1	180,2	1579	-2295	-716	36,5	321,3	-53,0	-272,8	-16,5	48,6
1150	1200	1175	21	201,2	1529	-2709	-1179	32,1	353,4	-56,9	-329,6	-24,8	23,8
1100	1150	1125	18,4	219,6	1454	-3190	-1736	26,7	380,2	-58,6	-388,3	-31,9	-8,1
1050	1100	1075	19,1	238,7	1386	-3688	-2301	26,5	406,7	-70,6	-458,9	-44,0	-52,2
1000	1050	1025	17,5	256,2	1324	-4152	-2827	23,1	429,8	-72,5	-531,4	-49,3	-101,5
950	1000	975	17,3	273,5	1250	-4518	-3267	21,6	451,5	-78,2	-609,5	-56,5	-158,1
900	950	925	16,4	289,9	1168	-4902	-3734	19,2	470,7	-80,5	-690,0	-61,3	-219,4
850	900	875	13,5	303,4	1082	-5324	-4242	14,6	485,3	-71,9	-761,9	-57,3	-276,6
800	850	825	14,1	317,5	996	-5866	-4869	14,0	499,3	-82,5	-844,4	-68,5	-345,1
750	800	775	11,4	328,9	889	-6521	-5631	10,1	509,4	-74,2	-918,6	-64,1	-409,2
700	750	725	7,8	336,7	797	-6996	-6198	6,2	515,6	-54,5	-973,1	-48,3	-457,5
650	700	675	3,7	340,4	733	-7262	-6529	2,7	518,3	-26,9	-1000,0	-24,2	-481,6

Sylgjujökull

Elevation (m a.s.l.)			ΔS (km^2)	ΣΔS (km^2)	b_w (mm)	b_s (mm)	b_n (mm)	ΔB_w (10^6m^3)	$\Sigma\Delta B_w$ (10^6m^3)	ΔB_s (10^6m^3)	$\Sigma\Delta B_s$ (10^6m^3)	ΔB_n (10^6m^3)	ΣB_n (10^6m^3)
1600	1650	1625	1,7	1,7	1970	-667	1302	3,3	3,3	-1,1	-1,1	2,2	2,2
1550	1600	1575	5,5	7,2	1924	-744	1179	10,5	13,9	-4,1	-5,2	6,5	8,7
1500	1550	1525	18,6	25,8	1848	-1008	839	34,4	48,2	-18,7	-24,0	15,6	24,3
1450	1500	1475	13,2	39,0	1802	-1195	607	23,8	72,0	-15,8	-39,7	8,0	32,3
1400	1450	1425	8,3	47,3	1733	-1379	354	14,4	86,4	-11,4	-51,1	2,9	35,2
1350	1400	1375	5,6	52,9	1654	-1570	84	9,2	95,6	-8,7	-59,9	0,5	35,7
1300	1350	1325	5,2	58,1	1568	-1806	-238	8,1	103,6	-9,3	-69,2	-1,2	34,5
1250	1300	1275	10,1	68,2	1521	-2032	-510	15,3	118,9	-20,4	-89,6	-5,1	29,3
1200	1250	1225	12	80,2	1488	-2327	-839	17,9	136,8	-28,0	-117,6	-10,1	19,2
1150	1200	1175	13,6	93,8	1422	-2793	-1371	19,4	156,2	-38,1	-155,7	-18,7	0,5
1100	1150	1125	12,8	106,6	1278	-3385	-2106	16,3	172,5	-43,2	-198,9	-26,9	-26,3
1050	1100	1075	12,3	118,9	1000	-3846	-2845	12,3	184,8	-47,2	-246,0	-34,9	-61,2
1000	1050	1025	10,9	129,8	750	-4220	-3470	8,1	192,9	-45,8	-291,8	-37,7	-98,9
950	1000	975	3,8	133,6	659	-4440	-3781	2,5	195,4	-16,8	-308,7	-14,3	-113,2
900	950	925	1,7	135,3	618	-4640	-4022	1,0	196,5	-7,8	-316,5	-6,8	-120,0
850	900	875	0,3	135,6	571	-4773	-4201	0,2	196,7	-1,5	-318,0	-1,3	-121,4

Köldukvíslarjökul

Elevation (m a.s.l.)			ΔS (km^2)	∑ΔS (km^2)	b_w (mm)	b_s (mm)	b_n (mm)	ΔB_w ($10^6 m^3$)	$\sum\Delta B_w$ ($10^6 m^3$)	ΔB_s ($10^6 m^3$)	$\sum\Delta B_s$ ($10^6 m^3$)	ΔB_n ($10^6 m^3$)	$\sum B_n$ ($10^6 m^3$)
1950	2000	1975	0,8	0,8	2207	-214	1992	1,8	1,8	-0,2	-0,2	1,7	1,7
1900	1950	1925	13,9	14,7	2337	-279	2057	32,6	34,4	-3,9	-4,1	28,7	30,3
1850	1900	1875	6,4	21,1	2277	-382	1895	14,6	48,9	-2,4	-6,5	12,1	42,4
1800	1850	1825	6	27,1	2216	-450	1765	13,4	62,3	-2,7	-9,2	10,6	53,1
1750	1800	1775	10,3	37,4	2241	-465	1775	23,1	85,4	-4,8	-14,0	18,3	71,4
1700	1750	1725	17	54,4	2063	-559	1504	35,0	120,5	-9,5	-23,5	25,5	96,9
1650	1700	1675	15,9	70,3	1880	-714	1166	29,9	150,4	-11,4	-34,9	18,5	115,5
1600	1650	1625	14,1	84,4	1763	-887	876	24,9	175,3	-12,5	-47,4	12,4	127,8
1550	1600	1575	18,7	103,1	1644	-1059	584	30,7	206,0	-19,8	-67,2	10,9	138,8
1500	1550	1525	20,3	123,4	1600	-1232	367	32,5	238,5	-25,0	-92,2	7,5	146,2
1450	1500	1475	19,4	142,8	1493	-1321	171	29,0	267,5	-25,7	-117,9	3,3	149,6
1400	1450	1425	15,3	158,1	1321	-1467	-146	20,2	287,6	-22,4	-140,3	-2,2	147,3
1350	1400	1375	15,1	173,2	1150	-1732	-582	17,4	305,0	-26,2	-166,5	-8,8	138,5
1300	1350	1325	17,3	190,5	1046	-2045	-999	18,1	323,1	-35,4	-201,9	-17,3	121,2
1250	1300	1275	18	208,5	979	-2463	-1484	17,6	340,7	-44,3	-246,2	-26,7	94,5
1200	1250	1225	17,4	225,9	923	-3028	-2105	16,0	356,8	-52,6	-298,8	-36,5	58,0
1150	1200	1175	16,3	242,2	868	-3566	-2698	14,2	370,9	-58,2	-357,0	-44,0	14,0
1100	1150	1125	14,8	257,0	809	-3985	-3175	12,0	382,9	-58,9	-415,8	-46,9	-32,9
1050	1100	1075	13,4	270,4	745	-4297	-3552	10,0	392,9	-57,6	-473,4	-47,6	-80,5
1000	1050	1025	10,5	280,9	680	-4524	-3843	7,2	400,0	-47,6	-521,1	-40,5	-121,0
950	1000	975	9,7	290,6	620	-4686	-4065	6,0	406,0	-45,3	-566,3	-39,3	-160,3
900	950	925	6,3	296,9	567	-4806	-4238	3,6	409,6	-30,5	-596,8	-26,9	-187,2
850	900	875	0,9	297,8	511	-4925	-4413	0,4	410,1	-4,3	-601,1	-3,8	-191,0

Dyngjujökull

Elevation (m a.s.l.)			ΔS (km^2)	∑ΔS (km^2)	b_w (mm)	b_s (mm)	b_n (mm)	ΔB_w ($10^6 m^3$)	$\sum\Delta B_w$ ($10^6 m^3$)	ΔB_s ($10^6 m^3$)	$\sum\Delta B_s$ ($10^6 m^3$)	ΔB_n ($10^6 m^3$)	$\sum B_n$ ($10^6 m^3$)
2000	2050	2025	0	0,0	2110	-293	1816	0,0	0,0	0,0	0,0	0,0	0,0
1950	2000	1975	3,3	3,3	2168	-217	1950	7,1	7,1	-0,7	-0,7	6,4	6,4
1900	1950	1925	12,7	16,0	2384	-207	2176	30,3	37,4	-2,6	-3,4	27,7	34,1
1850	1900	1875	25,1	41,1	2580	-355	2224	64,9	102,3	-8,9	-12,3	55,9	90,0
1800	1850	1825	14,8	55,9	2500	-497	2002	36,9	139,2	-7,4	-19,7	29,6	119,6
1750	1800	1775	15,7	71,6	2391	-579	1811	37,5	176,7	-9,1	-28,7	28,4	148,0
1700	1750	1725	28,1	99,7	2343	-639	1704	65,9	242,6	-18,0	-46,7	47,9	195,9
1650	1700	1675	73,5	173,2	2254	-669	1585	165,6	408,2	-49,1	-95,8	116,5	312,3
1600	1650	1625	118,8	292,0	2179	-686	1493	258,9	667,1	-81,5	-177,4	177,4	489,7
1550	1600	1575	95,5	387,5	2019	-842	1176	193,0	860,1	-80,5	-257,9	112,4	602,1
1500	1550	1525	87,8	475,3	1833	-922	911	161,0	1021,0	-80,9	-338,9	80,0	682,2
1450	1500	1475	73,7	549,0	1648	-1017	631	121,6	1142,6	-75,0	-413,9	46,5	728,7
1400	1450	1425	61,2	610,2	1457	-1107	349	89,2	1231,8	-67,8	-481,7	21,4	750,1
1350	1400	1375	49,5	659,7	1280	-1250	29	63,3	1295,2	-61,9	-543,6	1,5	751,6
1300	1350	1325	36,5	696,2	1176	-1509	-332	43,0	1338,1	-55,1	-598,7	-12,1	739,5
1250	1300	1275	39,9	736,1	1121	-1860	-738	44,7	1382,9	-74,2	-672,9	-29,5	710,0
1200	1250	1225	45,4	781,5	1076	-2352	-1276	48,9	1431,7	-106,9	-779,7	-58,0	652,0
1150	1200	1175	45,7	827,2	1010	-2965	-1954	46,1	1477,9	-135,4	-915,1	-89,2	562,7
1100	1150	1125	43	870,2	936	-3482	-2546	40,3	1518,2	-149,9	-1065,1	-109,6	453,1
1050	1100	1075	31,5	901,7	873	-3900	-3026	27,6	1545,7	-123,0	-1188,1	-95,5	357,6
1000	1050	1025	33	934,7	836	-4193	-3357	27,6	1573,3	-138,4	-1326,4	-110,8	246,9
950	1000	975	30,6	965,3	808	-4456	-3648	24,7	1598,0	-136,2	-1462,6	-111,5	135,4
900	950	925	25,7	991,0	785	-4670	-3884	20,2	1618,2	-120,1	-1582,7	-99,9	35,5
850	900	875	23,6	1014,6	769	-4828	-4059	18,2	1636,4	-114,1	-1696,8	-95,9	-60,4
800	850	825	21,6	1036,2	756	-4946	-4190	16,3	1652,7	-106,7	-1803,5	-90,4	-150,8
750	800	775	17,8	1054,0	736	-5035	-4299	13,1	1665,8	-89,4	-1892,9	-76,4	-227,1
700	750	725	5,4	1059,4	719	-5064	-4344	3,9	1669,6	-27,1	-1920,1	-23,3	-250,4

Brúarjökull

Elevation (m a.s.l.)			ΔS (km^2)	∑ΔS (km^2)	b_w (mm)	b_s (mm)	b_n (mm)	$ΔB_w$ (10^6m^3)	$∑ΔB_w$ (10^6m^3)	$ΔB_s$ (10^6m^3)	$∑ΔB_s$ (10^6m^3)	$ΔB_n$ (10^6m^3)	$∑B_n$ (10^6m^3)
1850	1900	1875	1,2	1,2	2555	-524	2030	3,0	3,1	-0,6	-0,6	2,4	2,5
1800	1850	1825	4,4	5,6	2551	-423	2127	11,3	14,4	-1,9	-2,5	9,4	11,9
1750	1800	1775	2,9	8,5	2447	-472	1974	7,0	21,4	-1,4	-3,9	5,6	17,5
1700	1750	1725	3,9	12,4	2360	-528	1831	9,3	30,6	-2,1	-5,9	7,2	24,7
1650	1700	1675	5,5	17,9	2306	-583	1722	12,7	43,3	-3,2	-9,2	9,5	34,2
1600	1650	1625	50,9	68,8	2260	-595	1665	115,1	158,5	-30,3	-39,5	84,8	119,0
1550	1600	1575	46	114,8	2238	-779	1458	102,9	261,4	-35,8	-75,3	67,1	186,1
1500	1550	1525	72,6	187,4	2158	-881	1276	156,6	418,0	-64,0	-139,3	92,6	278,7
1450	1500	1475	78,3	265,7	2062	-985	1076	161,5	579,5	-77,2	-216,4	84,3	363,0
1400	1450	1425	111,2	376,9	2185	-1065	1120	243,1	822,5	-118,5	-334,9	124,6	487,6
1350	1400	1375	155,9	532,8	2058	-1181	876	320,9	1143,4	-184,2	-519,1	136,7	624,3
1300	1350	1325	147,2	680,0	1920	-1287	632	282,6	1426,0	-189,5	-708,6	93,1	717,3
1250	1300	1275	141,8	821,8	1848	-1407	440	262,2	1688,2	-199,7	-908,3	62,5	779,8
1200	1250	1225	117,9	939,7	1739	-1594	145	205,1	1893,3	-188,0	-1096,3	17,1	797,0
1150	1200	1175	102,7	1042,4	1600	-1863	-262	164,4	2057,7	-191,3	-1287,7	-26,9	770,0
1100	1150	1125	83,4	1125,8	1435	-2195	-759	119,7	2177,4	-183,1	-1470,8	-63,4	706,7
1050	1100	1075	69,8	1195,6	1286	-2594	-1307	89,8	2267,2	-181,0	-1651,8	-91,3	615,4
1000	1050	1025	62,5	1258,1	1154	-3031	-1877	72,1	2339,3	-189,4	-1841,2	-117,3	498,1
950	1000	975	56,4	1314,5	1036	-3490	-2454	58,4	2397,7	-196,9	-2038,1	-138,5	359,6
900	950	925	46,3	1360,8	924	-3939	-3015	42,8	2440,6	-182,4	-2220,6	-139,6	220,0
850	900	875	42,6	1403,4	818	-4382	-3564	34,8	2475,4	-186,5	-2407,1	-151,7	68,3
800	850	825	38,1	1441,5	718	-4821	-4102	27,4	2502,8	-183,8	-2590,9	-156,4	-88,1
750	800	775	37	1478,5	596	-5377	-4781	22,1	2524,9	-199,1	-2790,0	-177,0	-265,1
700	750	725	25,6	1504,1	504	-5893	-5389	12,9	2537,8	-150,9	-2940,9	-138,0	-403,2
650	700	675	17,5	1521,6	433	-6194	-5760	7,6	2545,4	-108,1	-3049,0	-100,5	-503,7
600	650	625	3	1524,6	391	-6365	-5973	1,2	2546,5	-19,1	-3068,1	-17,9	-521,6

Eyjabakkajökull

Elevation (m a.s.l.)			ΔS (km^2)	∑ΔS (km^2)	b_w (mm)	b_s (mm)	b_n (mm)	$ΔB_w$ (10^6m^3)	$∑ΔB_w$ (10^6m^3)	$ΔB_s$ (10^6m^3)	$∑ΔB_s$ (10^6m^3)	$ΔB_n$ (10^6m^3)	$∑B_n$ (10^6m^3)
1550	1600	1575	0	0,0	2854	-1029	1825	0,3	0,3	0,0	-0,1	0,2	0,2
1500	1550	1525	1	1,0	2806	-1023	1783	2,7	3,0	-1,0	-1,1	1,7	1,9
1450	1500	1475	1,8	2,8	2767	-1048	1718	5,1	8,1	-1,9	-3,0	3,2	5,1
1400	1450	1425	2,5	5,3	2679	-1130	1548	6,8	14,9	-2,9	-5,9	3,9	9,0
1350	1400	1375	4,1	9,4	2580	-1225	1355	10,6	25,5	-5,0	-10,9	5,6	14,6
1300	1350	1325	13,7	23,1	2302	-1412	890	31,6	57,1	-19,4	-30,3	12,2	26,8
1250	1300	1275	13,4	36,5	1992	-1625	367	26,7	83,8	-21,8	-52,1	4,9	31,7
1200	1250	1225	14,4	50,9	1847	-1909	-61	26,6	110,4	-27,5	-79,6	-0,9	30,8
1150	1200	1175	12,1	63,0	1736	-2288	-551	21,0	131,4	-27,7	-107,3	-6,7	24,1
1100	1150	1125	10,4	73,4	1619	-2896	-1277	16,8	148,3	-30,1	-137,4	-13,3	10,9
1050	1100	1075	10,1	83,5	1507	-3519	-2012	15,2	163,5	-35,5	-172,9	-20,3	-9,4
1000	1050	1025	7,6	91,1	1393	-4029	-2636	10,5	174,0	-30,5	-203,4	-19,9	-29,4
950	1000	975	4,9	96,0	1292	-4347	-3055	6,4	180,4	-21,5	-224,8	-15,1	-44,5
900	950	925	4	100,0	1234	-4511	-3277	4,9	185,3	-17,9	-242,7	-13,0	-57,4
850	900	875	3,1	103,1	1218	-4642	-3424	3,7	189,0	-14,2	-256,9	-10,5	-67,9
800	850	825	3	106,1	1176	-4835	-3658	3,6	192,6	-14,7	-271,6	-11,1	-79,0
750	800	775	2,6	108,7	1108	-5141	-4033	2,9	195,5	-13,4	-285,0	-10,5	-89,6
700	750	725	3	111,7	1024	-5520	-4495	3,1	198,6	-16,8	-301,9	-13,7	-103,3
650	700	675	0,2	111,9	959	-5767	-4807	0,2	198,7	-0,9	-302,8	-0,8	-104,0

Hoffellsjökull

Elevation (m a.s.l.)			ΔS (km^2)	$\sum\Delta S$ (km^2)	b_w (mm)	b_s (mm)	b_n (mm)	ΔB_w (10^6m^3)	$\sum\Delta B_w$ (10^6m^3)	ΔB_s (10^6m^3)	$\sum\Delta B_s$ (10^6m^3)	ΔB_n (10^6m^3)	$\sum B_n$ (10^6m^3)
1450	1500	1475	0,9	0,9	2822	-1003	1818	2,6	2,6	-0,9	-0,9	1,7	1,7
1400	1450	1425	6,7	7,6	2870	-987	1883	20,8	23,4	-7,1	-8,1	13,6	15,3
1350	1400	1375	10,0	17,6	2715	-1040	1675	27,6	51,0	-10,6	-18,7	17,1	32,3
1300	1350	1325	15,4	33,0	2587	-1162	1424	42,1	93,1	-18,9	-37,6	23,2	55,6
1250	1300	1275	33,6	66,6	2367	-1375	992	82,7	175,9	-48,0	-85,6	34,7	90,2
1200	1250	1225	26,8	93,4	2223	-1547	675	57,4	233,3	-40,0	-125,6	17,5	107,7
1150	1200	1175	18,2	111,6	2067	-1778	288	37,1	270,4	-31,9	-157,5	5,2	112,9
1100	1150	1125	17,5	129,1	1923	-2034	-110	32,6	303,0	-34,4	-192,0	-1,9	111,0
1050	1100	1075	13,6	142,7	1783	-2359	-576	22,8	325,8	-30,2	-222,2	-7,4	103,6
1000	1050	1025	10,0	152,7	1667	-2627	-959	16,3	342,0	-25,6	-247,8	-9,4	94,3
950	1000	975	9,0	161,7	1543	-2872	-1328	13,4	355,4	-24,9	-272,7	-11,5	82,8
900	950	925	6,4	168,1	1421	-3125	-1703	9,1	364,5	-20,0	-292,7	-10,9	71,8
850	900	875	4,3	172,4	1302	-3332	-2029	5,7	370,2	-14,5	-307,2	-8,8	63,0
800	850	825	3,6	176,0	1269	-3464	-2194	4,5	374,7	-12,3	-319,5	-7,8	55,2
750	800	775	3,9	179,9	1191	-3656	-2464	4,6	379,3	-14,1	-333,6	-9,5	45,7
700	750	725	3,8	183,7	1085	-3844	-2759	3,9	383,2	-13,9	-347,5	-10,0	35,7
650	700	675	3,4	187,1	977	-4075	-3098	3,4	386,6	-14,1	-361,6	-10,7	25,0
600	650	625	2,5	189,6	867	-4386	-3519	2,2	388,8	-11,1	-372,7	-8,9	16,1
550	600	575	1,8	191,4	779	-4705	-3926	1,3	390,2	-8,1	-380,8	-6,8	9,3
500	550	525	1,5	192,9	703	-5011	-4307	1,1	391,3	-7,9	-388,8	-6,8	2,5
450	500	475	0,9	193,8	613	-5327	-4713	0,5	391,8	-4,7	-393,4	-4,1	-1,6
400	450	425	0,9	194,7	477	-5653	-5176	0,4	392,3	-5,3	-398,8	-4,9	-6,5
350	400	375	0,6	195,3	233	-6002	-5768	0,1	392,4	-3,8	-402,6	-3,7	-10,2
300	350	325	0,9	196,2	-73	-6390	-6464	0,0	392,4	-4,6	-407,2	-4,7	-14,8
250	300	275	2,2	198,4	-435	-6821	-7257	-0,6	391,8	-8,9	-416,1	-9,5	-24,3
200	250	225	3,3	201,7	-817	-7292	-8110	-2,2	389,6	-19,5	-435,6	-21,7	-46,0
150	200	175	2,6	204,3	-1148	-7893	-9042	-3,4	386,2	-23,6	-459,2	-27,0	-73,0
100	150	125	2,1	206,4	-1332	-8352	-9684	-3,1	383,0	-19,7	-478,9	-22,9	-95,9
50	100	75	2,8	209,2	-1409	-8638	-10048	-2,6	380,4	-16,0	-494,9	-18,6	-114,5
0	50	25	0,6	209,8	-1475	-8942	-10417	-3,9	376,5	-23,4	-518,3	-27,3	-141,8

Breiðamerkurjökull

Elevation (m a.s.l.)			ΔS (km^2)	$\sum\Delta S$ (km^2)	b_w (mm)	b_s (mm)	b_n (mm)	ΔB_w ($10^6 m^3$)	$\sum\Delta B_w$ ($10^6 m^3$)	ΔB_s ($10^6 m^3$)	$\sum\Delta B_s$ ($10^6 m^3$)	ΔB_n ($10^6 m^3$)	$\sum B_n$ ($10^6 m^3$)
1900	1950	1925	0,0	0,0	3176	1999	5176	0,3	0,3	0,2	0,2	0,4	0,4
1850	1900	1875	0,4	0,4	3122	2011	5133	1,2	1,4	0,7	0,9	1,9	2,3
1800	1850	1825	0,4	0,8	3048	1998	5046	1,4	2,8	0,9	1,8	2,4	4,7
1750	1800	1775	0,8	1,6	2977	1719	4696	3,0	5,8	1,7	3,6	4,7	9,4
1700	1750	1725	2,5	4,1	2900	520	3421	7,6	13,4	1,4	4,9	9,0	18,3
1650	1700	1675	5,8	9,9	2783	-169	2614	16,7	30,1	-1,0	3,9	15,7	34,0
1600	1650	1625	15,8	25,7	2503	-393	2109	42,9	73,0	-6,8	-2,8	36,2	70,2
1550	1600	1575	25,7	51,4	2360	-556	1803	61,3	134,3	-14,5	-17,3	46,8	117,0
1500	1550	1525	32,2	83,6	2293	-753	1539	73,3	207,6	-24,1	-41,4	49,2	166,3
1450	1500	1475	44,3	127,9	2333	-920	1413	107,2	314,9	-42,3	-83,7	64,9	231,2
1400	1450	1425	58,3	186,2	2285	-1042	1243	135,4	450,3	-61,7	-145,4	73,7	304,8
1350	1400	1375	88,7	274,9	2223	-1188	1034	198,9	649,1	-106,3	-251,8	92,5	397,4
1300	1350	1325	96,9	371,8	2181	-1329	852	207,6	856,7	-126,5	-378,3	81,1	478,5
1250	1300	1275	59,4	431,2	2113	-1437	675	121,7	978,4	-82,8	-461,1	38,9	517,4
1200	1250	1225	39,7	470,9	2052	-1580	472	81,6	1060,0	-62,8	-523,9	18,8	536,1
1150	1200	1175	32,6	503,5	1962	-1737	224	62,3	1122,3	-55,2	-579,0	7,1	543,3
1100	1150	1125	27,7	531,2	1858	-1902	-44	50,7	1173,0	-51,9	-630,9	-1,2	542,1
1050	1100	1075	24,1	555,3	1747	-2055	-307	41,6	1214,6	-48,9	-679,8	-7,3	534,8
1000	1050	1025	22,1	577,4	1644	-2207	-563	36,0	1250,5	-48,3	-728,1	-12,3	522,4
950	1000	975	24,5	601,9	1557	-2393	-835	37,9	1288,5	-58,3	-786,4	-20,3	502,1
900	950	925	27,4	629,3	1497	-2539	-1041	40,6	1329,0	-68,8	-855,1	-28,2	473,9
850	900	875	26,2	655,5	1394	-2747	-1353	35,5	1364,5	-70,0	-925,1	-34,5	439,4
800	850	825	26,1	681,6	1278	-2968	-1689	33,0	1397,5	-76,5	-1001,6	-43,5	395,9
750	800	775	25,3	706,9	1146	-3179	-2032	28,9	1426,3	-80,0	-1081,6	-51,1	344,8
700	750	725	23,9	730,8	1053	-3329	-2276	23,4	1449,7	-74,0	-1155,6	-50,6	294,2
650	700	675	30,8	761,6	1005	-3474	-2469	31,5	1481,3	-109,0	-1264,6	-77,5	216,7
600	650	625	26,2	787,8	873	-3688	-2814	22,4	1503,7	-94,6	-1359,2	-72,2	144,5
550	600	575	27,0	814,8	767	-3924	-3157	20,7	1524,3	-105,6	-1464,8	-85,0	59,6
500	550	525	15,7	830,5	715	-4160	-3444	11,1	1535,5	-64,7	-1529,5	-53,6	6,0
450	500	475	16,3	846,8	606	-4483	-3876	8,8	1544,3	-65,3	-1594,8	-56,5	-50,5
400	450	425	15,9	862,7	479	-4807	-4327	7,9	1552,2	-79,1	-1674,0	-71,2	-121,8
350	400	375	13,0	875,7	219	-5241	-5022	2,9	1555,1	-69,1	-1743,1	-66,2	-188,0
300	350	325	13,1	888,8	-161	-5689	-5850	-1,9	1553,2	-66,0	-1809,1	-67,9	-255,8
250	300	275	12,1	900,9	-572	-6134	-6707	-6,4	1546,8	-68,5	-1877,5	-74,9	-330,7
200	250	225	11,5	912,4	-940	-6531	-7472	-10,7	1536,1	-74,6	-1952,1	-85,3	-416,0
150	200	175	8,6	921,0	-1200	-6980	-8180	-11,3	1524,8	-65,5	-2017,6	-76,7	-492,8
100	150	125	7,9	928,9	-1336	-7381	-8717	-10,7	1514,2	-58,9	-2076,5	-69,6	-562,3
50	100	75	6,1	935,0	-1411	-7619	-9030	-10,4	1503,8	-56,1	-2132,6	-66,5	-628,8
0	50	25	3,0	938,0	-1450	-7773	-9223	-8,1	1495,7	-43,5	-2176,0	-51,6	-680,3

Síðujökull

Elevation (m a.s.l.)			ΔS (km^2)	$\sum\Delta S$ (km^2)	b_w (mm)	b_s (mm)	b_n (mm)	ΔB_w (10^6m^3)	$\sum\Delta B_w$ (10^6m^3)	ΔB_s (10^6m^3)	$\sum\Delta B_s$ (10^6m^3)	ΔB_n (10^6m^3)	$\sum B_n$ (10^6m^3)
1700	1750	1725	0,8	0,8	2798	-758	2040	2,4	2,4	-0,6	-0,6	1,7	1,7
1650	1700	1675	5,5	6,3	2503	-838	1665	13,9	16,2	-4,6	-5,3	9,2	10,9
1600	1650	1625	11,1	17,4	2375	-872	1503	26,3	42,5	-9,7	-14,9	16,7	27,6
1550	1600	1575	10,7	28,1	2465	-886	1578	26,5	69,0	-9,5	-24,5	17,0	44,5
1500	1550	1525	20,5	48,6	2477	-967	1510	50,7	119,7	-19,8	-44,2	30,9	75,4
1450	1500	1475	39	87,6	2295	-1185	1110	89,6	209,3	-46,3	-90,5	43,3	118,8
1400	1450	1425	25,9	113,5	2076	-1407	669	53,8	263,1	-36,5	-127,0	17,3	136,1
1350	1400	1375	21,2	134,7	1945	-1598	347	41,2	304,3	-33,8	-160,8	7,4	143,5
1300	1350	1325	17,3	152,0	1886	-1772	114	32,7	337,0	-30,7	-191,5	2,0	145,5
1250	1300	1275	15,9	167,9	1809	-1987	-177	28,8	365,8	-31,7	-223,2	-2,8	142,6
1200	1250	1225	21,1	189,0	1788	-2271	-482	37,8	403,6	-48,0	-271,2	-10,2	132,4
1150	1200	1175	18,3	207,3	1740	-2672	-932	31,8	435,4	-48,8	-319,9	-17,0	115,4
1100	1150	1125	17,2	224,5	1737	-2976	-1239	29,9	465,3	-51,3	-371,2	-21,4	94,1
1050	1100	1075	16,2	240,7	1704	-3272	-1567	27,6	492,9	-53,1	-424,3	-25,4	68,6
1000	1050	1025	20,5	261,2	1626	-3601	-1975	33,4	526,3	-73,9	-498,2	-40,5	28,1
950	1000	975	20,2	281,4	1494	-4056	-2561	30,2	556,5	-81,9	-580,1	-51,7	-23,6
900	950	925	21,6	303,0	1329	-4505	-3175	28,8	585,2	-97,4	-677,5	-68,7	-92,3
850	900	875	19,8	322,8	1190	-4814	-3623	23,5	608,8	-95,2	-772,7	-71,7	-163,9
800	850	825	21,3	344,1	1068	-5081	-4013	22,7	631,5	-108,0	-880,7	-85,3	-249,2
750	800	775	23,3	367,4	937	-5344	-4407	21,9	653,4	-124,7	-1005,5	-102,9	-352,1
700	750	725	23,6	391,0	810	-5677	-4867	19,1	672,5	-133,9	-1139,4	-114,8	-466,9
650	700	675	19,9	410,9	694	-6046	-5352	13,8	686,2	-120,0	-1259,4	-106,2	-573,2
600	650	625	10,9	421,8	604	-6270	-5666	6,6	692,8	-68,4	-1327,8	-61,8	-635,0
550	600	575	1,5	423,3	558	-6363	-5804	0,9	693,7	-9,8	-1337,6	-8,9	-643,9

Skaftárjökull

Elevation (m a.s.l.)			ΔS (km^2)	$\sum\Delta S$ (km^2)	b_w (mm)	b_s (mm)	b_n (mm)	ΔB_w (10^6m^3)	$\sum\Delta B_w$ (10^6m^3)	ΔB_s (10^6m^3)	$\sum\Delta B_s$ (10^6m^3)	ΔB_n (10^6m^3)	$\sum B_n$ (10^6m^3)
1350	1400	1375	2,3	2,3	1801	-1616	184	4,2	4,2	-3,8	-3,8	0,4	0,4
1300	1350	1325	5,4	7,7	1730	-1767	-36	9,3	13,5	-9,5	-13,2	-0,2	0,2
1250	1300	1275	4,2	11,9	1682	-2030	-347	7,1	20,6	-8,6	-21,8	-1,5	-1,2
1200	1250	1225	6,5	18,4	1639	-2374	-734	10,6	31,2	-15,4	-37,2	-4,8	-6,0
1150	1200	1175	7,9	26,3	1598	-2725	-1126	12,6	43,8	-21,5	-58,7	-8,9	-14,9
1100	1150	1125	11,2	37,5	1556	-3066	-1510	17,4	61,2	-34,2	-92,9	-16,8	-31,7
1050	1100	1075	12,9	50,4	1501	-3446	-1944	19,4	80,6	-44,5	-137,4	-25,1	-56,8
1000	1050	1025	12,9	63,3	1426	-3801	-2375	18,5	99,0	-49,2	-186,6	-30,7	-87,6
950	1000	975	8,5	71,8	1308	-4219	-2911	11,1	110,2	-36,0	-222,6	-24,8	-112,4
900	950	925	5,5	77,3	1209	-4599	-3390	6,6	116,8	-25,2	-247,7	-18,5	-130,9
850	900	875	5,3	82,6	1108	-5019	-3911	5,9	122,7	-26,8	-274,6	-20,9	-151,8
800	850	825	5	87,6	1009	-5516	-4507	5,0	127,8	-27,5	-302,1	-22,5	-174,3
750	800	775	4,8	92,4	912	-6002	-5090	4,4	132,2	-28,9	-331,0	-24,5	-198,9
700	750	725	4,4	96,8	807	-6651	-5843	3,6	135,7	-29,4	-360,4	-25,8	-224,7
650	700	675	2,6	99,4	707	-7142	-6435	1,8	137,6	-18,4	-378,8	-16,6	-241,3
600	650	625	0,7	100,1	623	-7247	-6623	0,4	138,0	-4,8	-383,6	-4,4	-245,7

Vestari Skaftárketill

Elevation (m a.s.l.)			ΔS (km^2)	$\sum\Delta S$ (km^2)	b_w (mm)	b_s (mm)	b_n (mm)	ΔB_w (10^6m^3)	$\sum\Delta B_w$ (10^6m^3)	ΔB_s (10^6m^3)	$\sum\Delta B_s$ (10^6m^3)	ΔB_n (10^6m^3)	$\sum B_n$ (10^6m^3)
1900	1950	1925	0,6	0,6	2602	-325	2276	1,5	1,5	-0,2	-0,2	1,3	1,3
1850	1900	1875	0,6	1,2	2590	-367	2223	1,6	3,1	-0,2	-0,4	1,4	2,7
1800	1850	1825	0,8	2,0	2542	-403	2138	2,0	5,0	-0,3	-0,7	1,6	4,3
1750	1800	1775	2,6	4,6	2410	-484	1925	6,2	11,2	-1,3	-2,0	5,0	9,3
1700	1750	1725	5,5	10,1	2174	-540	1633	12,0	23,3	-3,0	-5,0	9,0	18,3
1650	1700	1675	6,6	16,7	1999	-540	1386	13,3	36,5	-4,1	-9,0	9,2	27,5
1600	1650	1625	7,6	24,3	1934	-540	1257	14,7	51,2	-5,1	-14,2	9,5	37,0
1550	1600	1575	5,5	29,8	1880	-540	1122	10,3	61,5	-4,1	-18,3	6,1	43,2
1500	1550	1525	1,5	31,3	1864	-540	1071	2,8	64,3	-1,2	-19,5	1,6	44,8

Eystri Skaftárketill

Elevation (m a.s.l.)			ΔS (km^2)	$\sum\Delta S$ (km^2)	b_w (mm)	b_s (mm)	b_n (mm)	ΔB_w (10^6m^3)	$\sum\Delta B_w$ (10^6m^3)	ΔB_s (10^6m^3)	$\sum\Delta B_s$ (10^6m^3)	ΔB_n (10^6m^3)	$\sum B_n$ (10^6m^3)
1750	1800	1775	1,1	1,1	2397	-533	1864	2,6	2,6	-0,6	-0,6	2,0	2,0
1700	1750	1725	10,2	11,3	2175	-580	1594	22,2	24,8	-5,9	-6,5	16,3	18,3
1650	1700	1675	16,5	27,8	2053	-643	1409	33,9	58,7	-10,6	-17,1	23,3	41,6
1600	1650	1625	9,7	37,5	2011	-658	1353	19,4	78,1	-6,4	-23,5	13,1	54,6
1550	1600	1575	2,4	39,9	2008	-653	1354	4,9	83,0	-1,6	-25,1	3,3	57,9

Gjálp

Elevation (m a.s.l.)			ΔS (km^2)	$\sum\Delta S$ (km^2)	b_w (mm)	b_s (mm)	b_n (mm)	ΔB_w (10^6m^3)	$\sum\Delta B_w$ (10^6m^3)	ΔB_s (10^6m^3)	$\sum\Delta B_s$ (10^6m^3)	ΔB_n (10^6m^3)	$\sum B_n$ (10^6m^3)
1900	1950	1925	0,4	0,4	2627	-323	2304	1,0	1,0	-0,1	-0,1	0,9	0,9
1850	1900	1875	0,7	1,1	2609	-392	2216	1,9	2,9	-0,3	-0,4	1,6	2,5
1800	1850	1825	1,1	2,2	2554	-457	2096	2,9	5,8	-0,5	-0,9	2,4	4,9
1750	1800	1775	4,9	7,1	2460	-557	1903	12,0	17,8	-2,7	-3,6	9,2	14,1
1700	1750	1725	18,8	25,9	2259	-643	1615	42,4	60,2	-12,1	-15,7	30,3	44,4
1650	1700	1675	13,5	39,4	2162	-687	1474	29,2	89,3	-9,3	-25,0	19,9	64,3

Grímsvötn

Elevation (m a.s.l.)			ΔS (km^2)	$\sum\Delta S$ (km^2)	b_w (mm)	b_s (mm)	b_n (mm)	ΔB_w (10^6m^3)	$\sum\Delta B_w$ (10^6m^3)	ΔB_s (10^6m^3)	$\sum\Delta B_s$ (10^6m^3)	ΔB_n (10^6m^3)	$\sum B_n$ (10^6m^3)
1700	1750	1725	0,7	0,7	2141	-735	1405	1,6	1,6	-0,5	-0,5	1,0	1,0
1650	1700	1675	40,6	41,3	2095	-719	1376	85,1	86,7	-29,2	-29,8	55,9	56,9
1600	1650	1625	30,8	72,1	2008	-840	1167	61,8	148,5	-25,9	-55,6	36,0	92,9
1550	1600	1575	19,2	91,3	1964	-927	1037	37,7	186,3	-17,8	-73,4	19,9	112,8
1500	1550	1525	16,9	108,2	1950	-1053	896	33,0	219,3	-17,8	-91,3	15,2	128,0
1450	1500	1475	10	118,2	1934	-1214	719	19,4	238,7	-12,2	-103,5	7,2	135,2
1400	1450	1425	11,7	129,9	1929	-1340	589	22,6	261,2	-15,7	-119,1	6,9	142,1
1350	1400	1375	4,3	134,2	1949	-1323	626	8,5	269,7	-5,7	-124,9	2,7	144,8
1300	1350	1325	0,7	134,9	1989	-1223	765	1,5	271,2	-0,9	-125,8	0,6	145,4

Appendix C: Coordinates at velocity measurement stakes in 2016.

Position of velocity measurement stakes determined by GPS sub-metre differential (I), fast static (FS) and kinematic (K).
(Accuracy of horizontal position 0.5 – 1.0 m, and vertical accuracy 1-2 m for DGPS, about 1cm for fast static, and 3 cm for kinematic).
The station Hofn in Höfn í Hornafirði is used as a stationary reference for all measurements, ÍSN93 datum, h_l is elevation above ellipsoid, dL antenna height, N estimated difference between ellipsoid and sea-level, H elevation in metres above sea level ($H= h_l+N+dL$). X and Y are ÍSN93 Lambert conformal conic projected coordinates. M is a quality marker.

Site	time	Date	#	Calender Day	Year	Latitude		Longitude		h_l (m a. e.)	dL (m)	N (m)	H (m a. s. l.)	X	Y	M
B07-16	12,518	8	5	129	2016	64	25,78638	16	17,45627	1426,2	0,0	-67,1	1359,1	630474,7	439226,8	K
B07-16	10,943	10	10	284	2016	64	25,78578	16	17,45573	1422,7	-0,5	-67,1	1355,2	630475,2	439225,7	K
B09-16	20,130	7	5	128	2016	64	45,04895	16	5,45842	804,9	0,0	-66,7	738,2	638452,6	475406,7	K
B09-16	15,975	11	10	285	2016	64	45,04887	16	5,45995	798,3	0,0	-66,7	731,6	638451,4	475406,5	K
B10-16	19,491	7	5	128	2016	64	43,68713	16	6,69779	862,8	0,0	-66,7	796,1	637585,7	472834,0	K
B10-16	15,433	11	10	285	2016	64	43,68649	16	6,69631	856,6	0,0	-66,7	789,9	637586,9	472832,8	K
B11-16	19,255	7	5	128	2016	64	40,94366	16	10,49373	1026,0	0,0	-66,8	959,2	634801,8	467605,5	K
B11-16	13,854	11	10	285	2016	64	40,94850	16	10,48976	1021,2	0,0	-66,8	954,4	634804,6	467614,6	K
B12-16	18,234	7	5	128	2016	64	38,26636	16	14,12407	1145,8	0,0	-66,9	1078,9	632134,1	462508,2	K
B12-16	17,837	11	10	285	2016	64	38,27504	16	14,11588	1142,0	0,0	-66,9	1075,1	632139,9	462524,6	K
B13-16	21,179	7	5	128	2016	64	34,52647	16	19,70494	1285,2	0,0	-67,0	1218,2	627984,7	455374,5	K
B13-16	12,877	11	10	285	2016	64	34,53616	16	19,69331	1282,2	-0,3	-67,0	1214,9	627993,2	455392,9	K
B13ror15	9,800	8	5	129	2016	64	34,54414	16	19,70953	1284,8	0,0	-67,0	1217,8	627979,7	455407,2	K
B14-16	15,016	7	5	128	2016	64	31,63416	16	24,69878	1386,4	0,0	-67,1	1319,3	624219,7	449839,3	K
B14-16	14,684	11	10	285	2016	64	31,64201	16	24,68534	1383,1	0,0	-67,1	1316,0	624229,9	449854,3	K
B15-16	20,537	6	5	127	2016	64	28,48751	16	30,01639	1470,6	0,0	-67,2	1403,4	620199,7	443826,2	K
B15-16	18,789	11	10	285	2016	64	28,49210	16	30,00525	1466,4	0,0	-67,2	1399,2	620208,3	443835,1	K
B16-16	12,657	7	5	128	2016	64	24,11856	16	40,84751	1596,1	0,0	-67,3	1528,7	611821,2	435383,3	K
B16-16	17,307	14	10	288	2016	64	24,11883	16	40,84690	1592,2	0,0	-67,3	1524,9	611821,7	435383,9	K
B17-16	21,747	7	5	128	2016	64	36,73489	16	28,79601	1282,1	0,0	-67,1	1215,0	620566,6	459176,5	K
B17-16	14,061	11	10	285	2016	64	36,74339	16	28,78974	1279,4	0,0	-67,1	1212,3	620570,9	459192,5	K
B18-16	12,348	7	5	128	2016	64	31,58308	16	0,12763	1382,5	0,0	-66,9	1315,5	643864,0	450612,8	K
B18-16	11,783	10	10	284	2016	64	31,58845	16	0,13057	1378,7	-0,4	-66,9	1311,4	643861,2	450622,6	K
B19-16	13,214	8	5	129	2016	64	27,99417	15	55,97825	1506,7	0,0	-66,9	1439,8	647503,6	444111,7	K
B19-16	11,552	10	10	284	2016	64	27,99461	15	55,97858	1502,1	0,0	-66,9	1435,2	647503,3	444112,5	K
BB0-16	17,500	8	5	129	2016	64	22,71540	16	5,05440	1587,8	0,0	-66,9	1520,9	640686,0	433969,9	K
BB0-16	10,098	10	10	284	2016	64	22,71518	16	5,05531	1583,7	0,0	-66,9	1516,8	640685,3	433969,4	K
BB08-16	14,966	4	6	156	2016	64	37,18999	17	29,51508	1982,3	0,0	-67,9	1914,4	572142,7	458479,2	K
BB09-16	15,736	4	6	156	2016	64	36,51602	17	30,55471	1980,6	0,0	-67,9	1912,7	571343,5	457207,6	K
BB10-16	15,896	4	6	156	2016	64	35,95404	17	30,93248	1956,5	0,0	-67,9	1888,6	571066,7	456156,6	K
BB11-16	16,169	4	6	156	2016	64	36,00805	17	31,40758	1957,8	0,0	-67,9	1889,9	570685,4	456248,1	K
BB15-16	16,619	4	6	156	2016	64	38,10215	17	30,62676	1998,5	0,0	-67,9	1930,6	571216,6	460152,5	K
BB17-16	16,868	4	6	156	2016	64	38,58228	17	28,86616	1979,0	0,0	-67,9	1911,1	572597,8	461077,7	K
BB18-16	17,037	4	6	156	2016	64	39,51877	17	26,68567	1968,8	0,0	-67,9	1900,9	574291,6	462859,4	K
BB19-16	17,518	4	6	156	2016	64	39,10375	17	22,91469	1935,1	0,0	-67,8	1867,3	577313,0	462163,9	K
BB20-16	17,368	4	6	156	2016	64	38,96929	17	23,49472	1941,6	0,0	-67,9	1873,7	576857,5	461902,3	K
BB21-16	17,229	4	6	156	2016	64	38,66886	17	24,79352	1927,0	0,0	-67,9	1859,2	575837,4	461318,2	K
BB22-16	17,671	4	6	156	2016	64	38,43721	17	25,62078	1934,7	0,0	-67,9	1866,8	575189,3	460871,4	K
BB23-16	16,396	4	6	156	2016	64	37,13683	17	27,52905	1966,5	0,0	-67,9	1898,6	573728,2	458418,6	K
BB24-16	17,854	4	6	156	2016	64	37,19125	17	24,57016	1939,9	0,0	-67,9	1872,1	576084,3	458578,1	K
BB31-16	14,123	5	6	157	2016	64	42,04969	17	15,18152	1529,3	0,0	-67,6	1461,7	583318,5	467799,2	K
BB35-16	14,387	5	6	157	2016	64	40,99018	17	18,18294	1606,9	0,0	-67,7	1539,2	580986,1	465766,4	K
BB36-16	14,611	5	6	157	2016	64	40,13164	17	20,26209	1719,4	0,0	-67,8	1651,6	579374,7	464127,8	K
BB42-16	13,234	5	6	157	2016	64	35,54761	17	31,72620	1922,1	0,0	-67,9	1854,2	570451,1	455386,9	K
BB43-16	14,040	4	6	156	2016	64	34,91612	17	32,80232	1824,0	0,0	-67,9	1756,2	569619,4	454194,1	K
BB43b-16	13,016	5	6	157	2016	64	34,94985	17	32,82783	1825,0	0,0	-67,9	1757,2	569597,6	454256,2	K
BB44-16	13,683	4	6	156	2016	64	34,14560	17	35,90103	1749,6	0,0	-67,9	1681,8	567177,5	452706,9	K
BB45-16	13,566	4	6	156	2016	64	34,08236	17	36,05973	1740,4	0,0	-67,8	1672,5	567053,3	452586,6	K
BB46-16	13,259	4	6	156	2016	64	33,53921	17	36,60006	1727,9	0,0	-67,8	1660,1	566644,0	451568,2	K

Bor-16	18,758	6	6	158	2016	64	24,94384	17	20,14292	1473,9	0,0	-67,7	1406,2	580212,3	435921,2	K
Bor-16	10,787	16	10	290	2016	64	24,94034	17	20,14117	1468,0	0,0	-67,7	1400,3	580213,9	435914,8	K
BORTHNb	13,880	16	10	290	2016	64	25,06017	17	19,16411	1470,7	0,0	-67,7	1403,0	580992,6	436158,1	K
BORTHNb1	12,000	6	6	158	2016	64	25,06469	17	19,16350	1478,2	0,0	-67,7	1410,5	580992,9	436166,5	I
BORTHNb2	13,000	7	8	220	2016	64	25,06050	17	19,16736	1481,6	-0,4	-67,7	1413,5	580990,0	436158,6	I
Br1k	16,768	18	1	18	2016	64	5,73641	16	19,69599	186,5	0,0	-65,9	120,7	630251,9	401930,3	FS
Br1-16	17,569	18	1	18	2016	64	5,83997	16	19,72054	206,6	0,0	-65,9	140,8	630223,9	402121,7	FS
Br2k	16,217	19	1	19	2016	64	6,37974	16	22,54027	285,4	-1,2	-66,0	218,1	627892,6	403027,8	FS
Br2k	12,000	5	11	310	2016	64	6,37746	16	22,53938					627893,5	403023,6	I
Br3n	15,533	19	1	19	2016	64	8,48909	16	24,07551	459,1	-1,2	-66,3	391,6	626485,3	406892,3	FS
Br3O	15,533	19	1	19	2016	64	8,48909	16	24,07551	459,1	-1,2	-66,3	391,6	626485,3	406892,3	FS
Br3q	15,700	19	1	19	2016	64	8,48003	16	24,06190	458,5	-1,6	-66,3	390,6	626497,0	406875,9	FS
Br3-16	15,533	19	1	19	2016	64	8,48909	16	24,07551	459,1	-1,2	-66,3	391,6	626485,3	406892,3	FS
Br4esnjo	11,417	19	1	19	2016	64	10,43383	16	20,25252	558,3	0,2	-66,3	492,1	629432,5	410631,5	FS
Br4e-is	11,417	19	1	19	2016	64	10,43383	16	20,25252	558,3	-0,5	-66,3	491,5	629432,5	410631,5	FS
Br4-16	14,200	19	1	19	2016	64	10,93101	16	20,18430	603,5	-1,9	-66,4	535,2	629448,8	411556,8	FS
Br4-16	21,118	8	5	129	2016	64	10,88338	16	20,18523	600,0	0,0	-66,4	533,6	629451,8	411468,3	K
Br7-16	13,682	8	5	129	2016	64	22,14362	16	16,94145	1314,9	0,0	-67,0	1247,9	631178,6	432482,5	K
Br7-16	10,300	10	10	284	2016	64	22,11930	16	16,93848	1310,4	-0,7	-67,0	1242,7	631182,9	432437,5	K
Bru-16	20,505	7	5	128	2016	64	41,00285	15	55,22533	829,1	0,0	-66,7	762,3	646929,6	468282,4	K
Bru-16	14,591	10	10	284	2016	64	41,00457	15	55,22498	822,5	0,0	-66,7	755,7	646929,8	468285,6	K
Bud-16	21,015	7	5	128	2016	64	35,98980	15	59,87602	1205,0	0,0	-66,9	1138,1	643676,5	458800,8	K
Bud-16	12,871	10	10	284	2016	64	35,99880	15	59,87374	1201,1	0,0	-66,9	1134,2	643677,5	458817,6	K
D05-16	20,278	6	5	127	2016	64	42,24635	16	54,64840	1271,3	0,0	-67,4	1204,0	599622,4	468659,6	K
D05-16	15,347	14	10	288	2016	64	42,25333	16	54,63788	1267,3	0,0	-67,4	1199,9	599630,3	468672,9	K
D07-16	19,165	6	5	127	2016	64	38,29161	16	59,23101	1442,0	0,0	-67,5	1374,5	596215,6	461197,3	K
D07-16	14,751	14	10	288	2016	64	38,30362	16	59,21960	1438,7	0,0	-67,5	1371,2	596223,9	461219,9	K
D09-16	17,258	6	5	127	2016	64	31,81021	17	0,55819	1652,6	0,0	-67,6	1585,1	595537,7	449127,4	K
D09-16	14,091	14	10	288	2016	64	31,81436	17	0,55948	1649,3	0,0	-67,6	1581,8	595536,4	449135,0	K
D12-16	15,818	6	5	127	2016	64	28,96711	17	0,14278	1717,2	0,0	-67,6	1649,6	596036,8	443858,0	K
D12-16	13,625	14	10	288	2016	64	28,96754	17	0,14276	1714,3	0,0	-67,6	1646,7	596036,8	443858,8	K
E01-16	10,054	8	5	129	2016	64	41,06186	15	34,09628	769,7	0,0	-66,7	703,0	663709,5	469257,1	K
E01-16	15,358	10	10	284	2016	64	41,06158	15	34,09760	763,1	0,0	-66,7	696,4	663708,5	469256,5	K
E02-16	10,454	8	5	129	2016	64	39,13467	15	35,97798	1022,0	0,0	-66,8	955,2	662407,3	465600,7	K
E02-16	14,496	10	10	284	2016	64	39,14276	15	35,97550	1017,1	0,0	-66,8	950,3	662408,5	465615,8	K
E03-16	11,232	8	5	129	2016	64	36,66417	15	36,91310	1257,0	0,0	-66,9	1190,1	661909,3	460977,2	K
E03-16	13,251	10	10	284	2016	64	36,66813	15	36,91565	1252,3	0,0	-66,9	1185,5	661906,9	460984,4	K
E04-16	11,839	8	5	129	2016	64	34,95343	15	37,08986	1357,2	0,0	-66,8	1290,4	661938,5	457795,6	K
E04-16	12,427	10	10	284	2016	64	34,95420	15	37,08934	1352,9	-0,3	-66,8	1285,8	661938,8	457797,1	K
Fl01-16	17,946	8	5	129	2016	64	26,16440	15	55,62825	1415,4	0,0	-66,8	1348,6	647949,1	440729,6	K
Fl01-16	11,080	10	10	284	2016	64	26,15838	15	55,61463	1410,4	0,0	-66,8	1343,6	647960,6	440718,9	K
G02-16	17,997	8	6	160	2016	64	26,84951	17	17,71799	1631,4	0,0	-67,7	1563,7	582064,2	439512,6	K
G02-16	19,916	15	10	289	2016	64	26,84633	17	17,72097	1629,0	0,0	-67,7	1561,3	582062,0	439506,6	K
G03-16	17,811	8	6	160	2016	64	28,45075	17	16,34518	1725,7	0,0	-67,7	1658,0	583084,1	442516,5	K
G03-16	19,679	15	10	289	2016	64	28,44912	17	16,34610	1723,7	0,0	-67,7	1656,0	583083,5	442513,4	K
G04-16	17,589	8	6	160	2016	64	30,02733	17	15,04842	1754,6	0,0	-67,7	1686,9	584042,2	445473,2	K
G04-16	19,362	15	10	289	2016	64	30,02772	17	15,04808	1752,3	0,0	-67,7	1684,6	584042,5	445473,9	K
GengSigb	18,337	6	6	158	2016	64	40,17363	16	41,07042	1675,6	0,0	-67,3	1608,3	610549,8	465187,0	K
gb2-16	15,252	7	5	128	2016	64	34,10626	16	0,01014	1271,5	0,0	-66,9	1204,6	643735,6	455300,0	K
gb2-16	12,451	10	10	284	2016	64	34,11369	16	0,01146	1267,6	0,0	-66,9	1200,7	643733,9	455313,8	K
Go1-16	13,022	5	6	157	2016	64	33,97271	17	24,93917	1827,4	0,0	-67,8	1759,6	575940,1	452592,6	K
Go1-16	17,768	15	10	289	2016	64	33,97134	17	24,93833	1825,0	0,0	-67,8	1757,2	575940,8	452590,0	K
Go1seisa	20,543	5	6	157	2016	64	33,97493	17	24,93220	1827,3	0,0	-67,8	1759,5	575945,5	452596,8	K
HAAB-16	12,079	10	6	162	2016	64	20,97420	17	24,11570	1798,4	0,0	-67,5	1730,9	577208,2	428465,6	K
HAAB-16	11,225	16	10	290	2016	64	20,97439	17	24,11569	1795,5	0,0	-67,5	1728,0	577208,2	428466,0	K
Hof01-16	12,504	8	5	129	2016	64	32,30691	15	35,84253	1208,2	0,0	-66,7	1141,5	663197,6	452938,9	K
Hof01-16	12,840	10	10	284	2016	64	32,30041	15	35,84176	1203,4	0,0	-66,7	1136,7	663198,8	452926,9	K
HveDvb1b	15,258	6	6	158	2016	64	40,44693	16	41,60961	1706,1	0,0	-67,3	1638,8	610102,5	465678,8	K

K01-16	12,340	6	5	127	2016	64	35,16276	17	51,79858	1126,3	0,0	-67,6	1058,7	554446,2	454341,5	K
K01-16	17,019	15	10	289	2016	64	35,16405	17	51,80537	1121,0	0,0	-67,6	1053,4	554440,8	454343,8	K
K02-16	11,573	6	5	127	2016	64	34,81247	17	49,67798	1244,7	0,0	-67,6	1177,1	556151,0	453721,7	K
K02-16	16,401	15	10	289	2016	64	34,81502	17	49,69004	1239,8	0,0	-67,6	1172,1	556141,3	453726,3	K
K03-16	10,844	6	5	127	2016	64	34,24763	17	46,40186	1364,4	0,0	-67,7	1296,7	558787,0	452722,1	K
K03-16	16,207	15	10	289	2016	64	34,25003	17	46,41679	1360,5	0,0	-67,7	1292,8	558775,0	452726,3	K
K04-16	13,782	6	5	127	2016	64	33,20469	17	42,26625	1556,1	0,0	-67,7	1488,4	562129,6	450850,6	K
K04-16	16,459	15	10	289	2016	64	33,20792	17	42,28797	1552,0	0,0	-67,7	1484,2	562112,1	450856,2	K
K05-16	14,522	6	5	127	2016	64	33,44738	17	35,43519	1749,8	0,0	-67,8	1682,0	567578,5	451418,2	K
K05-16	16,954	15	10	289	2016	64	33,44459	17	35,44976	1745,9	0,0	-67,8	1678,1	567566,9	451412,8	K
K06-16	16,234	5	6	157	2016	64	38,35233	17	31,36633	2017,3	0,0	-67,9	1949,4	570616,5	460603,3	K
K06-16	18,000	15	10	289	2016	64	38,35200	17	31,36070					570621,0	460602,8	I
K07-16	9,479	6	5	127	2016	64	29,11772	17	42,03436	1602,3	0,0	-67,7	1534,6	562471,0	443262,4	K
K07-16	15,861	15	10	289	2016	64	29,11770	17	42,03607	1598,7	0,0	-67,7	1531,0	562469,6	443262,4	K
S01-16	15,605	4	5	125	2016	64	7,01219	17	49,97499	800,1	0,0	-66,8	733,2	556867,4	402072,9	K
S01-16	12,964	15	10	289	2016	64	7,01425	17	49,97600	798,1	0,0	-66,8	731,2	556866,5	402076,7	K
S02-16	14,380	4	5	125	2016	64	12,16588	17	48,96097	1075,7	0,0	-67,1	1008,7	557511,5	411662,3	K
S02-16	11,098	15	10	289	2016	64	12,15661	17	48,96481	1070,6	0,0	-67,1	1003,5	557508,7	411645,0	K
S04e	10,709	15	10	289	2016	64	15,97419	17	48,48000	1216,7	0,0	-67,2	1149,5	557767,4	418744,3	K
S04o	10,589	15	10	289	2016	64	16,14849	17	48,23894	1222,3	0,0	-67,2	1155,1	557956,0	419071,7	K
S04-16	18,039	4	5	125	2016	64	16,17412	17	48,20572	1227,4	0,0	-67,2	1160,2	557981,9	419119,9	K
S04-16	10,758	15	10	289	2016	64	16,16294	17	48,21734	1223,0	0,0	-67,2	1155,8	557972,9	419098,9	K
Skf01-16	11,254	9	5	130	2016	64	17,99511	16	4,97864	1350,7	0,0	-66,6	1284,1	641151,5	425211,7	K
Skf01-16	20,848	9	10	283	2016	64	17,99276	16	4,96368	1345,7	-0,4	-66,6	1278,7	641163,7	425207,9	K
T01-16	21,173	3	5	124	2016	64	19,48713	18	8,22802	800,7	0,0	-67,3	733,4	541728,8	425011,5	K
T01-16	15,879	16	10	290	2016	64	19,48743	18	8,22781	792,2	0,0	-67,3	724,9	541729,0	425012,1	K
T02-16	22,016	3	5	124	2016	64	19,59893	18	3,96425	1004,2	0,0	-67,3	937,0	545162,2	425268,0	K
T02-16	15,058	16	10	290	2016	64	19,59910	18	3,97002	997,3	0,0	-67,3	930,1	545157,5	425268,3	K
T03-16	11,266	4	5	125	2016	64	20,20676	17	58,59171	1142,2	0,0	-67,3	1074,9	549473,5	426464,3	K
T03-16	14,548	16	10	290	2016	64	20,20537	17	58,60069	1117,1	0,0	-67,3	1049,8	549466,3	426461,6	K
T04-16	13,354	4	5	125	2016	64	21,32921	17	51,48191	1290,9	0,0	-67,4	1223,5	555163,3	428647,6	K
T04-16	13,605	16	10	290	2016	64	21,32606	17	51,49329	1286,6	0,0	-67,4	1219,2	555154,2	428641,5	K
T05-16	15,207	4	5	125	2016	64	22,27330	17	42,98377	1413,3	0,0	-67,5	1345,9	561968,5	430532,6	K
T05-16	15,433	15	10	289	2016	64	22,27032	17	42,99491	1409,6	0,0	-67,5	1342,2	561959,7	430526,9	K
T05rorg	15,016	15	10	289	2016	64	22,27277	17	43,06658	1408,9	2,7	-67,5	1344,1	561901,9	430530,3	K
T06-16	18,215	4	5	125	2016	64	24,26818	17	36,52071	1535,8	0,0	-67,6	1468,2	567086,5	434348,2	K
T06-16	12,893	16	10	290	2016	64	24,26442	17	36,53146	1531,5	0,0	-67,6	1463,8	567078,0	434341,0	K
T07-16	21,839	5	5	126	2016	64	25,29045	17	31,18522	1632,5	0,0	-67,7	1564,8	571329,0	436344,4	K
T07-16	11,662	16	10	290	2016	64	25,28847	17	31,19361	1628,6	0,0	-67,7	1560,9	571322,3	436340,6	K
T08-16	22,222	5	5	126	2016	64	26,28397	17	27,75461	1705,9	0,0	-67,8	1638,1	574038,8	438255,6	K
T08-16	11,244	16	10	290	2016	64	26,28357	17	27,75604	1702,3	0,0	-67,8	1634,5	574037,6	438254,8	K

Appendix D: Measured surface velocity on Vatnajökull in 2016.

Site	Calendar day date	#	Calendar day date	#	# of days	translation (m)	(°)	velocity (cm/day)	(m/annum)
B07-16	160508	129	161010	284	155	1,19	159	0,77	2,81
B09-16	160507	128	161011	285	157	1,22	263	0,78	2,84
B10-16	160507	128	161011	285	157	1,67	135	1,06	3,88
B11-16	160507	128	161011	285	157	9,50	19	6,05	22,09
B12-16	160507	128	161011	285	157	17,35	22	11,05	40,33
B13-16	160507	128	161011	285	157	20,21	27	12,87	46,97
B13ror15	151024	297	160508	129	197	4,52	27	2,30	8,38
B14-16	160507	128	161011	285	157	18,08	36	11,52	42,03
B15-16	160506	127	161011	285	158	12,33	46	7,80	28,48
B16-16	160507	128	161014	288	160	0,70	44	0,44	1,60
B17-16	160507	128	161011	285	157	16,52	18	10,52	38,40
B18-16	160507	128	161010	284	156	10,22	347	6,55	23,91
B19-16	160508	129	161010	284	155	0,86	342	0,55	2,02
BB0-16	160508	129	161010	284	155	0,84	241	0,54	1,97
Bor-16	160606	158	161016	290	132	6,63	168	5,02	18,34
BORTHNb	151025	298	161016	290	357	21,41	187	6,00	21,89
Br1k	150415	105	160118	18	278	2,09	155	0,75	2,74
Br2k	150415	105	160119	19	279	9,42	178	3,37	12,32
Br2k	160119	19	161105	310	291	4,28	170	1,47	5,37
Br3n	101013	286	160119	19	1923	133,53	147	6,94	25,34
Br3O	130131	31	160119	19	1083	70,04	148	6,47	23,61
Br3q	150415	105	160119	19	279	20,31	150	7,28	26,58
Br4esnjo	150415	105	160119	19	279	250,59	182	89,82	327,83
Br4-16	160119	19	160508	129	110	88,21	180	80,19	292,71
Br7-16	160508	129	161010	284	155	45,10	177	29,10	106,21
Bru-16	160507	128	161010	284	156	3,20	5	2,05	7,48
Bud-16	160507	128	161010	284	156	16,77	6	10,75	39,23
D05-16	160506	127	161014	288	161	15,39	33	9,56	34,90
D07-16	160506	127	161014	288	161	24,03	22	14,92	54,47
D09-16	160506	127	161014	288	161	7,75	352	4,82	17,58
D12-16	160506	127	161014	288	161	0,80	1	0,49	1,81
E01-16	160508	129	161010	284	155	1,17	244	0,76	2,76
E02-16	160508	129	161010	284	155	15,11	8	9,75	35,59
E03-16	160508	129	161010	284	155	7,61	345	4,91	17,92
E04-16	160508	129	161010	284	155	1,49	16	0,96	3,50
Fl01-16	160508	129	161010	284	155	15,61	136	10,07	36,76
G02-16	160608	160	161015	289	129	6,36	202	4,93	17,98
G03-16	160608	160	161015	289	129	3,11	194	2,41	8,79
G04-16	160608	160	161015	289	129	0,77	21	0,60	2,18
gb2-16	160507	128	161010	284	156	13,80	356	8,85	32,29
Go1-16	160605	157	161015	289	132	2,62	165	1,99	7,26
HAAB-16	160610	162	161016	290	128	0,35	1	0,27	1,00
Hof01-16	160508	129	161010	284	155	12,05	177	7,78	28,38

K01-16	160506	127	161015	289	162	5,92	294	3,66	13,34
K02-16	160506	127	161015	289	162	10,72	296	6,62	24,16
K03-16	160506	127	161015	289	162	12,72	290	7,85	28,67
K04-16	160506	127	161015	289	162	18,36	289	11,33	41,36
K05-16	160506	127	161015	289	162	12,73	246	7,86	28,69
K06-16	160605	157	161015	289	132	4,53	98	3,43	12,51
K07-16	160506	127	161015	289	162	1,37	268	0,85	3,09
S01-16	160504	125	161015	289	164	3,90	348	2,38	8,68
S02-16	160504	125	161015	289	164	17,45	190	10,64	38,83
S04e	60925	268	161015	289	3671	397,28	204	10,82	39,50
S04o	151026	299	161015	289	355	40,36	205	11,37	41,49
S04-16	160504	125	161015	289	164	22,73	204	13,86	50,59
Skf01-16	160509	130	161009	283	153	12,83	110	8,38	30,60
T01-16	160503	124	161016	290	166	0,58	17	0,35	1,28
T02-16	160503	124	161016	290	166	4,66	274	2,81	10,24
T03-16	160504	125	161016	290	165	7,68	250	4,65	16,98
T04-16	160504	125	161016	290	165	10,86	238	6,58	24,02
T05-16	160504	125	161015	289	164	10,52	238	6,42	23,42
T05rorg	151027	300	161015	289	354	20,12	240	5,68	20,75
T06-16	160504	125	161016	290	165	11,09	231	6,72	24,54
T07-16	160505	126	161016	290	164	7,67	241	4,68	17,07
T08-16	160505	126	161016	290	164	1,37	237	0,83	3,04

Appendix E: Melt water runoff to selected rivers in summer 2016, derived from summer balance.

ΔS: area in a given elevation range where summer balance is negative, **∑ΔS**: cumulative area above a given elevation, **ΔQ_s**: melt water runoff from a given elevation range, **$\sum\Delta Q_s$** : cumulative melt water runoff from an area above given elevation.

Tungnaá water drainage basin

Elevation (m a. s. l.)		ΔS km²	∑ΔS km²	ΔQ_s ($10^6 m^3$)	$\sum\Delta Q_s$ ($10^6 m^3$)
1350	1400	0,4	0,4	0,6	0,6
1300	1350	6,1	6,4	10,8	11,4
1250	1300	10,2	16,7	20,6	32,0
1200	1250	10,9	27,6	25,1	57,1
1150	1200	9,9	37,5	27,8	85,0
1100	1150	11,9	49,4	39,9	124,9
1050	1100	11,9	61,4	45,4	170,2
1000	1050	9,6	71,0	40,5	210,7
950	1000	9,6	80,6	43,3	254,0
900	950	9,2	89,8	44,6	298,6
850	900	7,8	97,5	41,3	339,9
800	850	7,7	105,2	44,8	384,7
750	800	7,0	112,1	45,3	430,0
700	750	4,7	116,9	33,0	463,0
650	700	2,1	119,0	15,3	478,3

Sylgja water drainage basin

Elevation (m a. s. l.)		ΔS km²	∑ΔS km²	ΔQ_s ($10^6 m^3$)	$\sum\Delta Q_s$ ($10^6 m^3$)
1300	1350	1,1	1,1	2,1	2,1
1250	1300	3,6	4,7	7,3	9,4
1200	1250	5,9	10,5	13,6	23,0
1150	1200	8,3	18,8	22,6	45,6
1100	1150	6,1	24,9	20,2	65,8
1050	1100	6,9	31,8	26,4	92,2
1000	1050	5,1	36,9	21,3	113,6
950	1000	1,8	38,7	7,8	121,4
900	950	0,7	39,3	3,1	124,5
850	900	0,0	39,4	0,3	124,8

Western Skaftá cauldron water drainage basin

Elevation (m a. s. l.)		ΔS km²	∑ΔS km²	ΔQ_s ($10^6 m^3$)	$\sum\Delta Q_s$ ($10^6 m^3$)
1700	1750	2,5	2,5	1,4	1,4
1650	1700	7,2	9,7	4,3	5,8
1600	1650	8,5	18,2	5,7	11,5
1550	1600	5,4	23,6	4,1	15,6
1500	1550	1,5	25,1	1,2	16,8

Eastern Skaftár cauldoron water drainage basin

Elevation (m a. s. l.)		ΔS km^2	∑ΔS km^2	$ΔQ_s$ (10^6m^3)	$∑ΔQ_s$ (10^6m^3)
1750	1800	2,4	2,4	1,2	1,2
1700	1750	9,9	12,3	5,7	6,9
1650	1700	14,9	27,2	9,6	16,6
1600	1650	9,7	36,9	6,4	23,0
1550	1600	2,4	39,3	1,6	24,5

Grímsvötn water drainage basin

Elevation (m a. s. l.)		ΔS km^2	∑ΔS km^2	$ΔQ_s$ (10^6m^3)	$∑ΔQ_s$ (10^6m^3)
1900	1950	0,4	0,4	0,1	0,1
1850	1900	1,3	1,8	0,5	0,6
1800	1850	1,7	3,4	0,7	1,4
1750	1800	4,3	7,7	2,4	3,7
1700	1750	18,6	26,3	12,0	15,7
1650	1700	53,3	79,6	38,1	53,8
1600	1650	30,9	110,4	25,9	79,7
1550	1600	19,3	129,7	17,8	97,6
1500	1550	16,8	146,4	17,7	115,3
1450	1500	10,0	156,5	12,2	127,4
1400	1450	11,7	168,2	15,7	143,1
1350	1400	4,3	172,5	5,7	148,9
1300	1350	0,7	173,2	0,9	149,8

Kaldakvísl water drainage basin

Elevation (m a. s. l.)		ΔS km^2	∑ΔS km^2	$ΔQ_s$ (10^6m^3)	$∑ΔQ_s$ (10^6m^3)
1950	2000	1,7	1,7	0,4	0,4
1900	1950	14,7	16,4	4,4	4,8
1850	1900	6,9	23,4	2,8	7,6
1800	1850	6,5	29,8	3,0	10,6
1750	1800	11,4	41,2	5,4	16,0
1700	1750	20,2	61,5	11,3	27,3
1650	1700	17,1	78,5	12,1	39,4
1600	1650	14,5	93,0	12,8	52,3
1550	1600	19,1	112,1	20,2	72,4
1500	1550	25,3	137,4	31,2	103,6
1450	1500	28,8	166,2	36,9	140,6
1400	1450	24,0	190,1	34,3	174,9
1350	1400	22,1	212,3	37,2	212,1
1300	1350	21,2	233,5	42,5	254,6
1250	1300	22,4	255,9	53,5	308,2
1200	1250	21,7	277,5	63,0	371,1
1150	1200	20,0	297,5	68,9	440,0
1100	1150	18,0	315,5	69,8	509,7
1050	1100	16,9	332,3	71,0	580,7
1000	1050	14,6	347,0	65,0	645,7
950	1000	10,4	357,4	48,8	694,4
900	950	6,3	363,7	30,5	724,9
850	900	0,9	364,6	4,3	729,2

Jökulsá á Fjöllum water drainage basin

Elevation (m a. s. l.)		ΔS km^2	∑ΔS km^2	ΔQ_s ($10^6 m^3$)	$\sum\Delta Q_s$ ($10^6 m^3$)
1950	2000	3,7	3,7	0,8	0,8
1900	1950	15,4	19,2	3,5	4,3
1850	1900	28,3	47,4	10,4	14,7
1800	1850	20,0	67,4	9,6	24,3
1750	1800	22,0	89,4	12,2	36,4
1700	1750	34,7	124,1	21,6	58,1
1650	1700	80,8	204,9	53,0	111,0
1600	1650	121,1	326,1	83,3	194,3
1550	1600	100,5	426,6	84,4	278,8
1500	1550	93,6	520,2	86,3	365,1
1450	1500	80,6	600,8	82,1	447,2
1400	1450	69,8	670,5	77,3	524,5
1350	1400	56,3	726,8	70,3	594,9
1300	1350	43,3	770,2	65,5	660,3
1250	1300	47,2	817,4	88,3	748,6
1200	1250	51,6	868,9	121,2	869,8
1150	1200	51,4	920,4	152,2	1022,0
1100	1150	44,8	965,2	155,6	1177,6
1050	1100	32,3	997,5	125,8	1303,4
1000	1050	33,5	1030,9	140,3	1443,8
950	1000	31,0	1061,9	137,9	1581,7
900	950	26,0	1087,9	121,5	1703,2
850	900	23,7	1111,7	114,6	1817,8
800	850	21,6	1133,2	106,7	1924,5
750	800	17,8	1151,0	89,4	2013,9
700	750	5,4	1156,4	27,1	2041,1

Kreppa and Kverká water drainage basin

Elevation (m a. s. l.)		ΔS km^2	∑ΔS km^2	ΔQ_s $(10^6 m^3)$	$\sum\Delta Q_s$ $(10^6 m^3)$
1900	1950	0,1	0,1	0,0	0,0
1850	1900	1,3	1,4	0,7	0,7
1800	1850	4,4	5,8	1,9	2,6
1750	1800	2,7	8,5	1,3	3,9
1700	1750	3,8	12,3	2,0	5,9
1650	1700	5,2	17,5	3,0	8,9
1600	1650	41,4	58,9	23,3	32,2
1550	1600	20,5	79,4	15,9	48,1
1500	1550	13,4	92,8	11,8	59,9
1450	1500	16,3	109,1	15,7	75,6
1400	1450	19,8	128,9	21,3	96,9
1350	1400	25,5	154,4	30,5	127,4
1300	1350	20,0	174,4	26,2	153,6
1250	1300	15,5	189,9	22,0	175,6
1200	1250	17,7	207,6	27,9	203,5
1150	1200	17,7	225,3	31,2	234,7
1100	1150	16,9	242,2	34,9	269,6
1050	1100	11,1	253,3	27,2	296,8
1000	1050	13,4	266,7	39,2	336,0
950	1000	15,1	281,8	51,7	387,7
900	950	13,5	295,3	51,7	439,4
850	900	14,2	309,5	60,1	499,5
800	850	11,0	320,5	50,6	550,1
750	800	10,5	331,0	54,5	604,6
700	750	4,8	335,8	27,9	632,5
650	700	1,8	337,6	11,0	643,5

Hálslón water drainage basin

Elevation (m a. s. l.)		ΔS km^2	∑ΔS km^2	ΔQ_s $(10^6 m^3)$	$\sum\Delta Q_s$ $(10^6 m^3)$
1600	1650	11,2	11,2	7,5	7,5
1550	1600	31,8	43,0	24,8	32,3
1500	1550	63,6	106,7	56,1	88,4
1450	1500	67,6	174,3	67,2	155,6
1400	1450	97,7	272,0	103,9	259,6
1350	1400	131,7	403,7	155,3	414,9
1300	1350	129,4	533,1	165,9	580,8
1250	1300	126,1	659,2	177,3	758,1
1200	1250	99,2	758,4	158,6	916,7
1150	1200	84,7	843,1	159,5	1076,2
1100	1150	66,5	909,6	148,2	1224,4
1050	1100	58,7	968,3	154,2	1378,6
1000	1050	49,4	1017,7	151,1	1529,7
950	1000	41,4	1059,2	145,6	1675,2
900	950	32,9	1092,0	131,1	1806,3
850	900	28,5	1120,5	126,7	1933,1
800	850	27,2	1147,7	133,2	2066,3
750	800	26,6	1174,3	144,6	2210,9
700	750	20,8	1195,1	123,0	2333,9
650	700	15,7	1210,7	97,1	2431,0
600	650	3,0	1213,7	19,1	2450,1

Jökulsá á Fljótsdal water drainage basin

Elevation (m a. s. l.)		ΔS km^2	∑ΔS km^2	ΔQ_s $(10^6 m^3)$	$\sum \Delta Q_s$ $(10^6 m^3)$
1500	1550	0,0	0,0	0,0	0,0
1450	1500	0,9	1,0	1,0	1,0
1400	1450	1,9	2,9	2,0	3,1
1350	1400	2,8	5,8	3,3	6,3
1300	1350	5,4	11,2	6,8	13,1
1250	1300	16,2	27,4	23,0	36,1
1200	1250	16,0	43,4	25,9	62,0
1150	1200	17,3	60,7	32,6	94,5
1100	1150	15,0	75,7	33,6	128,2
1050	1100	12,4	88,1	34,8	163,0
1000	1050	11,9	100,0	40,0	203,0
950	1000	8,8	108,8	33,9	236,9
900	950	5,5	114,3	23,1	260,0
850	900	4,4	118,7	19,1	279,1
800	850	3,2	121,9	14,7	293,9
750	800	3,0	124,9	14,7	308,6
700	750	2,6	127,5	13,4	322,0
650	700	3,0	130,6	16,8	338,9
600	650	0,2	130,7	0,9	339,8

Hornafjarðarfljót water drainage basin

Elevation (m a. s. l.)		ΔS km^2	∑ΔS km^2	$ΔQ_s$ (10^6m^3)	$∑ΔQ_s$ (10^6m^3)
1450	1500	1,0	1,0	1,0	1,0
1400	1450	8,2	9,2	8,2	9,2
1350	1400	12,7	21,8	13,5	22,7
1300	1350	19,1	40,9	22,8	45,5
1250	1300	37,9	78,9	52,3	97,9
1200	1250	29,1	108,0	45,0	142,8
1150	1200	20,5	128,4	36,5	179,3
1100	1150	19,1	147,5	38,8	218,1
1050	1100	14,5	162,0	34,0	252,1
1000	1050	11,4	173,4	29,8	281,9
950	1000	10,7	184,2	30,5	312,4
900	950	8,2	192,3	25,2	337,6
850	900	5,5	197,8	18,3	356,0
800	850	4,4	202,2	15,2	371,1
750	800	4,2	206,3	15,2	386,3
700	750	3,7	210,1	14,4	400,6
650	700	3,6	213,6	14,5	415,1
600	650	2,6	216,3	11,6	426,7
550	600	1,9	218,2	8,9	435,6
500	550	1,9	220,1	9,3	444,9
450	500	1,3	221,4	6,7	451,6
400	450	1,3	222,7	7,5	459,1
350	400	0,8	223,6	5,1	464,2
300	350	0,9	224,5	5,8	470,1
250	300	1,5	225,9	10,0	480,1
200	250	2,9	228,8	20,9	501,0
150	200	3,1	232,0	24,8	525,8
100	150	2,4	234,4	20,3	546,1
50	100	1,8	236,2	16,0	562,1
0	50	2,6	238,9	23,4	585,5

Jökulsá á Breiðamerkursandi water drainage basin

Elevation (m a. s. l.)		ΔS km^2	∑ΔS km^2	ΔQ_s ($10^6 m^3$)	$\sum\Delta Q_s$ ($10^6 m^3$)
1700	1750	1,0	1,0	0,4	0,4
1650	1700	4,2	5,2	2,1	2,6
1600	1650	13,8	19,0	6,9	9,5
1550	1600	19,0	38,0	10,9	20,4
1500	1550	23,2	61,2	17,6	38,0
1450	1500	36,2	97,4	33,2	71,2
1400	1450	51,2	148,6	53,1	124,3
1350	1400	84,2	232,8	100,3	224,6
1300	1350	83,4	316,2	109,8	334,3
1250	1300	51,6	367,9	74,0	408,3
1200	1250	35,1	403,0	55,6	463,9
1150	1200	28,2	431,2	49,1	513,1
1100	1150	24,1	455,3	46,0	559,0
1050	1100	20,5	475,7	42,4	601,4
1000	1050	17,6	493,3	39,4	640,9
950	1000	18,9	512,2	45,4	686,2
900	950	20,0	532,3	50,6	736,8
850	900	19,9	552,2	54,5	791,3
800	850	20,1	572,3	59,2	850,5
750	800	19,5	591,9	61,8	912,3
700	750	19,2	611,1	63,8	976,1
650	700	27,6	638,7	95,3	1071,4
600	650	18,4	657,1	67,9	1139,2
550	600	18,7	675,8	73,1	1212,3
500	550	7,6	683,3	31,3	1243,5
450	500	6,5	689,8	29,3	1272,8
400	450	6,4	696,2	31,0	1303,8
350	400	5,3	701,4	27,3	1331,1
300	350	5,7	707,1	32,1	1363,2
250	300	5,5	712,6	33,1	1396,3
200	250	5,9	718,5	37,9	1434,1
150	200	5,3	723,8	37,0	1471,1
100	150	4,9	728,7	36,2	1507,3
50	100	4,8	733,5	36,7	1544,0
0	50	3,9	737,4	30,0	1574,1

Breiðárlón/Fjallsárlón water drainage basin

Elevation (m a. s. l.)		ΔS km^2	∑ΔS km^2	$ΔQ_s$ ($10^6 m^3$)	∑$ΔQ_s$ ($10^6 m^3$)
1700	1750	0,0	0,0	0,0	0,0
1600	1650	0,4	0,4	0,0	0,0
1550	1600	3,1	3,5	0,8	0,8
1500	1550	5,6	9,1	2,8	3,6
1450	1500	4,9	14,0	3,5	7,1
1400	1450	5,3	19,3	4,8	11,8
1350	1400	6,3	25,7	6,8	18,6
1300	1350	12,6	38,3	17,5	36,2
1250	1300	6,5	44,7	9,5	45,7
1200	1250	5,6	50,4	8,9	54,6
1150	1200	4,9	55,2	8,4	63,0
1100	1150	4,5	59,7	8,5	71,5
1050	1100	5,0	64,6	10,0	81,5
1000	1050	6,0	70,6	12,6	94,1
950	1000	6,9	77,5	16,5	110,6
900	950	8,3	85,8	21,3	131,9
850	900	6,6	92,4	18,3	150,2
800	850	8,1	100,5	24,1	174,3
750	800	8,7	109,2	27,7	202,0
700	750	6,2	115,4	20,8	222,7
650	700	7,1	122,5	24,7	247,4
600	650	7,9	130,4	29,0	276,5
550	600	8,6	139,0	34,1	310,6
500	550	8,7	147,6	36,2	346,8
450	500	9,1	156,7	40,4	387,2
400	450	11,0	167,7	52,4	439,7
350	400	8,9	176,6	46,9	486,6
300	350	6,9	183,5	39,3	525,8
250	300	6,9	190,4	42,7	568,6
200	250	7,1	197,4	46,6	615,2
150	200	5,3	202,7	37,2	652,3
100	150	4,3	207,1	32,0	684,3
50	100	4,1	211,1	30,9	715,2
0	50	3,3	214,4	25,6	740,8

Skeiðarársandur (Gígja) water drainage basin (Gígja)

Elevation (m a. s. l.)		ΔS km^2	∑ΔS km^2	ΔQ_s ($10^6 m^3$)	$\sum\Delta Q_s$ ($10^6 m^3$)
1700	1750	1,4	1,4	0,8	0,8
1650	1700	19,7	21,1	12,1	12,9
1600	1650	80,9	102,0	48,8	61,7
1550	1600	82,0	184,0	62,1	123,7
1500	1550	105,5	289,5	93,7	217,4
1450	1500	96,3	385,8	102,2	319,6
1400	1450	92,7	478,5	113,9	433,5
1350	1400	81,5	559,9	113,4	546,9
1300	1350	69,9	629,9	108,4	655,4
1250	1300	62,9	692,8	109,0	764,4
1200	1250	52,5	745,3	101,2	865,6
1150	1200	44,8	790,1	96,7	962,3
1100	1150	37,2	827,4	87,8	1050,1
1050	1100	30,5	857,9	78,7	1128,8
1000	1050	24,6	882,4	68,2	1197,0
950	1000	23,1	905,5	68,1	1265,1
900	950	23,4	928,9	74,2	1339,3
850	900	28,4	957,3	98,5	1437,8
800	850	21,2	978,6	81,2	1519,0
750	800	18,6	997,2	76,9	1595,9
700	750	20,1	1017,2	88,4	1684,2
650	700	14,2	1031,4	67,6	1751,8
600	650	11,6	1043,0	58,3	1810,1
550	600	13,9	1056,8	73,9	1884,0
500	550	9,4	1066,2	52,7	1936,7
450	500	6,3	1072,5	37,5	1974,2
400	450	6,6	1079,1	41,2	2015,4
350	400	9,2	1088,3	60,5	2075,9
300	350	12,3	1100,5	85,0	2160,9
250	300	12,7	1113,3	91,8	2252,7
200	250	12,6	1125,9	94,4	2347,1
150	200	10,5	1136,4	81,7	2428,9
100	150	8,9	1145,3	71,1	2499,9
50	100	7,9	1153,2	64,5	2564,5
0	50	0,2	1153,4	1,4	2565,9

Súla water drainage basin

Elevation (m a. s. l.)		ΔS km^2	∑ΔS km^2	ΔQ_s $(10^6 m^3)$	$\sum\Delta Q_s$ $(10^6 m^3)$
1700	1750	0,5	0,5	0,4	0,4
1650	1700	1,5	2,0	1,2	1,6
1600	1650	2,5	4,5	2,2	3,8
1550	1600	4,0	8,6	3,8	7,6
1500	1550	5,9	14,4	5,8	13,4
1450	1500	11,1	25,5	12,4	25,8
1400	1450	11,0	36,5	13,7	39,5
1350	1400	9,3	45,8	13,7	53,2
1300	1350	8,2	54,0	13,1	66,3
1250	1300	6,6	60,5	11,7	78,1
1200	1250	7,9	68,5	15,8	93,8
1150	1200	8,8	77,3	19,8	113,6
1100	1150	15,2	92,4	35,7	149,3
1050	1100	16,0	108,4	40,3	189,6
1000	1050	16,7	125,1	45,8	235,4
950	1000	18,0	143,1	54,9	290,3
900	950	15,4	158,5	52,1	342,4
850	900	11,4	169,8	41,2	383,7
800	850	11,9	181,7	45,7	429,4
750	800	7,4	189,1	31,5	460,8
700	750	5,9	195,0	27,8	488,7
650	700	5,1	200,1	25,1	513,8
600	650	5,6	205,7	28,7	542,5
550	600	11,1	216,8	58,9	601,4
500	550	10,5	227,3	58,5	659,9
450	500	7,3	234,5	43,4	703,2
400	450	6,5	241,0	40,6	743,9
350	400	5,1	246,1	33,2	777,0
300	350	2,7	248,8	18,7	795,7
250	300	1,0	249,8	7,6	803,3
200	250	0,8	250,6	6,2	809,5
150	200	0,7	251,3	5,3	814,8
100	150	0,7	252,0	5,7	820,5
50	100	0,7	252,8	6,1	826,7

Djúpá water drainage basin

Elevation (m a. s. l.)		ΔS km^2	∑ΔS km^2	ΔQ_s $(10^6 m^3)$	$\sum \Delta Q_s$ $(10^6 m^3)$
1450	1500	0,0	0,0	0,1	0,1
1400	1450	0,3	0,4	0,5	0,7
1350	1400	0,7	1,1	1,2	1,9
1300	1350	3,5	4,6	6,2	8,1
1250	1300	3,4	8,0	6,6	14,7
1200	1250	3,0	11,0	6,7	21,4
1150	1200	3,5	14,5	9,1	30,5
1100	1150	5,3	19,9	15,2	45,7
1050	1100	6,1	26,0	19,9	65,5
1000	1050	9,2	35,2	32,8	98,3
950	1000	7,3	42,4	29,5	127,9
900	950	7,8	50,2	35,4	163,2
850	900	6,7	56,9	32,2	195,4
800	850	8,0	64,8	40,4	235,9
750	800	6,6	71,4	35,1	271,0
700	750	3,7	75,1	20,9	291,8
650	700	2,9	78,0	17,3	309,2
600	650	1,0	79,0	6,3	315,5

Brunná water drainage basin

Elevation (m a. s. l.)		ΔS km^2	∑ΔS km^2	ΔQ_s $(10^6 m^3)$	$\sum \Delta Q_s$ $(10^6 m^3)$
1050	1100	0,0	0,0	0,0	0,0
1000	1050	0,9	1,0	3,5	3,5
950	1000	2,5	3,5	10,3	13,8
900	950	4,3	7,8	19,5	33,2
850	900	4,2	12,0	20,1	53,3
800	850	4,2	16,2	20,8	74,1
750	800	4,6	20,7	24,1	98,3
700	750	5,6	26,4	31,8	130,1
650	700	4,8	31,2	29,0	159,2
600	650	3,2	34,4	20,1	179,2
550	600	0,5	34,9	3,3	182,5

Hverfisfljót water drainage basin

Elevation (m a. s. l.)		ΔS km^2	∑ΔS km^2	ΔQ$_s$ ($10^6 m^3$)	∑ΔQ$_s$ ($10^6 m^3$)
1700	1750	0,9	0,9	0,7	0,7
1650	1700	5,5	6,4	4,6	5,3
1600	1650	9,1	15,5	7,9	13,2
1550	1600	9,6	25,1	8,6	21,8
1500	1550	19,9	45,0	19,3	41,1
1450	1500	41,1	86,1	48,4	89,5
1400	1450	27,6	113,7	38,9	128,4
1350	1400	24,1	137,8	38,6	166,9
1300	1350	22,8	160,6	40,3	207,2
1250	1300	18,1	178,7	35,9	243,1
1200	1250	20,2	198,9	45,7	288,9
1150	1200	14,6	213,5	38,9	327,8
1100	1150	11,1	224,6	33,2	361,0
1050	1100	9,6	234,1	31,2	392,2
1000	1050	9,0	243,1	32,4	424,6
950	1000	8,9	252,0	35,9	460,5
900	950	8,6	260,5	38,5	499,0
850	900	7,8	268,3	37,5	536,5
800	850	7,3	275,5	36,8	573,3
750	800	10,1	285,6	53,5	626,9
700	750	12,1	297,7	68,7	695,5
650	700	10,5	308,2	63,7	759,3
600	650	6,2	314,4	39,0	798,2
550	600	1,0	315,4	6,5	804,8

Skaftá water drainage basin

Elevation (m a. s. l.)		ΔS km^2	∑ΔS km^2	ΔQ$_s$ ($10^6 m^3$)	∑ΔQ$_s$ ($10^6 m^3$)
1650	1700	2,2	2,2	1,7	1,7
1600	1650	15,6	17,8	12,6	14,3
1550	1600	22,7	40,4	17,6	31,9
1500	1550	30,8	71,2	29,6	61,5
1450	1500	24,5	95,7	30,8	92,2
1400	1450	22,3	118,0	32,4	124,6
1350	1400	20,5	138,5	32,2	156,9
1300	1350	22,5	161,0	39,1	196,0
1250	1300	15,6	176,6	31,0	227,0
1200	1250	21,0	197,6	48,6	275,6
1150	1200	22,7	220,2	61,2	336,8
1100	1150	23,7	243,9	72,9	409,7
1050	1100	24,2	268,1	84,2	493,9
1000	1050	26,2	294,3	101,7	595,6
950	1000	20,6	314,9	88,9	684,5
900	950	16,7	331,7	78,9	763,4
850	900	14,4	346,0	73,3	836,7
800	850	14,8	360,8	82,5	919,3
750	800	12,3	373,1	74,7	993,9
700	750	9,7	382,8	63,5	1057,4
650	700	5,8	388,6	39,9	1097,3
600	650	1,1	389,7	7,9	1105,2

Appendix F: MODIS satellite images of Vatnajökull and vicinity 2015-2016.

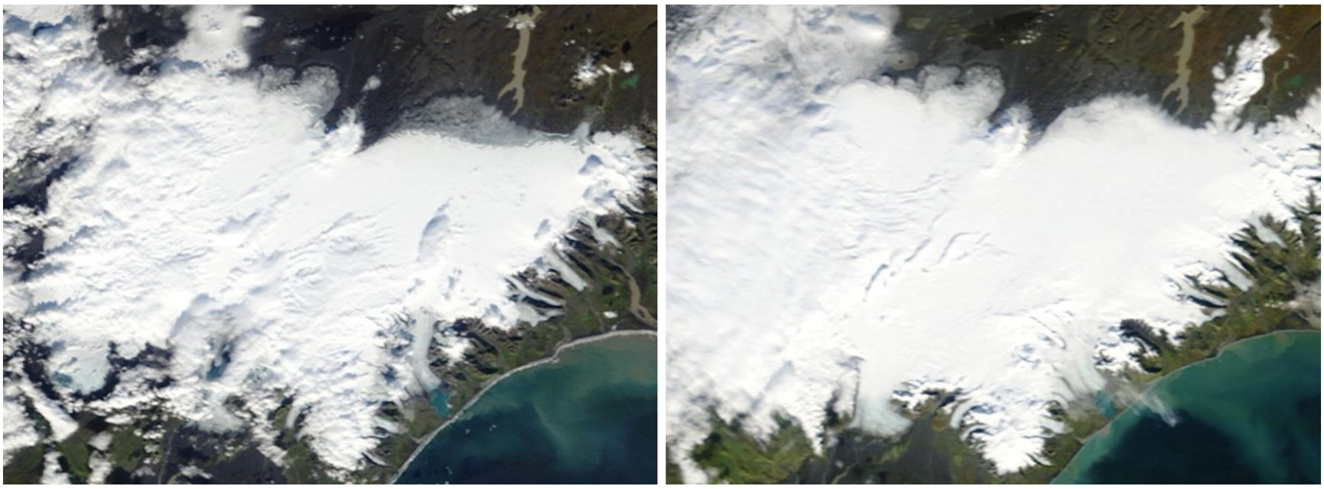

Left: September 10th 2015, still melt and upward migration of the snowline in the north.
Right: October 9th, winter has settled in, fresh snow on most of the glacier.

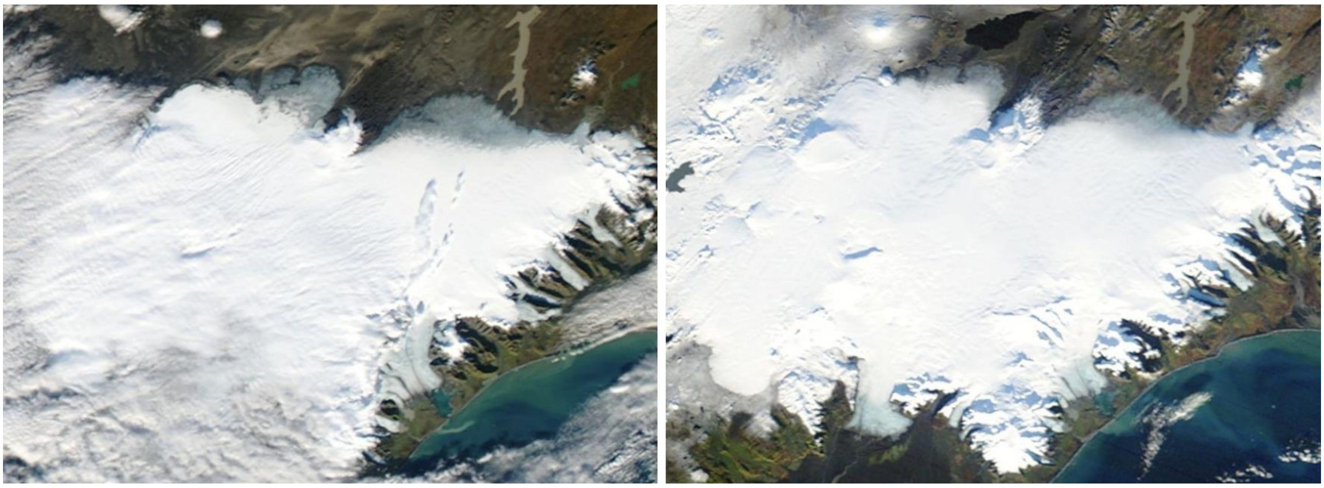

Left: October 17th, the fresh snow on the ablation zone of the N outlets (visible on Oct. 9th) has melted and the snowline has raised slightly. Note the dust storm to the ENE from the region north of Bárðarbunga and Dyngjujökull. Snow cover up to 1.2 m was measured north of Grímsvötn and on Bárðarbunga in the autumn mass balance expedition (October 22-28th).
Right: November 9th; The ~ 80 km^2 fresh lave field in Holuhraun is clearly visible, and so is the ice free surface of Hálslón.

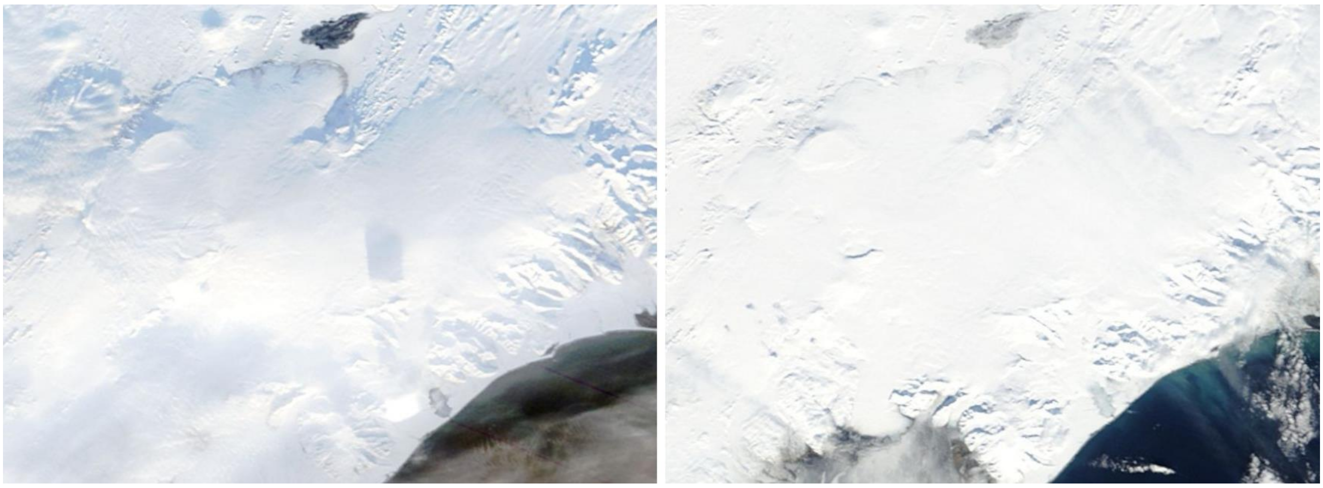

Left: January 28th 2016. Snow everywhere except where snow has melt away from the cooling Holuhraun and the dark tephra ands on Dyngjujökull is visible through thin snow.
Right: March 9th. Snow in the low land getting thinner, now Skeiðarársandur is snow free.

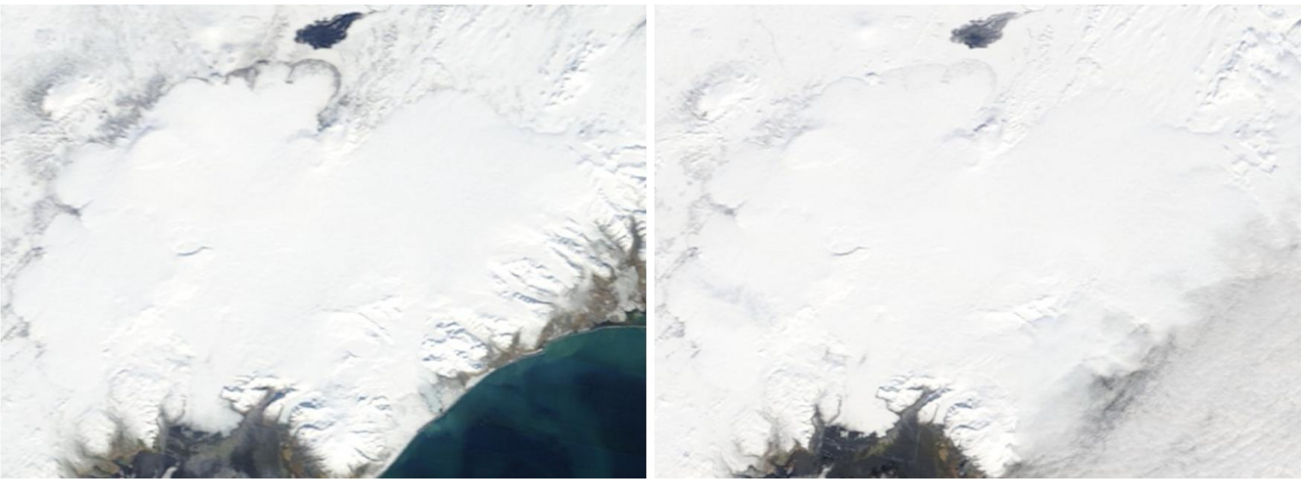

March 17th and 31st left and right respectively, height of winter. No snow in the south lowland and snow-cover in the west and north highland is very thin.

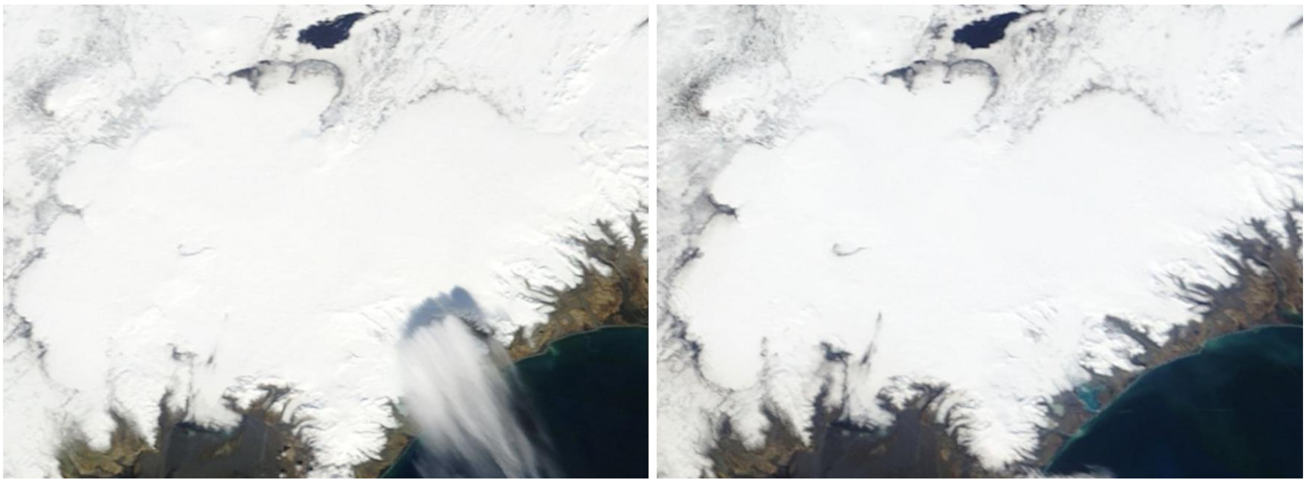

Left: April 25th, and May 15th. Not much has visibly changed since March, except that some melting has started in the highland and even on the glacier snouts..

Left: June 2nd. Start of summer, most of the snow has melted in the western and northern highland, Hágöngulón is still frozen over. Right: June 24th. The thin snow on the snout of the northern outlets has melted, snowline is rising on all visible outlets.

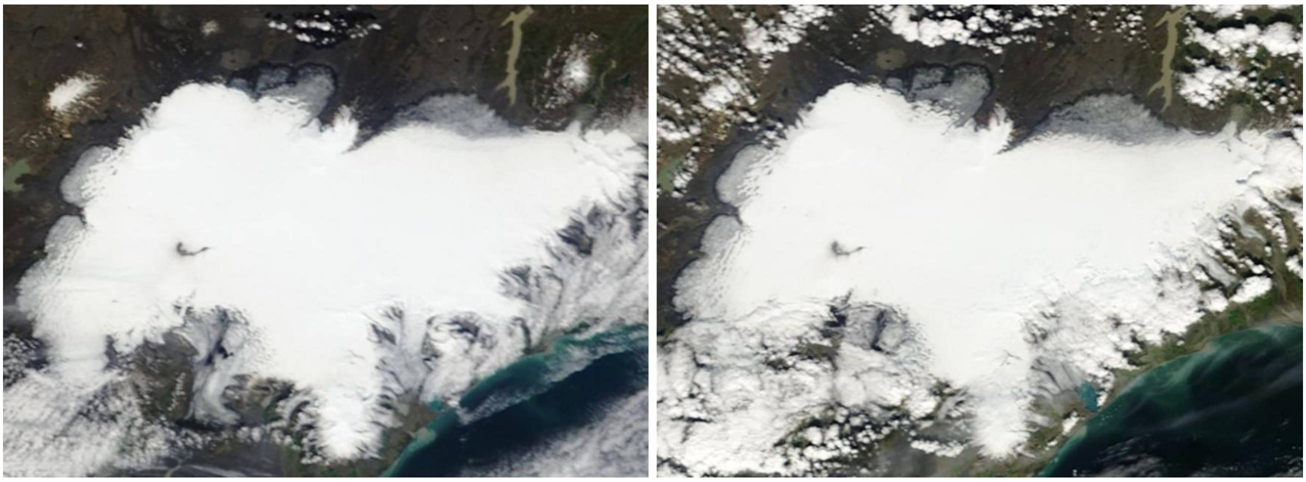

Left: July 18th, the first cloud free day over Vatnajökull in July. Some dust (brownish surface) is visible in areas just above th2 snowline. Right: August 6th. The snowline is migrating upwards on all visible outlets.

Left: August 20th. Snowline still migrating upwards and the surface seems dirtier than on the 6th. Note the dirt patches south of Grímsvötn. Right: August 29th. The snowline seem to have stopped migrating upwards, and the now whiter surface at higher elevations (above ~1400 m), snowfall, is first sign of autumn. The dirty patch south of Grímsvötn is now covered with snow.

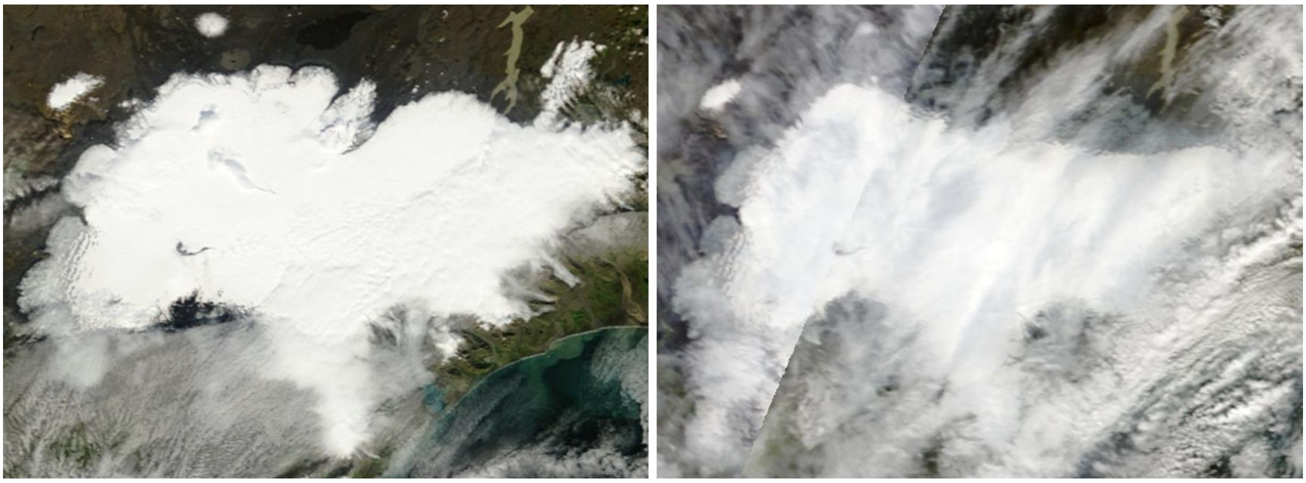

Left: September 3rd. Snow now covers most of the northern outlets. Right: the snow on the northern outlet ablation zone in seen on the image from September 3rd has melted. The snow line is apparently higher now than the last day of August, there is still melting below ~1300 m.

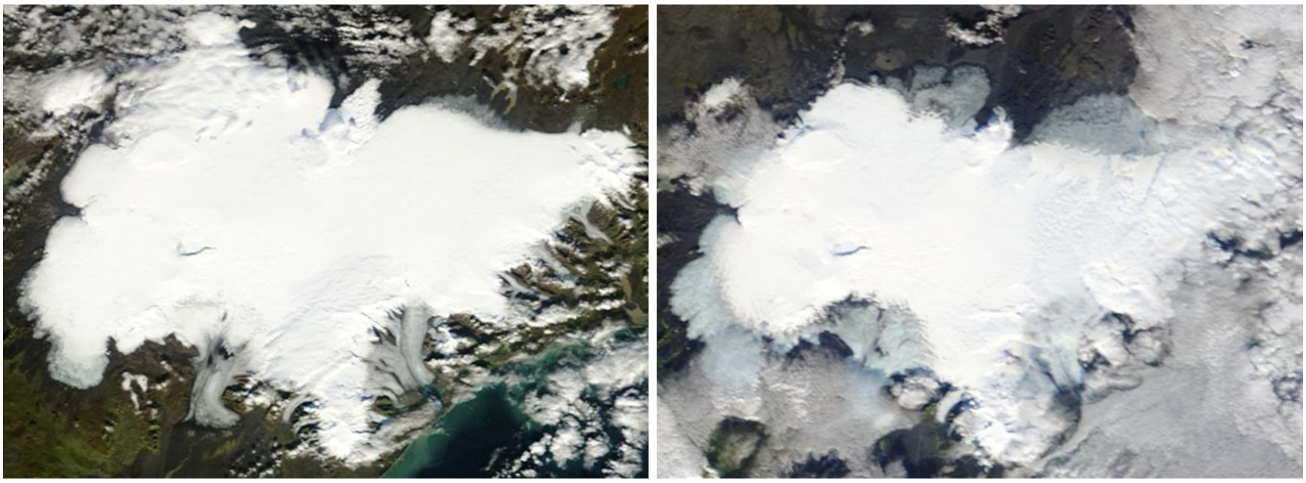

Left: September 26th. Since September 3rd there has been snowfall above ~800 m a.s.l..
Right: October 15th. Again most of the autumn snow has melted from ablation zone of all visible outlets. When the image was acquired the summer balance expedition to glacier was ongoing. Autumn snow up to 2 m (at Háabunga) was measured in the accumulation zone, but bare ice in most of the ablation zone.

The images are either from the MODIS Aqua or MODIS Terra satellites, visible light, 250 m resolution.
http://rapidfire.sci.gsfc.nasa.gov/
The Moderate Resolution Imaging Spectroradiometer (MODIS) flies onboard NASA's Aqua and Terra satellites as part of the NASA-centered international Earth Observing System. Both satellites orbit the Earth from pole to pole, seeing most of the globe every day. Onboard Terra, MODIS sees the Earth during the morning, while Aqua MODIS orbits the Earth in the afternoon.

On the next pages MODIS images for all days of May, June, July, August and September 2016 are shown in 1km resolution.

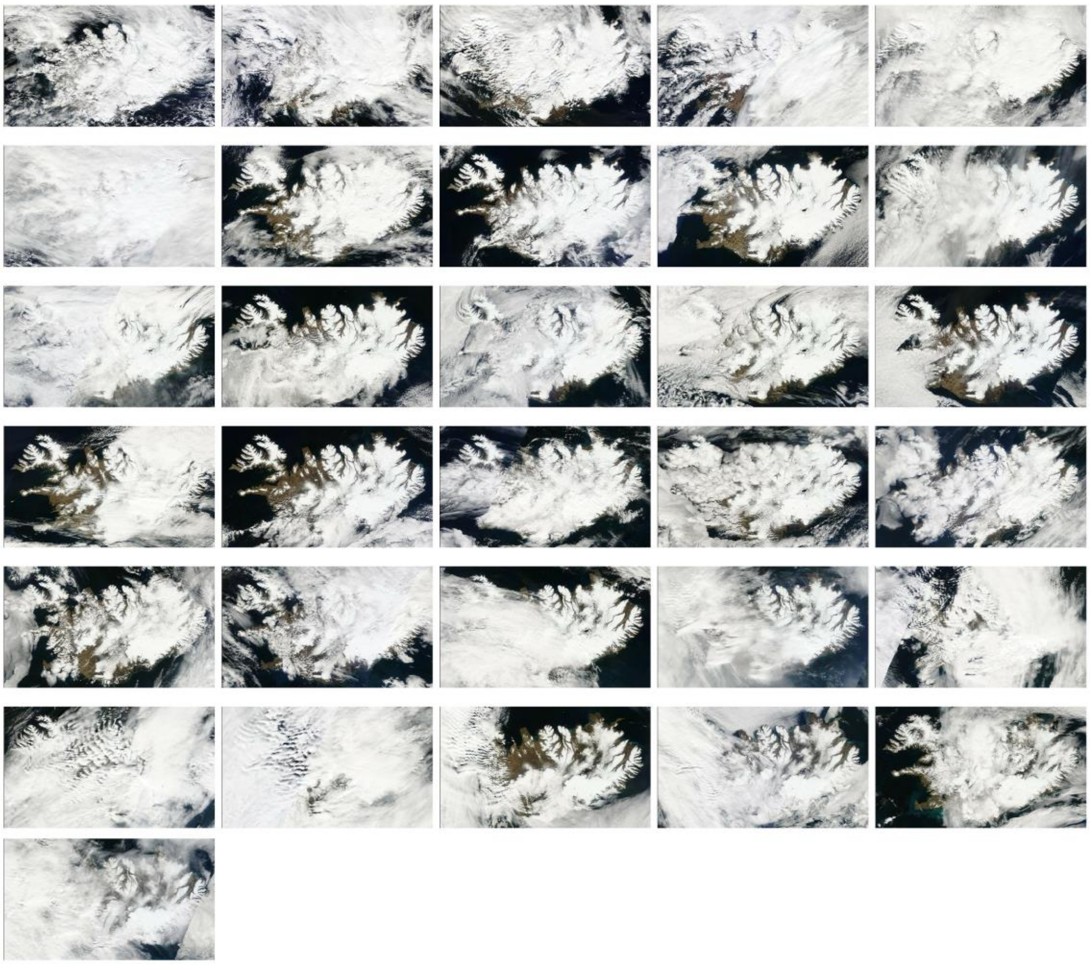

MODIS: May 2016 (read from left to right and downwards).

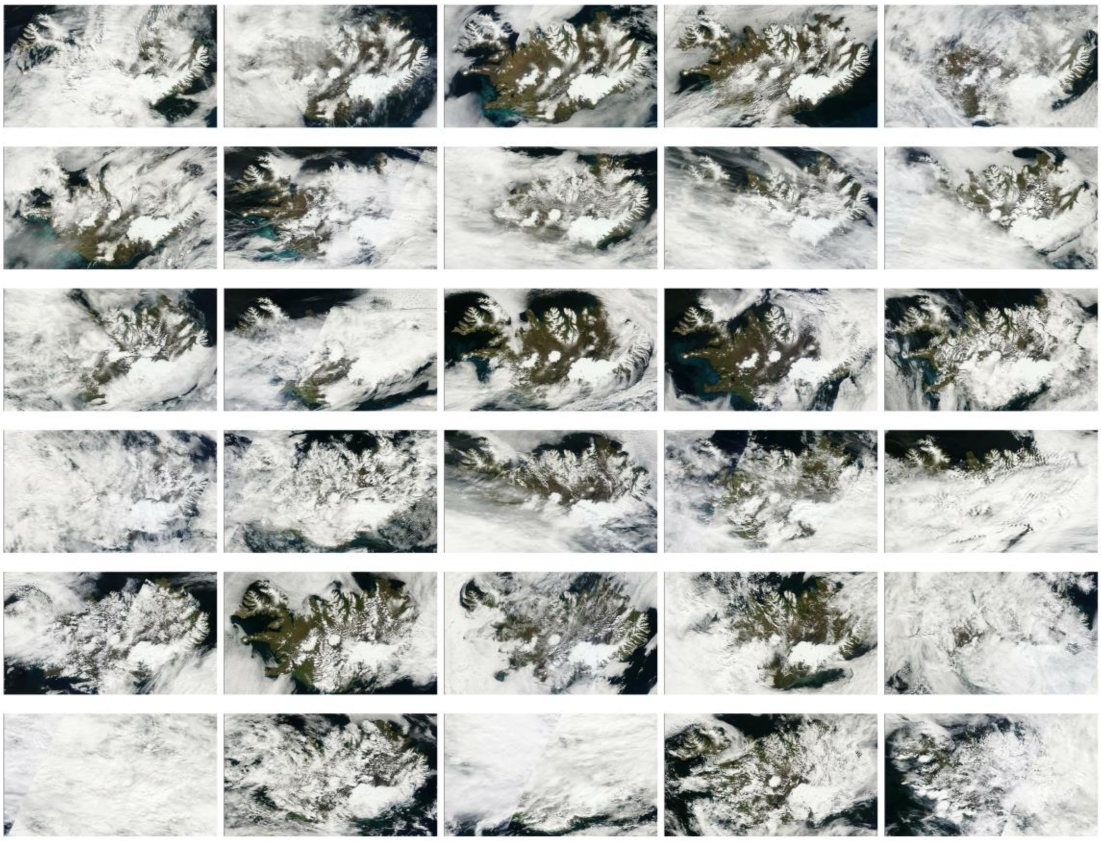

MODIS: June 2016 (read from left to right and downwards).

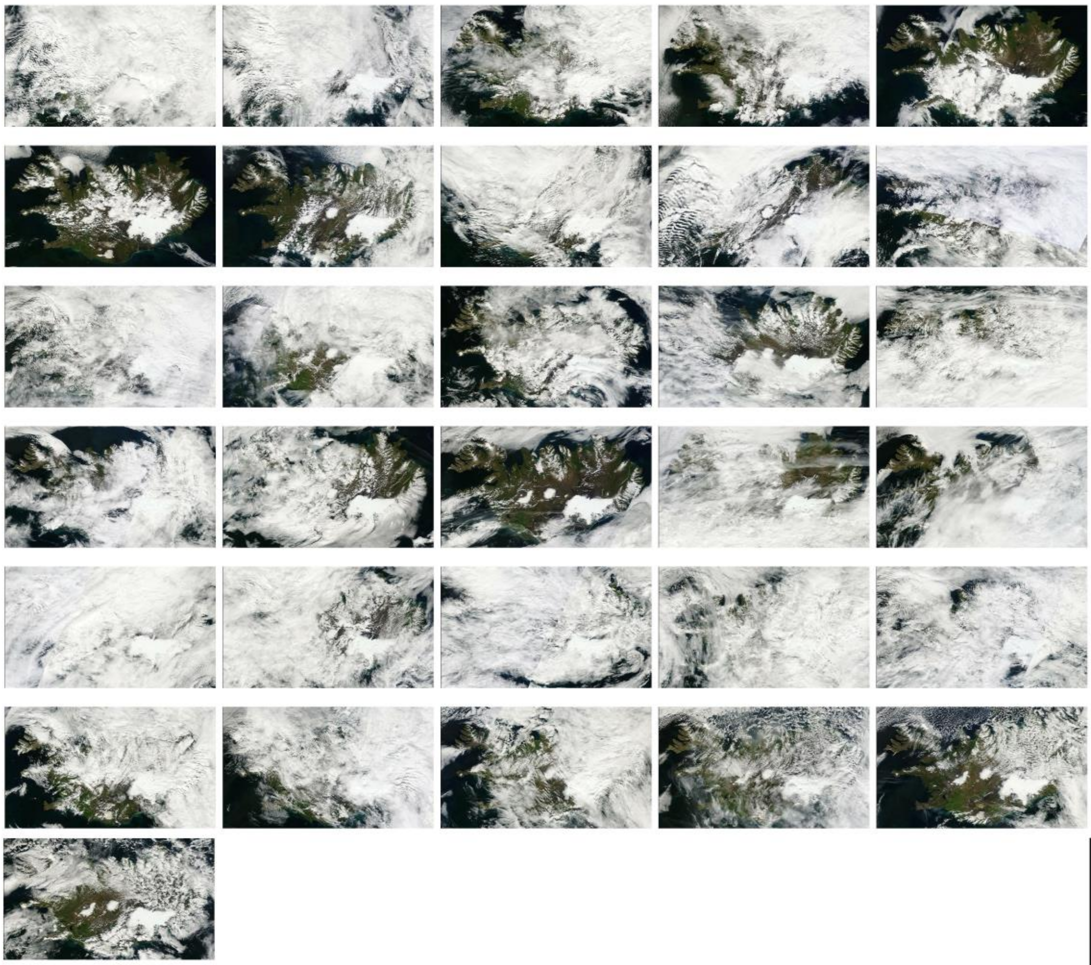

MODIS: July 2016 (read from left to right and downwards).

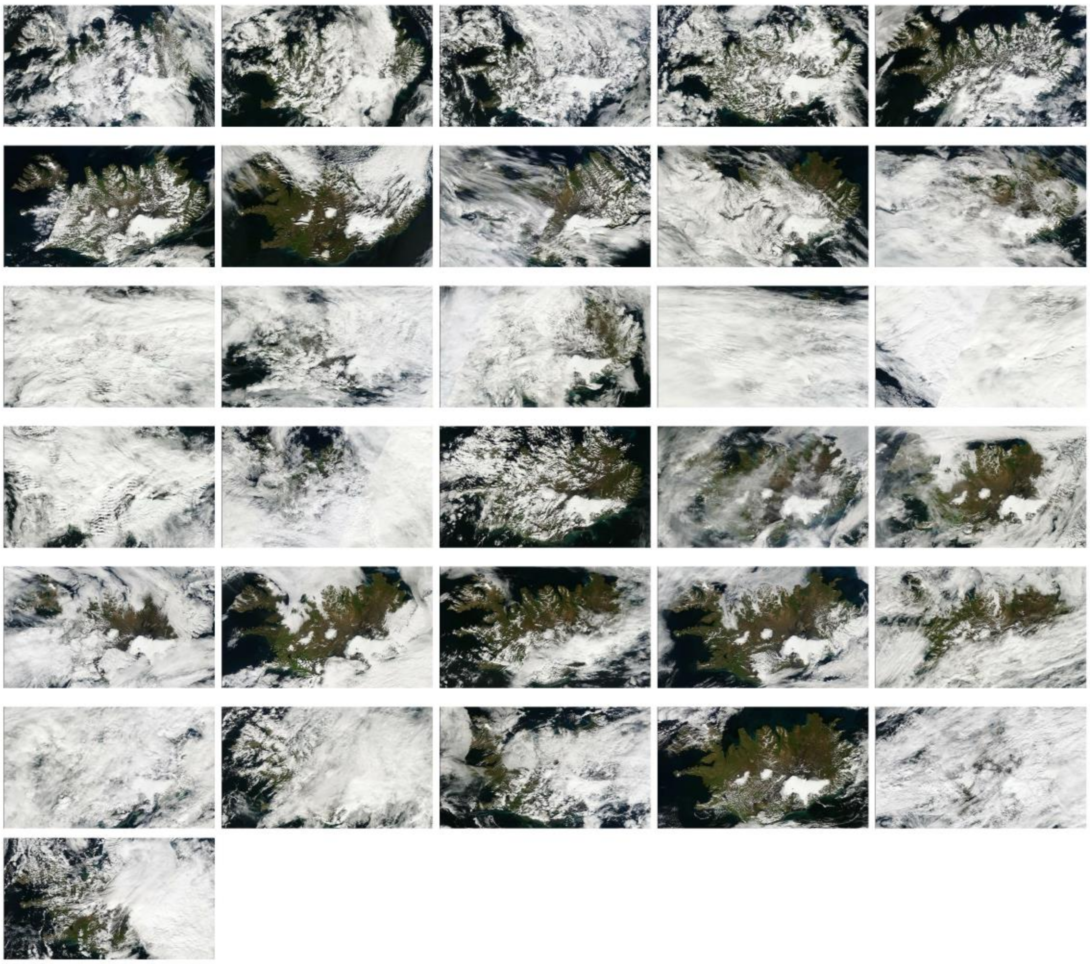

MODIS: August 2016 (read from left to right and downwards).

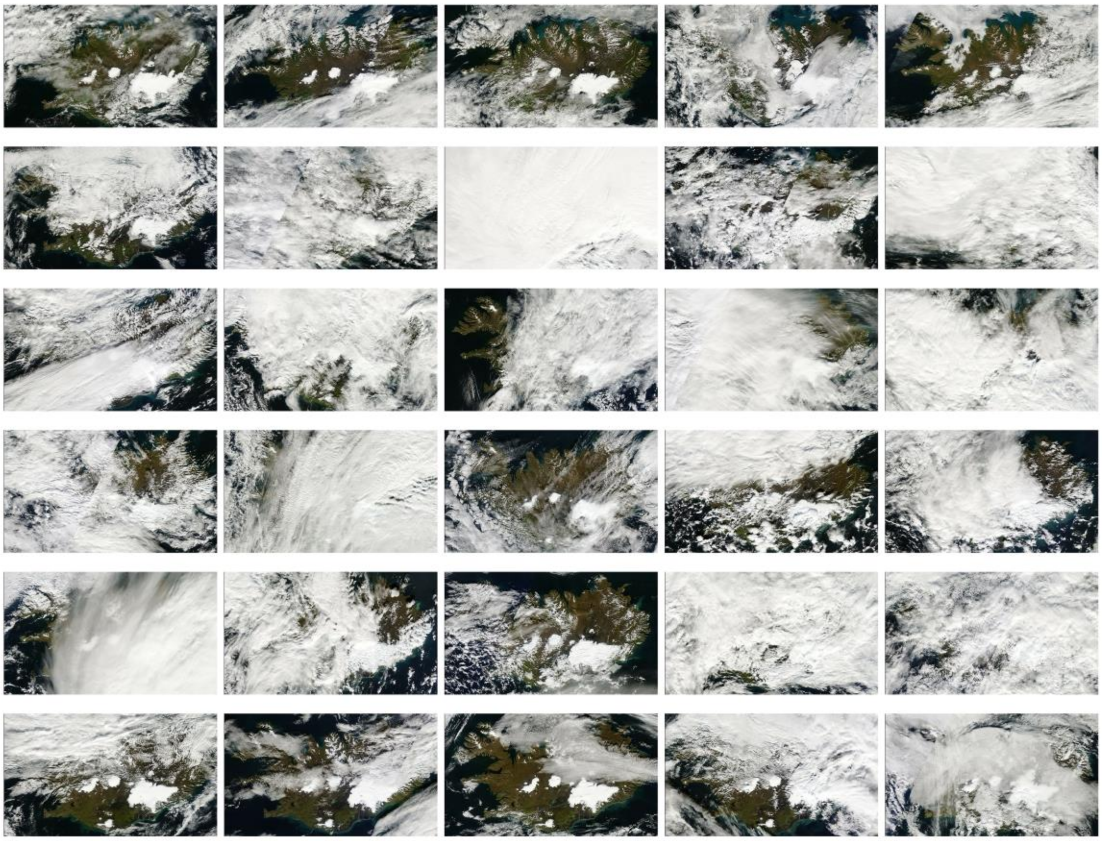

MODIS: September 2016 (read from left to right and downwards).

Landsvirkjun

Háaleitisbraut 68
103 Reykjavik
landsvirkjun.is

landsvirkjun@lv.is
Sími: 515 90 00